UNIVERSITAT POLITÈCNICA DE CATALUNYA
BARCELONATECH
Facultat de Matemàtiques i Estadística

Doctoral Degree in Applied Mathematics
School of Mathematics and Statistics
Universitat Politècnica de Catalunya

Mechanics of epithelial layers subjected to controlled pressure

by

Nimesh Ramesh Chahare

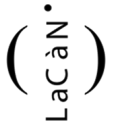

LaCàN: Laboratory of Mathematical and Computational Modeling

Advisor: Marino Arroyo and Xavier Trepat
Barcelona, March 7, 2023

"... If you want knowledge, you must take part in the practice of changing reality. If you want to know the taste of a pear, you must change the pear by eating it yourself..."

Abstract

Mechanics of epithelial layers subjected to controlled pressure

Nimesh Ramesh Chahare

Epithelial sheets form specialized 3D structures suited to their physiological roles, such as branched alveoli in the lungs, tubes in the kidney, and villi in the intestine. To generate and maintain these structures, epithelia must undergo complex 3D deformations across length and time scales. How epithelial shape arises from active stresses, viscoelasticity, and luminal pressure remains poorly understood. To address this question, we developed a microfluidic chip and a computational framework to engineer 3D epithelial tissues with controlled shape and pressure. In the setup, an epithelial monolayer is grown on a porous surface with circular low adhesion zones. On applying hydrostatic pressure, the monolayer delaminates into a spherical cap from the circular zone. This simple shape allows us to calculate epithelial tension using Laplace's law. Through this approach, we subject the monolayer to a range of lumen pressures at different rates and hence probe the relation between strain and tension in different regimes while computationally tracking actin dynamics and their mechanical effect at the tissue scale. Slow pressure changes relative to the actin dynamics allow the tissue to accommodate large strain variations. However, under sudden pressure reductions, the tissue develops buckling patterns and folds with different degrees of symmetry-breaking to store excess tissue area. These insights allow us to pattern epithelial folds through rationally directed buckling. Our study establishes a new approach for engineering epithelial morphogenetic events.

Keywords: epithelial monolayers, actomyosin cytoskeleton, morphogenesis, mechanobiology, microfluidics

Contents

Abstract i

Contents iii

List of Figures vii

I Introduction and motivation 1

1 Epithelial Layers 5
1.1 Introduction . . . 5
1.2 Key components . . . 6
1.2.1 Cell structure . . . 6
1.2.2 Microenvironment . . . 8
1.2.3 Cell-Matrix interaction . . . 9
1.3 Role in disease and development . . . 9
1.4 Forms of epithelia . . . 10

2 The mechanical basis of Morphogenesis 13
2.1 The complexity of the morphogenesis . . . 13
2.2 On growth and form . . . 14
2.3 Mechanobiology . . . 16
2.3.1 Synthetic substrates . . . 17
2.3.2 Geometric control . . . 18
2.3.3 Mechanical control . . . 19
2.3.4 3D systems . . . 21

3 Active tissue mechanics 23
3.1 Force generation with actin . . . 23
3.1.1 Actin filaments . . . 24
3.1.2 Actin networks . . . 25
3.1.3 Actin cortex . . . 26
3.2 Actin structures at a larger scale . . . 26
3.3 Timescales of the actin cytoskeleton . . . 28
3.4 Controlling cortical tension . . . 29

3.5 Modeling active tissue dynamics . . . 30
3.5.1 Vertex models . . . 31
3.5.2 Continuum models . . . 32
3.5.3 Active surface models . . . 34

4 Bottom up morphogenesis **37**
4.1 Learn by building . . . 37
4.2 How to build tissue structures? . . . 39
4.2.1 Controlling geometry and physical forces . . . 39
4.2.2 Manipulating biochemical signaling . . . 40
4.2.3 Exploiting mechanical instabilities . . . 42
4.3 Tissue hydraulics . . . 45
4.3.1 Hydraulic control of morphogenesis . . . 45
4.3.2 Mechanics of domes . . . 47

5 Structure of the thesis **51**
5.1 What is to be done? . . . 51
5.2 Objectives . . . 52
5.3 Thesis outline . . . 52

II Results **55**

6 A microfluidic system for generating 3D epithelia with controlled pressure and shape **57**
6.1 Introduction . . . 57
6.2 Monolayer inflator . . . 58
6.3 Fabrication of the device . . . 58
6.4 Protein patterning and inverted cell culture . . . 59
6.5 Pressure control . . . 60
6.6 Imaging the epithelial domes . . . 61
6.7 Light-sheet MOLI . . . 61
6.8 Summary and Discussion . . . 62

III Appendices **65**

A Methods and Materials **67**
A.1 Fabrication of microfluidic devices . . . 67
A.2 Patterning protein on the device . . . 68
A.3 Cell culture in the device . . . 68
A.4 Confocal Microscopy . . . 69
A.5 Device protein patterning and cell culture in Light-Sheet device . . . 69
A.6 Light-sheet microscopy . . . 70
A.7 Analysis of the kymographs . . . 70

A.8 Qualitative analysis of the buckling event 71

List of Figures

1.1 **The Anatomy Lesson of Dr. Frederik Ruysch**, 1670 by Adriaen Backer. . . 5
1.2 **Polarity of epithelia** Actin and myosin is distributed heterogenously in epithelial monolayers (Chen *et al.*, 2018). 6
1.3 **Mechanics of cytoskeletal filaments**: Schematic and sizes of actin filaments, intermediate filaments and microtubules; along with the strain response to shear stress. *Adapted from (Leggett* et al.*, 2021)* 7
1.4 **Intercellular forces through actomyosin cables and cadherins**: Schematic showing mechanical connections between adhesions and tissue force transmission with actomyosin cytoskeleton and adhesion proteins. (Ladoux and Mège, 2017) 8
1.5 **Cell-matrix interaction with respect to matrix stiffness and cell density**: In higher tension condition, the nucleus gets deformed triggering mechanotransduction causing alterations in cytoskeleton and tractions.(Xi *et al.*, 2018) 9
1.6 **Forms of epithelial tissues**: Simple squamous, cuboidal, columnar epithelia and pseudostratified epithelia 11

2.1 **Multiscale imaging and tracking of embryo cell dynamics**: Top panels show in toto imaging of germlayer specification; red is mesendoderm, blue is epiblast, and yellow is endoderm. Bottom panel shows data analysis of long term pan embryo cell dynamics (Shah *et al.*, 2019) 15
2.2 **D'Arcy Thompson's fishes** and his theory of transformation. (Thompson, 1979, Wolfram, 2017) 16
2.3 **Mechanobiological strategies for studying morphogenesis** (Vianello and Lutolf, 2019) 19

3.1 **Actin and Myosin**: (A) Electron micrograph of Actin filament with zoomed in images of barbed and pointed end. (B) Same for Myosin II minifilament with clearly visible two globular heads and a long tail. (C-D) Actin network can apply pushing force through polymerization of single filaments or network expansion. (E,F) While myosin activity would lead to contraction of the networks. *Adapted from A-B (Alberts, 2015) and C-F (Clarke and Martin, 2021)* 24

3.2 **Forms of actin networks**: (A) Actin treadmilling: where highlighted actins move from positive end to negative end as the filament polymerizes and depolymerizes from both ends. (C) In an adherent cells, there are many different kinds of actin structures from contractile network to gel-like cortex. (B,D,E,F) Actin structures can be thought as meshwork of actin filaments (red) with crosslinkers(green). Different crosslinkers produce distinct form of actin network. *Adapted from (Alberts, 2015)* 25
3.3 **Actin organization at different scales**:(A) Electron micrograph of actin cortex of mitotic Hela cells (Kelkar *et al.*, 2020). (B) Different forms of actin organization in circular fibroblast cell (Jalal *et al.*, 2019) Scale= $10\mu m$. (C) Supracellular actin ring during wound closure (Brugués *et al.*, 2014) Scale= $20\mu m$. (D) Dorsal closure of amnioserosa with actin network (Ducuing and Vincent, 2016) Scale= $10\mu m$. (E) Supra-cellular organization of actin for cellularization of coenocyte. Circle is $60\mu m$ (Dudin *et al.*, 2019). (F) Hydra with actin network, whose nematic defects determines morphogenesis (Maroudas-Sacks *et al.*, 2021) Scale= $100\mu m$. 27
3.4 **Morphogenesis driven by actin at tissue scale**: (A) Apical contraction or basal relaxation both results in the same curvature. (B) However, amount of deformation will depend on the contractility gradient. (C) Lateral surface of cells can also undergo expansion or contraction leading to cell rearrangements or tissue folding. (D-G) Supracellular actin cables plays vital role in creating boundaries or causing large scale deformations. *Adapted from (Clarke and Martin, 2021)* 28
3.5 **Molecular pathway and timescale of actin network related processes**: (A) Timescales of different actin driven cellular processes, ranging from cytoskeletal fluid deformation to large-scale tissue deformations (Wyatt *et al.*, 2016). (B) Molecular signaling of RhoGTPase. RhoGEFs return GDP for GTP to activate RhoA. In turn RhoA results in actomyosin contractility (Kelkar *et al.*, 2020). 29
3.6 **D'Arcy Thompson's forms of tissues:** (A-B) Thompson equates cell aggregates to coalescence of bubbles like in a froth. (C) A dragon fly wing is a clear example of this organization. 30
3.7 **Vertex model for cells in a monolayer** (Gómez-González *et al.*, 2020). . . . 31
3.8 **Stress strain behavior of materials**: (A) materials being stretched or compressed. (B) Quasistatic deformations yield stress-strain curves. (C) Creep test where strain response is characterized at constant stress. 33
3.9 **Active nematics**: (Xi *et al.*, 2018) 35
3.10 **Active surface models**: (A) Tissues or cell surfaces can be modeled as surface with stresses and torques along the thickness. (B) Internal and external forces actin on a surface element (Salbreux and Jülicher, 2017) 36

4.1 **A conceptual representation of two approaches to understanding mechanics: reconstruction (bottom-up) and deconstruction (top-down).** In reality, they are not separate from each other. These methods inform each other, with past top-down research guiding new reconstruction, and new engineered cells or tissues furthering our understanding of the field in innovative directions. 38
4.2 **Controlling geometry and physical forces:** The concept of scaffolding can be divided into two categories: static and dynamic scaffolds. (A) Static scaffolds are microfabricated structures that cells can adapt to and respond to geometrical cues, leading to the formation of a specific tissue organization (Brassard *et al.*, 2021). (B) In contrast, dynamic scaffolds consist of cell-laden matrices that are deformable, and their curvature can change dynamically due to external pressure or mechanical forces (Blonski *et al.*, 2021, Chan *et al.*, 2018). (C) Biohybrid assemblies can incorporate active contraction or pushing to create hybrid structures, such as origami folding triggered by fibroblast contraction (He *et al.*, 2018), or cells carving out an intestinal crypt-like geometry from a softer matrix (Gjorevski *et al.*, 2016). 40
4.3 **Manipulating biochemical signaling:** Biochemical signaling and mechanics are interdependent in morphogenetic processes (A). The transport of signaling molecules can affect the cytoskeleton and mechanical properties of cells, while mechanical forces can also influence biochemical signaling. Microfluidics (D) is one method used to control biochemical signaling by providing opposing morphogen gradients through multiple channels (Demers *et al.*, 2016). Alternatively, cells can be genetically engineered to undergo apical constriction (C) or produce morphogen gradients (E) locally to form curved geometries (Cederquist *et al.*, 2019, Martínez-Ara *et al.*, 2022). Mesenchyme condensation (B) is another approach used to program curvature in developing tissues (Hughes *et al.*, 2018, Palmquist *et al.*, 2022). 41
4.4 **D'Arcy Thompson compares biological budding to splashes** (A) of fluids and Rayleigh-Plateau instability (Thompson, 1979) (B), where liquid splits up into smaller droplets. This mechanism could also be seen in organogenesis of mammary tissue (C, D) (Fernández *et al.*, 2021). 42
4.5 **Compressive stresses** occur frequently in many systems (A). We can consider epithelia and matrix as thin sheet supported by a compliant substrate. Thus, the tissue folding could be understood as buckling of sheets (B) or wrinkling or creasing of thin film supported by an hydrogel (C). 43

4.6 **Examples of mechanical instabilities**: (A) Synthetic mini brains illustrate the wrinkling of the outer layer with swelling mimicking gyrification (Tallinen *et al.*, 2016). (B, D) Other way around where inner layer of lung or intestinal epithelia develops folds when embedded into a hydrogel or muscle shell (Shyer *et al.*, 2013, Varner *et al.*, 2015). (C) It is also shown that simple epithelial tissues embedded into a shell would also buckle (Trushko *et al.*, 2020). (D) (Wyatt *et al.*, 2020) used matrix independent tissue with compression to illustrate that the epithelial tissue itself can undergo buckling. *Panel A, D are adpated from (Collinet and Lecuit, 2021) and C from (Matejčić and Trepat, 2020)* 45

4.7 **Tissue hydraulics** plays an essential role in establishing (A) embryonic axis through lumen coarsening, and later the pressure regulates the size of the embryo. Laplace's law acts on the spherical cavities between cells to the whole blastocyst (Chan *et al.*, 2019, Collinet and Lecuit, 2021, Dumortier *et al.*, 2019). (B) Interestingly, if the inflated structure is surrounded by a mesh you see a stressball effect, where material inflates through the mesh. Similar phenomena is visible in growth and inflation of the lizard lungs. The smooth muscle constrains the deformation leading to stressball morphogenesis (Palmer *et al.*, 2021). (C) In cnidarians, the different orientation of F-actin leads to different shapes of the organism (Stokkermans *et al.*, 2022). 46

4.8 **Historical development of epithelial domes**:(A) Distended epithelium was observed in explant cultures in 1930-50s. (B) With MDCK cell line, spontaneously forming domes/hemicysts were characterized (Leighton *et al.*, 1969, Valentich *et al.*, 1979). (C,D) In our lab, shape and size of the domes were controlled with micropatterning adhesion protein (Latorre *et al.*, 2018). The pressure and tension was measured with Laplace's law and traction force microscopy. (E-F) For non-spherical domes, curved monolayer stress microscopy technique was implemented by segmenting the dome shape (Marín-Llauradó *et al.*, 2022). 48

4.9 **Ways of measuring pressure and tension**: (A) Earlier studies tried to estimate tension through geometry and thickness of the monolayer (Tanner *et al.*, 1983). (B) Later, pressure was measured by puncturing the dome with a micro-needle. However, the measurement of pressure is static, because the dome deflated after the puncturing (Choudhury *et al.*, 2022). (C) Traction force microscopy technique provides a viable non-invasive solution for measuring pressure under to domes (Latorre *et al.*, 2018). 49

Part I

Introduction and motivation

The central focus of this thesis is the epithelial tissue monolayer. From the perspective of a mechanical engineer, these monolayers are endlessly fascinating. These monolayers are remarkable in their ability to change shape, self-heal, and continuously deform or jam as needed (Xi *et al.*, 2018). They represent the simplest system for gaining a physical understanding of biological morphogenesis, as epithelia can be found everywhere in the body, covering the skin and lining various cavities and organs. The shapes of epithelial monolayers can range from simple spherical blastocysts to highly branched and folded lungs, and they are formed and maintained through constant adaptation and renewal. This thesis aims to explore the physical principles behind epithelial shape by combining theoretical and experimental approaches in the study of simple epithelial monolayers.

The chapters in this part serve as a comprehensive overview of all the key topics related to my PhD research. They begin with a brief introduction to epithelial tissue and its constituent parts, followed by a discussion on the role of mechanics in morphogenesis and various modeling approaches. This part concludes with a review of the growing field of "bottom-up" morphogenesis, where researchers are building biological systems from scratch.

Chapter 1

Epithelial Layers

1.1 Introduction

Figure 1.1: **The Anatomy Lesson of Dr. Frederik Ruysch**, 1670 by Adriaen Backer.

The term "epithelia" was first introduced by Dutch botanist Frederick Ruysch in the early 18th century (see fig 1.1). He used it to describe the tissue he observed while dissecting the lips of a cadaver, and the word is derived from Greek roots "epi," meaning top, and "thele," meaning nipple. [1] A few decades later, Swiss scientist Albrecht von Haller began using the term "epithelium/epithelia" to describe the fibers of the body, following the old Renaissance theory that the body was made of fibers, which were believed to be a fundamental building

[1] Ruysch is referred to as a "Artist of death" because of his famous anatomical collection. He was the first to use arterial embalming, which allowed for visualizing and dissecting smallest arteries. He also was part of the macabre practice of public dissections (Halley, 2019).

block of living things. [2] It was thought that these fibers and tissues arranged in different arrays gave rise to biological structures (MacCord, 2012, Zampieri *et al.*, 2014). This theory wasn't far off, as epithelial tissues make up more than 60% of the cells in a vertebrate's body and are found ubiquitously, covering the organs both inside and out (Alberts, 2015).

Epithelial cells are polarized, i.e., their apical side (faces the lumen of the organ), which differs in shape and composition from the basolateral side (see fig 1.2). Its polar organization is reflected in the vectorial functions like creating and maintaining concentration gradients between the separated compartments (Marchiando *et al.*, 2010). Typical examples of these are transporting epithelia such as those of the renal tubule, absorptive epithelia of the intestine, and secretory epithelial cells like hepatocytes (Alberts, 2015). In addition, polarized epithelia guide the developmental process by determining the fate of cells leading to symmetry-breaking events in the embryo (Kim *et al.*, 2018).

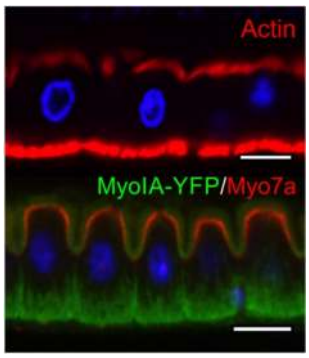

Figure 1.2: **Polarity of epithelia** Actin and myosin is distributed heterogenously in epithelial monolayers (Chen *et al.*, 2018).

1.2 Key components

The function of epithelia primarily depends on the tissue's structure and the surrounding microenvironment. It can be divided into three aspects: cell structure, microenvironment, and cell-matrix interactions.

1.2.1 Cell structure

The cell cytoskeleton plays a crucial role in maintaining cell shape and supporting vital functions such as cell division and migration (Alberts, 2015). The Eukaryotic cell cytoskeleton is composed primarily of filamentous proteins, including three main types of filaments that differ in size and protein composition: microtubules, actin filaments, and intermediate filaments (see fig 1.3). Microtubules, with a diameter of approximately 25 nm, are the largest and made of the protein tubulin. Actin filaments, with a diameter of only 6 nm, are the smallest. Intermediate filaments, with a diameter of around 10 nm, are composed of several different subunit proteins and have a diameter intermediate between the other two types (Mofrad, 2009). All three filament types dynamically respond to signals from the microenvironment and cell networks.

Mechanically, actin filaments have higher extensional stiffness than microtubules but break at lower extensions. Intermediate filaments have intermediate extensional stiffness and can sustain larger extensions while showing a nonlinear stiffening response (Wen and Janmey, 2011). Differences in strength and stability arise from the properties of individual subunits.

[2] Finding a fundamental unit of living entities comes from the philosophy of Gottfried W. Leibniz. It was based on the idea of "monad". Thanks to progress in microscopy and philosophy, naturalists were able to put together ideas for cells, fibers, and even cytoskeleton!(Zampieri *et al.*, 2014)

The persistence length can range from $1\mu m$ for intermediate filaments to $1mm$ for microtubules (Fletcher and Mullins, 2010). Actin filaments, being the stiffest, have a persistence length of a few microns.

The assembly and disassembly of these filaments are dictated by the dynamics of their macromolecular components and accompanying proteins. The combination of actin filaments and myosin motors forms the actomyosin cortex, which is essential in producing intra- and intercellular forces. In epithelial tissue, the actomyosin cortex and intercellular junctions make cell-to-cell contacts stronger and provide tissue integrity (Braga, 2016) (see fig 1.4). A good example of these tissue-level structures can be observed in wound healing assays, where cells surrounding the wound create a ring of actin to close it (Brugués *et al.*, 2014). In Chapter 3, we will delve into the actomyosin network in more detail.

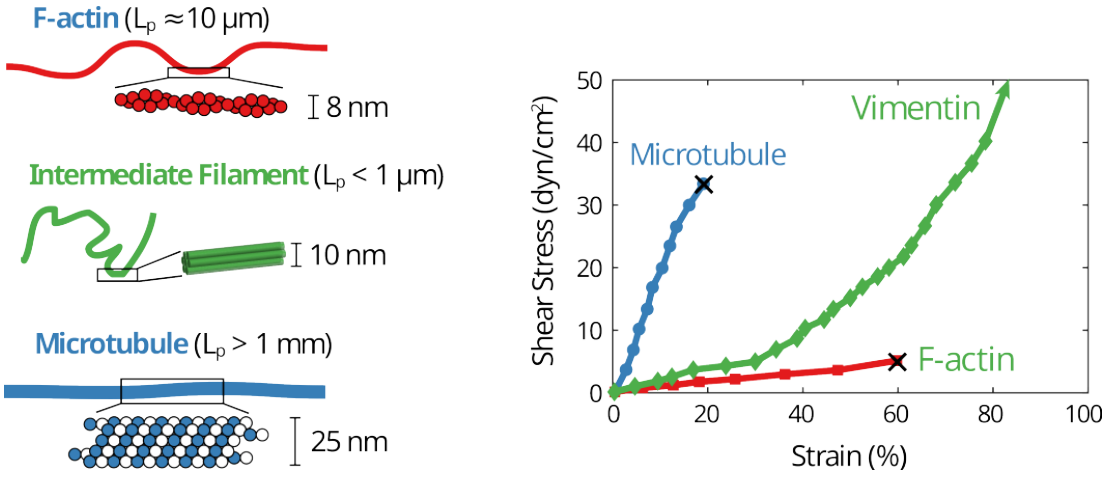

Figure 1.3: **Mechanics of cytoskeletal filaments**: Schematic and sizes of actin filaments, intermediate filaments and microtubules; along with the strain response to shear stress. *Adapted from (Leggett* et al.*, 2021)*

Multiple membrane molecules can facilitate cell adhesion, including cadherins. Cadherins are a crucial component for epithelial cell cohesion and the formation of adherens junctions, which transmit forces between cells. This key factor is involved in the mechanical regulation of cell division and tissue rearrangement during development and homeostasis (Godard and Heisenberg, 2019, Mertz *et al.*, 2013). Desmosomes, another type of intercellular junction, are coupled with intermediate filaments and provide mechanical resilience to cell layers (Hatzfeld *et al.*, 2017, Latorre *et al.*, 2018). Tight junctions serve as a barrier and regulate the active transport of ions across epithelial layers, playing an important role in controlling fluid pressure in tissues (Chan and Hiiragi, 2020, Marchiando *et al.*, 2010).

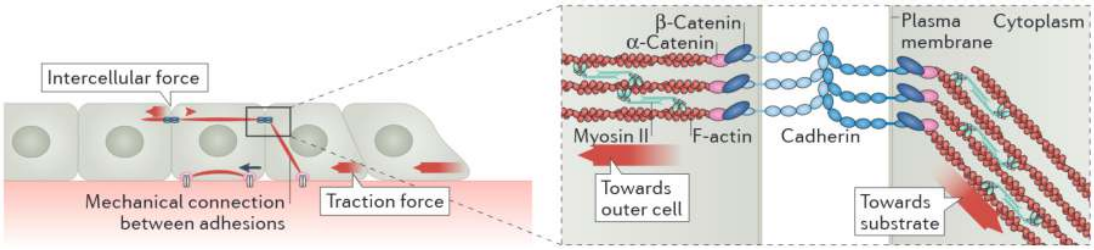

Figure 1.4: **Intercellular forces through actomyosin cables and cadherins**: Schematic showing mechanical connections between adhesions and tissue force transmission with actomyosin cytoskeleton and adhesion proteins. (Ladoux and Mège, 2017)

1.2.2 Microenvironment

The extracellular matrix (ECM) is the substrate or cell environment to which cells adhere. It is also referred to as the matrix, mesenchyme, or cellular microenvironment. The ECM serves many functions. It endows tissues with strength, thereby maintaining their shape. Additionally, it serves as a biologically active scaffolding that allows cells to migrate or adhere. The ECM also plays a role in regulating the phenotype of cells. It provides an aqueous environment that facilitates the diffusion of nutrients, ions, hormones, and metabolites between the cell and the capillary network (Alberts, 2015).

Moreover, the ECM is subjected to mechanical forces such as blood flow in endothelia, air flow in respiratory epithelia, or hydrostatic pressure in the mammary gland and bladder (Walma and Yamada, 2020, Waters *et al.*, 2012). It has been shown that the ECM regulates cell shape, orientation, movement, and overall function in response to biophysical forces (Alberts, 2015).

The ECM is a fibrous network of proteins, consisting of collagen, elastin, and proteoglycans as its primary structural components. Collagen is one of the most abundant proteins in the body, while Elastin is the most elastic and chemically stable protein. Proteoglycans can sequester significant water as well as growth factors and proteases. The water content of the ECM allows it to deform as a poroelastic material, absorbing water upon stretching and releasing it under compression, causing a hydraulic fracture effect (Casares *et al.*, 2015). The collagen network can also remodel under the influence of cells and mechanical forces (Humphrey *et al.*, 2014).

Most ECM components undergo continuous turnover, some quickly and some slowly. For example, the half-life of collagen in the periodontal ligament is a few days, whereas that in the vasculature may be several months (Humphrey *et al.*, 2014). In response to altered physical stimuli, disease, or injury, the rates of collagen synthesis and degradation can increase many times, allowing for a rapid response.

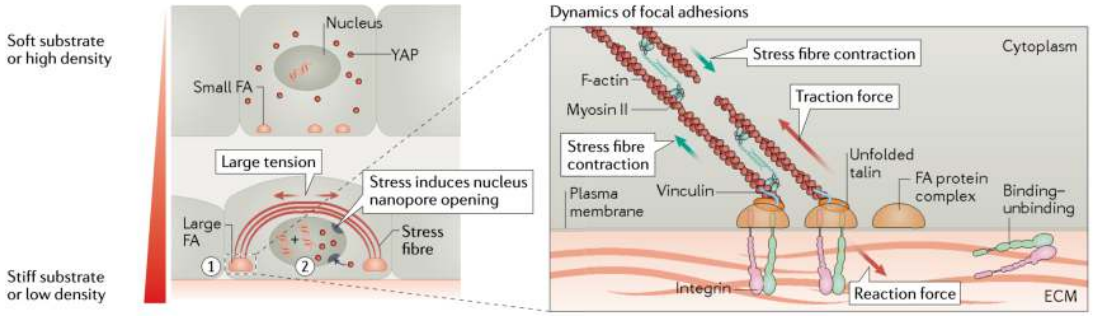

Figure 1.5: **Cell-matrix interaction with respect to matrix stiffness and cell density**: In higher tension condition, the nucleus gets deformed triggering mechanotransduction causing alterations in cytoskeleton and tractions.(Xi *et al.*, 2018)

1.2.3 Cell-Matrix interaction

The cells and the extracellular matrix (ECM) are in a dynamic relationship, constantly exchanging information and influencing each other. The cells sense the biophysical cues in the ECM through sensors such as integrins and focal adhesion complexes, which are responsible for cell-substrate adhesion (Kechagia *et al.*, 2019) (see fig 1.5). These adhesions allow cells to respond to various stimuli such as matrix stiffness, ligand density, and chemotactic gradients (Fortunato and Sunyer, 2022). It has also been shown that cells can respond to the viscoelasticity of the matrix (Elosegui-Artola *et al.*, 2022).

In addition to sensing the ECM, cells also contribute to its composition by secreting ECM components or remodeling the substrate (Malandrino *et al.*, 2018). This interplay between the cells and ECM can impact the tissue behavior fundamentally, as the connections between focal adhesions and the nucleus can affect the expression of transcriptional factors (Lomakin *et al.*, 2020, Venturini *et al.*, 2020). The precise control of cell-cell and cell-substrate interactions enables cells to transform into intricate shapes, such as curved forms in cell sheets (Schamberger *et al.*, 2022).

1.3 Role in disease and development

Maintaining epithelial integrity and homeostasis is crucial for survival, and mechanisms have evolved to ensure these processes are sustained during growth and in response to damage. Epithelial cells have one of the fastest turnover rates in the body, with the entire gut cell lining turning over in 5–7 days (Barker, 2014). This constant cell division and death pose a risk for tumor formation; it is know that 90% of cancers emerging in simple epithelia (Eisenhoffer and Rosenblatt, 2013, Torras *et al.*, 2018). Additionally, the high rate of cell turnover can disrupt the barrier function, as gaps should not emerge around dividing or dying cells.

If the fluid compartmentalization goes awry, it can have profound implications for epithelial

and stromal homeostasis, fluid and electrolyte balance, and the development of inflammatory states. Several bacterial toxins are known to target junctions, causing changes in the tight junction protein ZO1, which compromises the barrier function and leads to pathologies such as diarrhea and colitis (Fasano *et al.*, 1991). In cancer, the compromised ZO1 barrier is essential to allow metastatic cells to break into and out of blood vessels. The leaky barrier also enables a growing epithelial tumor to access luminal fluids as an additional source of nutrients (Mullin *et al.*, 2005).

Furthermore, epithelia participate in physiological events such as epithelial–mesenchymal transition (EMT), which is a developmental process where epithelial cells gradually transform into mesenchymal-like cells by losing their epithelial functionality. EMT plays a vital role in normal biological functions such as repair and differentiation, as well as abnormal pathological activity such as organ fibrosis and promoting carcinoma progression (Alberts, 2015). EMT endows cells with stem cell properties, enabling cell migration to distant organs and subsequent differentiation into multiple cell types during development and the initiation of metastasis (Thiery *et al.*, 2009).

Epithelia undergo drastic shape changes with deformation and reorganization from the embryonic to the adult stage. It's not surprising that any malfunction in this process can lead to damage and disorder, resulting in congenital malformations, which are a major cause of infant mortality worldwide (Clarke and Martin, 2021). Additionally, epithelial dysfunction is a precursor to diseases such as chronic obstructive pulmonary disease, asthma, cystic fibrosis, and pulmonary fibrosis (Carlier *et al.*, 2021).

1.4 Forms of epithelia

The structure and arrangement of epithelial cells are crucial for maintaining the integrity and homeostasis of tissues and organs (see fig 1.6). Simple epithelia are single-cell layers where all cells come in contact with the underlying basal lamina and have a free surface on the apical side. The shape of the cells can vary, ranging from flat to cuboidal to columnar. Stratified epithelia, on the other hand, have two or more layers of cells. Additionally, there is pseudostratified epithelia, which appears to be stratified, but it is a monolayer where the nuclei of the cells are positioned in a manner that gives the appearance of a stratified epithelium.

The classification of epithelia was first established in the 19th century based on their structure and physiological characteristics. Germ layer theory, developed by embryologists, further expanded the epithelial nomenclature (MacCord, 2012). During early embryogenesis, three layers emerge: endoderm, mesoderm, and ectoderm. The ectoderm forms the epithelia lining the skin, mouth, and nervous system, while the endoderm gives rise to the digestive tract, respiratory system, and liver. The mesoderm, in turn, develops the endothelia covering much of the circulatory and lymphatic systems.

It is important to note that not all tissues classified as epithelia, mentioned in this thesis, are purely composed of epithelial cells. They may be a mixture of different cell types that have

epithelial-like characteristics. The focus of this thesis is on packed cell monolayers, which can form and self-organize into various 3D shapes, ranging from simple spheres to complex branched tubules. The thesis will explore the role of mechanics in epithelial morphogenesis.

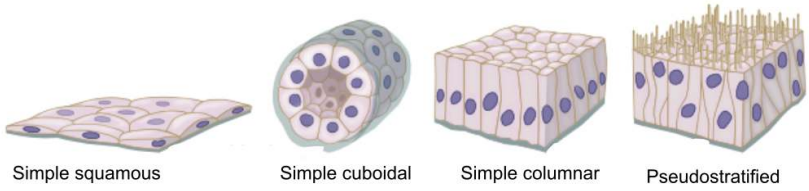

Figure 1.6: **Forms of epithelial tissues**: Simple squamous, cuboidal, columnar epithelia and pseudostratified epithelia

Chapter 2

The mechanical basis of Morphogenesis

2.1 The complexity of the morphogenesis

Epithelial cells play a crucial role in the formation of transient structures during embryonic development, such as the neural tube, somites, and precardiac epithelium, which serve as the precursor for the development of complex organs. During this process, different types of epithelia acquire distinct morphological forms and perform specific functions, including branched lungs, looped gut, kidney tubules, thyroid follicles, and sinusoids in the liver. The regulation of epithelial morphogenesis is a complex and hierarchical process that involves coordinated events at multiple spatial and temporal scales (Trepat and Sahai, 2018).

Some processes appear to be happening fast at the local level, such as cell shape changes through apical constrictions, which lead to global changes, such as the formation of a ventral furrow in a Drosophila embryo (Martin *et al.*, 2009). At the same time, chemical signaling events that activate these processes are slow and occur at a global level. The same complexity can be seen in in vitro systems, where a cluster of dissociated stem cells can assemble into an organoid or gastruloid and undergo global folds in response to appropriate culture conditions (Collinet and Lecuit, 2021).

The underlying mechanisms of epithelial morphogenesis are intricate and involve multiple factors, including genes responding to morphogen gradients, molecular machinery involved in apical constriction, and mechanical stresses that cause tissue-scale deformations. To fully understand the phenomenon of epithelial morphogenesis, it is essential to study these processes in detail, at multiple levels of complexity (Lecuit *et al.*, 2011, Schöck and Perrimon, 2002).

Rudolf Virchow's third tenet of the cell theory states that "omnis cellula e cellula," meaning "all cells come from cells" (Virchow *et al.*, 1860). [1] Although all tissues originate from cells

[1]The famous epigram was coined by François-Vincent Raspail. Virchow is regarded as influential biomedical scientist of 19th century, but more interesting part is as a radical who took part in the March revolution of 1848. He

that contain essentially the same genetic information, each tissue has a distinct architecture and function. This raises several questions, such as: what makes cells different from each other? Are differences due to genes, environmental factors, or both? What drives shape changes in tissue morphogenesis? Over the last two centuries, the field of developmental biology has addressed many of these questions, but it has also raised new issues and left others unanswered.

Until last decade, the focus of the field had been on tracking and mapping patterns of cell movements to patterns of gene or protein expression (Gorfinkiel and Martinez Arias, 2021). While these studies are influential and important for understanding morphogenetic patterns, they fall short in explaining how cells and tissues are physically shaped (Odell *et al.*, 1981, Veenvliet *et al.*, 2021). This is because the physical understanding of tissues has been limited to kinematic descriptions, which only describe tissue deformation or cell motion. However, we know that cells and tissues actively drive shape changes and movements through the generation of mechanical forces (Lecuit *et al.*, 2011). Thus, to have an integrated understanding of morphogenesis, we must consider the role of forces and mechanics.

2.2 On growth and form

Throughout history, the form of both animate and inanimate objects has been closely linked to their intended function. In fact, the 20th century architecture principle "Form Follows Function" highlights the idea that the organization of a structure should be based on its intended purpose. Similarly, in developmental biology, self-assembling systems such as intestinal organoids, cancer spheroids, and gastruloids are perfect examples of this principle in action, as each structure emerges from a set of cells in a suitable environment, adapting to perform a specific biological function (Gjorevski *et al.*, 2016, Ishiguro *et al.*, 2017, Morizane and Bonventre, 2017, Vianello and Lutolf, 2019).

However, the opposite design principle appears to be at work in numerous in vitro experiments that involve a controlled cellular environment. In such experiments, geometric constraints appear to drive biological function (Xi *et al.*, 2018). For instance, seeding stem cells in a bio-printed three-dimensional geometry of the gastrointestinal tract led to the production of functional tissues with physiological characteristics of the intestine. The curvature of the structure can even control the formation of villus-like structures (Brassard *et al.*, 2021).

In a way, assembly of biological systems treads the line between self-organization and programmed material. Advanced microscopy techniques have allowed us to witness the intricacies of developmental processes with unprecedented clarity (see fig 2.1). We can now observe cells and their motion throughout the morphogenetic process, from the formation of a spherical embryo to the creation of a complete organism (Shah *et al.*, 2019). Cells undergo shape changes and large-scale flows as they undergo morphogenesis, driven by mechanical forces in concert with biochemical processes (Labernadie and Trepat, 2018, Lecuit *et al.*, 2011,

was one of the first to advocate for the social origins of illness (Brown and Fee, 2006, Wright and Poulsom, 2012).

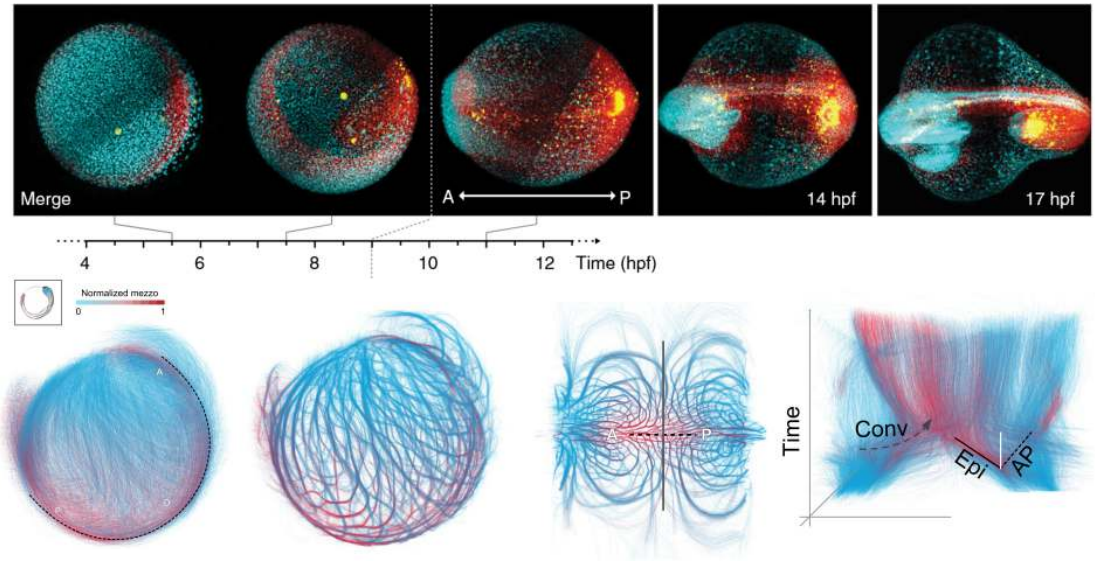

Figure 2.1: **Multiscale imaging and tracking of embryo cell dynamics**: Top panels show in toto imaging of germlayer specification; red is mesendoderm, blue is epiblast, and yellow is endoderm. Bottom panel shows data analysis of long term pan embryo cell dynamics (Shah *et al.*, 2019)

Trepat and Sahai, 2018). Thus, the dichotomy of form and function is incomplete without considering the physical laws of mechanics.

Over a century ago, D'Arcy Wentworth Thompson wrote the influential book "On Growth and Form" (Thompson, 1979), in which he explored the relationship between geometry, physics, and biology in the context of morphogenesis. Thompson used examples to show how mathematical principles can explain biological phenomena, such as his theory of transformations, which demonstrates how related species can be represented geometrically (see fig 2.2). According to Thompson's daughter, he even used to draw pictures of dogs on rubber sheets and stretch them to show children how poodles could become dachshunds (wol). This distortion of shape represents significant alterations in various forces or rates of growth throughout the developmental processes of different organisms.

Thompson's approach was highly speculative, but his goal was to identify general principles behind the diverse forms and patterns found in biology. He compared growth curves of haddock, trees, and tadpoles, and found logarithmic spirals in shells, horns, and leaf arrangements. [2] Essentially, this book emphasized two points: first, all material forms of living things—cells, tissues, and organs—must obey the laws of physics, and second, quantitative measurements

[2]Funnily, He criticized the zoologists and morphologists of the time of assigning shapes to psychical instinct of the organism or some divine interference for creating the perfect shapes: "He finds a simple geometric construction, for instance in the honeycomb structure, he would fain refer it to psychical instinct or design rather than in the operation of physical forces. ... When he sees in snail, or nautilus, or tiny foraminiferal or radiolarian shell a close approach to sphere or spiral, he is prone of old habit to believe that after all it is something more than a spiral or a sphere, and that in this "something more" there lies what neither mathematics nor physics can explain

are necessary to unravel the physical principles of biology.

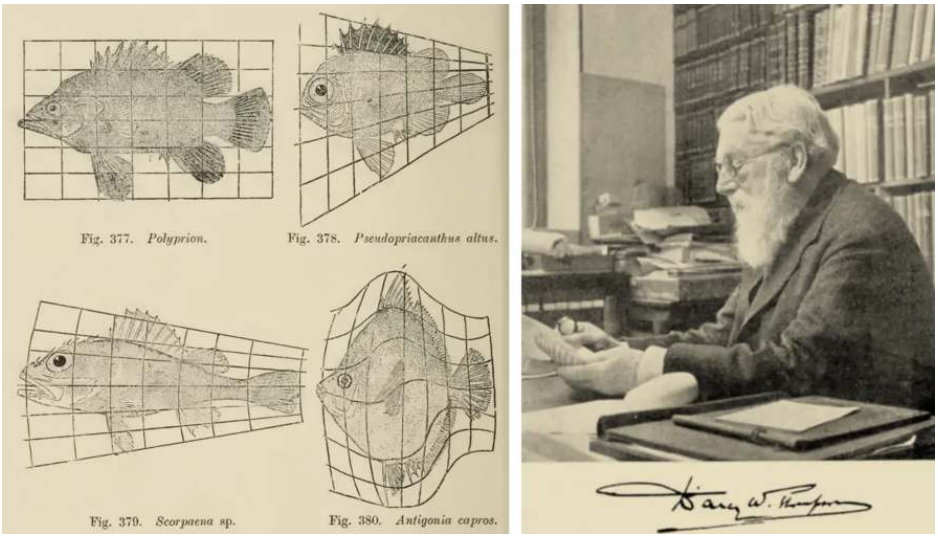

Figure 2.2: **D'Arcy Thompson's fishes** and his theory of transformation. (Thompson, 1979, Wolfram, 2017)

Thompson's work continues to inspire researchers even today. Right as I began my Ph.D., the centenary of the book's publication was being celebrated in the fields of developmental biology and biophysics (nat, 2017a,b, Heer and Martin, 2017). Even more so by the field of mechanobiology, an interdisciplinary field that studies the role of biophysical forces in cell and tissue functioning.

2.3 Mechanobiology

The cells within epithelial tissue can be viewed as mathematical systems that integrate multiple input cues to result in an output behavior. These inputs can be mechanical or chemical, such as the stretching of lungs or the presence of morphogen gradients during embryonic development. The outputs can include cell deformation, migration, differentiation, or proliferation (Kumar *et al.*, 2017). Some outputs can even feedback into the system as an input, such as when cells remodel the matrix (Malandrino *et al.*, 2018). Mechanochemical switches at the membrane, cell-cell junctions, or cell-matrix adhesions mediate the sensing of the environment, triggering a biochemical cascade that leads to a cellular response (Roca-Cusachs *et al.*, 2017). This interplay between biochemistry and mechanics is known as mechanotransduction.

During morphogenesis, mechanotransduction occurs at various scales, ranging from a single cell to complex multicellular tissue. To understand the role of different variables, experiments at different scales are necessary. It has been observed that individual cells can sense their environment and respond by altering their behavior through mechanical or biochemical processes. Whereas, multicellular systems can transmit forces and information at a longer

length scale, allowing for emergent characteristics such as collective migrations, oscillations, rearrangements, and even turbulent flows (Heer and Martin, 2017, Lecuit *et al.*, 2011, Trepat and Sahai, 2018).

An excellent demonstration of the interaction between tissues and their environment is provided by the phenomenon of durotaxis. Epithelial cells can detect changes in the stiffness of the extracellular matrix and migrate towards areas of higher rigidity. This migration towards stiffer regions has been observed both in vitro, where cells in a monolayer collectively expand and relocate to stiffer areas, and in vivo, such as during the migration of neural crest cells in *Xenopus laevis* (Shellard and Mayor, 2021, Sunyer *et al.*, 2016). It is worth noting that the migration of neural crest cells themselves generates the durotactic gradient. In another example, during Drosophila oogenesis, the disorganized matrix is remodeled by cells to create a polarized matrix that aligns with the actin bundles in the follicular epithelium. This alignment is achieved through the coordinated rotation of cells and can guide the directed motion of cells along the polarized fibers (Cetera *et al.*, 2014, Haigo and Bilder, 2011).

The interplay between individual cells, their neighbors, and exogenous stimuli makes it difficult to decouple various biophysical aspects of the environment, such as forces, pressures, matrix stiffness, spatial confinement, porosity, or viscoelasticity. Direct force measurements in and out of tissues are also challenging. To address these challenges, researchers from various disciplines have attempted to recreate experimental systems with precise control over the biochemical and mechanical environments of cells (Xi *et al.*, 2018). This has been made possible through continuous technological advancements in fluorescent probes, imaging, microfabrication, and force measurements (Roca-Cusachs *et al.*, 2017). In the following section, I will provide an overview of relevant techniques and experiments in the field of mechanobiology.

2.3.1 Synthetic substrates

The use of Polyacrylamide and soft PDMS gels has enabled researchers to investigate mechanical interactions at cell-substrate adhesion (see fig 2.3 A). Simply seeding cells on hydrogels of different stiffnesses reveals a significant impact on the actin cytoskeleton, cell shape, and lineage specification (Engler *et al.*, 2006, Yeung *et al.*, 2005). These substrates, because of their known elastic response, are also utilized in techniques like traction force microscopy (TFM) to measure the forces exerted by cells and tissues on the substrate (Gómez-González *et al.*, 2020, Harris *et al.*, 1980) (see fig 2.3 D). TFM studies have shown that cells and tissues can exert greater forces on stiffer substrates as a result of the remodeling of the cytoskeleton (Elosegui-Artola *et al.*, 2016). Higher matrix stiffness has also been found to induce the translocation of Yes-associated protein (YAP) from the cytoplasm to the nucleus, which is considered a sensor for mechanotransduction (Elosegui-Artola *et al.*, 2017). However, increasing extracellular matrix (ECM) ligand density alone can induce YAP nuclear translocation without changing substrate stiffness (Stanton *et al.*, 2019).

2.3.2 Geometric control

The shape of cells or tissues on 2D substrates can be controlled using micropatterned adhesion proteins or microfabricated stencils. Protein patterning techniques are used to pattern adhesion promoting proteins and control cell attachment and spreading, while microfabricated stencils physically confine cells in a particular geometry (see fig 2.3 B C). When cells are confined, they respond by reorganizing their actin cytoskeleton and focal adhesion complexes to match the shape imposed on them (Vignaud *et al.*, 2012). Confined tissues undergo larger-scale rearrangements, leading to the formation of fascinating topological defects or oscillations (Balasubramaniam *et al.*, 2021, Guillamat *et al.*, 2022, Tlili *et al.*, 2018). Through these experiments, we can uncover the mechanisms of force transmission and regulation of collective cell migration and epithelial growth in two dimensions (Deforet *et al.*, 2014, Nelson *et al.*, 2005, Vedula *et al.*, 2012).

Embryonic stem cells subjected to 2D confinement have been shown to differentiate based on the shape and size of the confinement. For example, a circular monolayer of stem cells can reproduce the tissue patterning of a 3D gastruloid (Warmflash *et al.*, 2014), and confinement in a triangular shape can lead to high tension at the vertices and activate Wnt signaling, promoting differentiation to mesoderm (Muncie *et al.*, 2020). Moreover, advancements in photopatterning technologies allow for precise control of multiple proteins on the same substrate (Guyon *et al.*, 2021, Prahl *et al.*, 2022), enabling the establishment of complex co-culture systems that mimic in vivo events.

Not just 2D shape, epithelial monolayers are also able to respond to curvature by regulating cell migration, orientation, cell/nucleus size, and shape (Marín-Llauradó *et al.*, 2022, Schamberger *et al.*, 2022) (see fig 2.3 C). For example, an epithelial monolayer on hemispheres of elastomers acts as a fluid with increasing curvature (Tang *et al.*, 2022). On a smaller scale, cells attached to corrugated hydrogels show variations in lamins, chromatin condensation, and cell proliferation rate in response to curvature (Luciano *et al.*, 2021). Bio-printing of three-dimensional tissue architectures can also create functional tissues (Brassard *et al.*, 2021, Breau *et al.*, 2022).

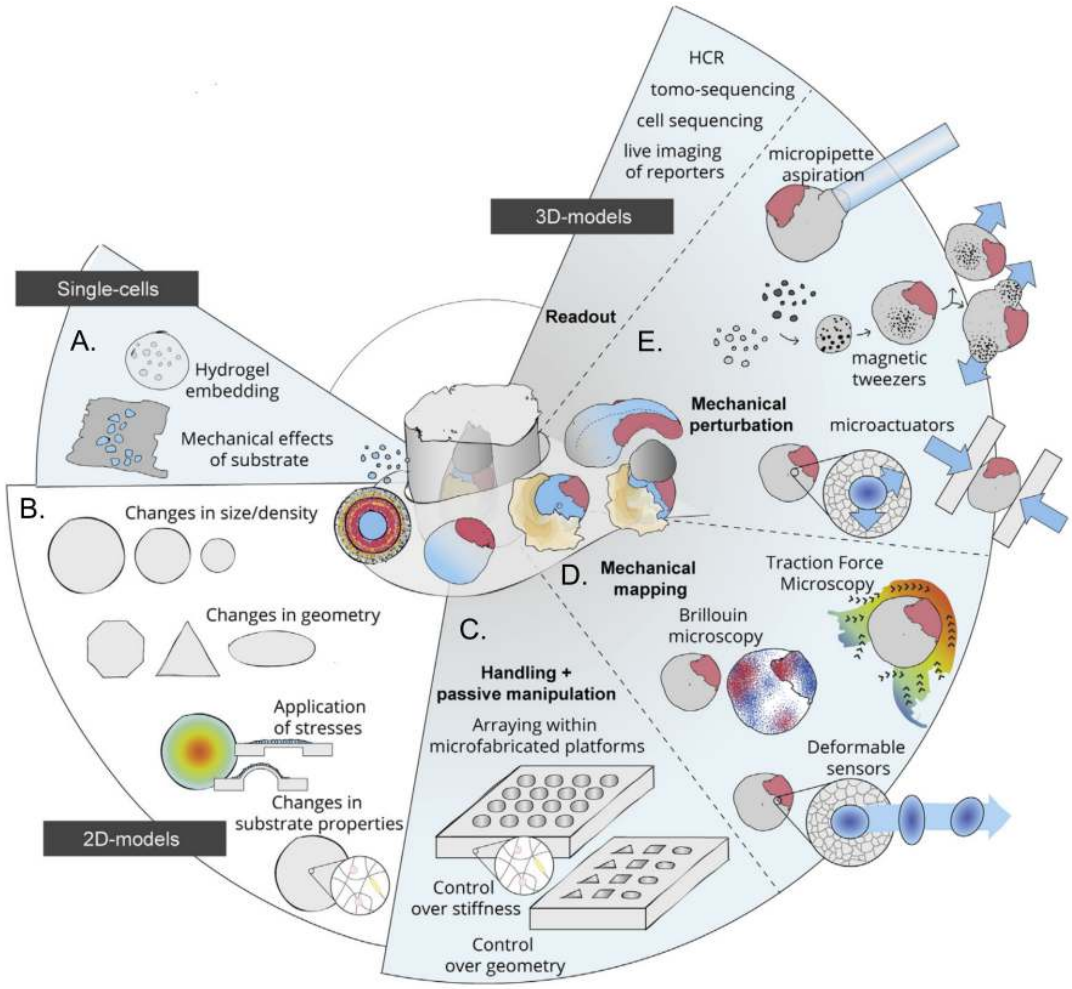

Figure 2.3: **Mechanobiological strategies for studying morphogenesis** (Vianello and Lutolf, 2019)

2.3.3 Mechanical control

Living systems have mechanical control in addition to spatial control, as physical forces emerge from growth, deformation, and remodeling of the extracellular matrix (ECM) and fluid pressure in closed geometries. For example, the intestinal epithelia are stretched during peristaltic movements in the gut and lung alveoli deformations during breathing. Compression can also guide morphogenetic events that involve tissue bending and folding, such as the formation of the optic cup, gut villi, and cortical convolutions in the brain (Okuda *et al.*, 2018, Shyer *et al.*, 2013, Tallinen *et al.*, 2016).

To study tissue behavior under external perturbation, cells and tissues are probed at the

molecular and subcellular scales using techniques such as atomic force microscopy, magnetic beads, optical tweezers, and micropipettes (Bao and Suresh, 2003) (see fig 2.3 E). At a larger scale, various types of stretching devices, tissue rheometers, and force plates can be used (Xi *et al.*, 2018). These experiments reveal that cells exhibit complex viscoelastic behavior at different levels of deformation and different regions of the cytoskeleton (Mofrad, 2009). The response of tissues to stretching can vary depending on the timescale of the stretch and the reorganization of cells within the tissue (Guillot and Lecuit, 2013). Rheological experiments also help to uncover the role of signaling pathways, such as YAP transcription factors, in mechanosensation (Wagh *et al.*, 2021).

The microfluidic system, also known as "cells on a chip," has emerged as a valuable tool for investigating cell behavior under controlled biophysical conditions that mimic in vivo conditions (Ingber, 2018). This system allows for the application of stretch or shear forces, as well as the creation of a controlled microenvironment that mimics the organ-level cues present in the body. For instance, the surface tension at the air-liquid interface in the lungs and the fluid flow through the vasculature, as well as the cyclic mechanical stretch of the tissue-tissue interface due to breathing, can be replicated using this approach (Huh *et al.*, 2010).

In the context of developmental biology, the use of microfluidic systems has allowed for the study of self-organization and embryo functions under controlled physical conditions. The co-culture of iPSC-derived motoneurons and brain microvascular endothelial cells in a microfluidic system has produced the in vivo-like maturation of spinal cord neural tissue, representing a new avenue for exploring the complex interplay between physical and biological factors in development (Samal *et al.*, 2019, Sances *et al.*, 2018).

As mentioned earlier, the tissue-matrix interaction plays a critical role in sensing and rapidly transmitting forces (Serra-Picamal *et al.*, 2012, Sunyer *et al.*, 2016, Tambe *et al.*, 2011). However, in early embryonic epithelia where little or no ECM is present, stresses generated by actomyosin contraction of the cells in one tissue are transmitted over long ranges via intercellular adhesions to other tissues. Thus, studying a simple free-standing epithelial monolayer is very appealing in terms of characterizing the mechanical response to stretch at different time scales.

Only two techniques are available for this: first, Harris and colleagues created a suspended monolayer by culturing a cell monolayer on a collagen matrix on two rods, and later removed the matrix using enzymatic digestion (Harris *et al.*, 2012). Second, epithelial domes, where MDCK cells pump ions to form fluid-filled blisters, have been used (Lever, 1979). Recently, my colleagues, Ernest Latorre and Ariadna Marin-Llaurado, have enhanced control over the curvature, shape, and size of the domes (Latorre *et al.*, 2018, Marín-Llauradó *et al.*, 2022), details on this system in the next chapter. These experiments showed that elasticity measurements of the monolayer were two orders of magnitude larger than those of individual cellular parts, and the monolayer could sustain more than 200% strain before the rupture of cell-cell junctions. The cell cytoskeleton, particularly the actomyosin network and cadherin junctions, actively remodel during stretching, while the keratin network reinforces monolayer integrity at higher

strains (Duque *et al.*, 2023, Latorre *et al.*, 2018). With sustained stretching, the tissue undergoes significant realignment and rearrangement via division (Wyatt *et al.*, 2015). Experiments on tissue devoid of the matrix also revealed epithelial actions such as superelasticity and buckling (Latorre *et al.*, 2018, Wyatt *et al.*, 2020).

2.3.4 3D systems

In vitro experiments with 2D or 2.5D cell systems have improved our understanding of cell mechanics in morphogenesis by allowing us to measure deformations and forces and control environmental conditions that are inaccessible in vivo. However, to gain a deeper understanding of cell mechanics, systems closer to the in vivo environment must be probed.

Cell aggregates are a promising in vitro system for probing cell mechanics, where synthetic matrix and mechanical measurement tools can be used. The response of cell clusters to the matrix, while similar to planar tissues, is more complex and includes sensitivity to matrix stiffness, confinement, and ECM concentration, as well as the ability to undergo 3D shape transformations (see fig 2.3 E). Our lab has demonstrated that cell aggregates perform durotaxis and exhibit wetting behavior dependent on stiffness (Pallarès *et al.*, 2022, Pérez-González *et al.*, 2019). Additionally, cell aggregates in suspension behave like viscous droplets and can be used to measure rheological properties, such as when squeezed between plates or probed with AFM or a micropipette (Xi *et al.*, 2018). The viscoelastic properties of cell aggregates can even be measured by coalescing two aggregates (Oriola *et al.*, 2022).

In recent years, the use of hydrogel systems for the culturing cell aggregates has gained significant attention. Hydrogels, such as polyethylene glycol (PEG), polyacrylamide, collagen, or Matrigel, serve as a supportive environment for cell growth. Naturally extracted hydrogels like Matrigel provide a similar architecture to the native ECM. When embedded into a hydrogel, polarized epithelia tend to form a spherical structure with a hollow lumen, which can be induced to form branching morphogenesis by hepatocyte growth factor (Bryant and Mostov, 2008).

Cell-driven self-assembly in organoids leads to tissue formation that mimics organ features, but achieving reproducibility in shape and composition is often challenging (Hofer and Lutolf, 2021, Nelson *et al.*, 2008). Synthetic hydrogels with control over ligand presentation, crosslinking, and degradability have proven useful for epithelial organoids, allowing for control over cell fate (Gjorevski *et al.*, 2022, 2016).

3D gel-based culture systems with spatiotemporal control over the mechanical properties corresponding to in vivo-like functional structures have also been developed (Torras *et al.*, 2018). Interestingly, recent publications show tissue transformation from planar to complex organ-resembling tissue without fine environmental control. For example, intestinal epithelium mechanically compartmentalizes itself, and 2D stem cells transform into a 3D neural tube (Karzbrun *et al.*, 2021, Pérez-González *et al.*, 2021).

In developing embryos, both embryonic and extraembryonic fluids generate frictional and tensional stresses when flowing, or hydrostatic pressures when confined within spaces (Chan and Hiiragi, 2020, Vianello and Lutolf, 2019). The challenge of measuring these forces

has led to the use of various techniques, including micropipette aspiration. Micropipette experiments, where a needle is inserted into the embryo to control pressure, have revealed that the internal hydrostatic pressure determines the embryonic size and dictates cell fate allocation (Chan *et al.*, 2019) (see fig 2.3 E). As a fluid-filled structure, the hydrostatic pressure inside the embryo corresponds to tension in its surfaces, and changes in luminal volumes are sensed by cells through increased cortical tension, inducing changes in cell shape and cytoskeleton organization (Chan *et al.*, 2019, Choudhury *et al.*, 2022). Micropipette aspiration has also been effective in measuring the surface tension of individual cells or whole blastomeres (Dumortier *et al.*, 2019), thus providing insight into the role of the actin cortex in regulating preimplantation embryonic contractility (Firmin *et al.*, 2022, Özgüç *et al.*, 2022).

The measurement of forces within embryos has also been approached through the insertion of deformable probes, such as hydrogels, oil, or magnetic droplets (Campàs *et al.*, 2014, Dolega *et al.*, 2017, Serwane *et al.*, 2017). The shape changes of these probes allow for measurement of local forces and osmotic pressures (Mongera *et al.*, 2023).

In addition to embryos, explant systems have been utilized to study organogenesis in the brain, gut, and lungs. Lung explant research has been particularly useful in understanding different aspects of shape formation, which occurs under the influence of pressure and growth factors. The explant system allows for direct control over the chemical and mechanical environment at specific stages of development. Work with mouse airway epithelium has shown that pressure and matrix stiffness impact the number of lung branches (Nelson *et al.*, 2017, Palmer *et al.*, 2021, Varner *et al.*, 2015).

Other tools such as optical tweezers, laser ablation, and optogenetic excitations have been used at different levels to probe the mechanics of development (Gómez-González *et al.*, 2020, Lecuit *et al.*, 2011). However, independent control over multiple factors remains difficult and force measurement remains indirect.

In conclusion, epithelial tissues are highly sensitive to various biophysical forces and constantly undergo remodeling at different scales and timeframes. There are multiple techniques available to manipulate and study these tissues, from single cells to embryos, with controlled forces and deformation. Due to its dynamic behavior, epithelial tissue can be considered an active material. The focus of this thesis is to develop a system that can control and measure physical forces to understand epithelial behavior as an active material. In the following chapter, we will delve into the molecular machinery responsible for driving these active tissues.

Chapter 3

Active tissue mechanics

3.1 Force generation with actin

In the field of morphogenesis, cells are central to the formation of specific structures through changes in their shape. Early embryologists posited the existence of a mysterious external vital force that guides the morphogenesis of individual cells in tissues (Thompson, 1979). However, as research progressed, particularly experiments by Wilhelm His and Wilhelm Roux, it became clear that the physical forces generated within the cell itself (Clarke and Martin, 2021). In the present day, we now understand, what was unknowable in the 19th century, that the machinery responsible for generating these physical forces is the actin cytoskeleton.

Specifically, the actomyosin cortex forms a mesh containing actin filaments and myosin motors just beneath the plasma membrane of a cell (Alberts, 2015). This mesh is organized into various higher-order arrays capable of dynamic remodeling, giving rise to the complex shapes and structures we observe in the world around us. We can understand the actomyosin cortex step by step, starting from its basic organization of single actin filaments to higher-order supracellular actomyosin cables.

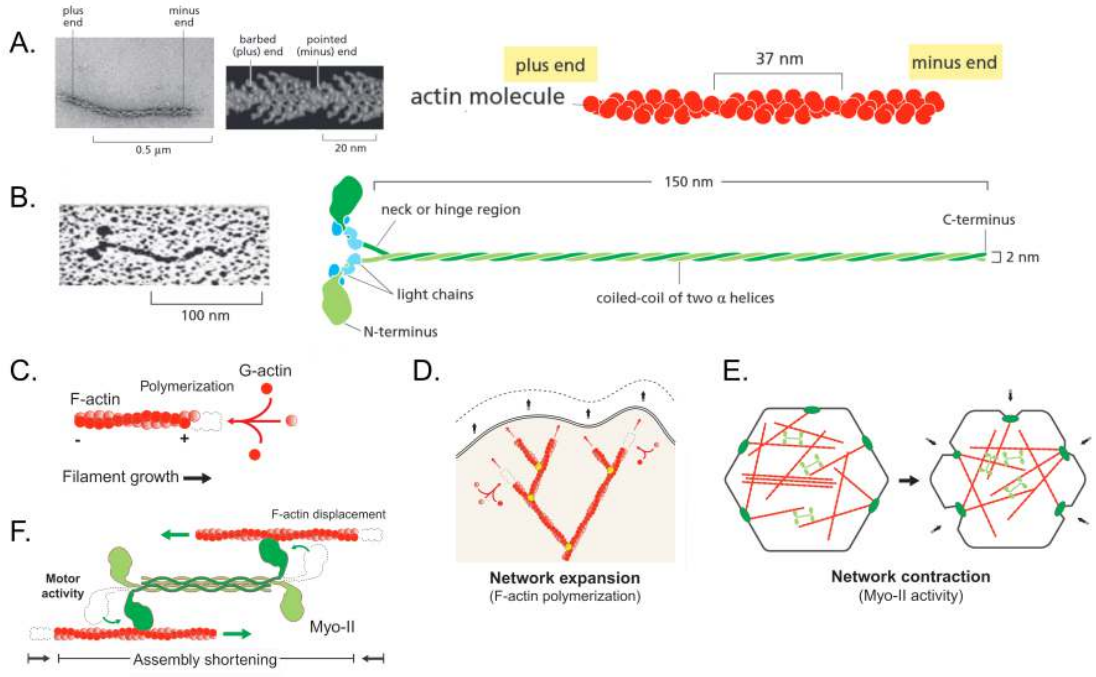

Figure 3.1: **Actin and Myosin**: (A) Electron micrograph of Actin filament with zoomed in images of barbed and pointed end. (B) Same for Myosin II minifilament with clearly visible two globular heads and a long tail. (C-D) Actin network can apply pushing force through polymerization of single filaments or network expansion. (E,F) While myosin activity would lead to contraction of the networks. *Adapted from A-B (Alberts, 2015) and C-F (Clarke and Martin, 2021)*

3.1.1 Actin filaments

The actin filaments are helical polymers composed of G-actin proteins (see fig 3.1 A). The asymmetrical nature of these proteins leads to the development of two distinct ends, referred to as the barbed and pointed ends, that can be differentiated based on their appearance in electron micrographs. The actin filaments are known for their dynamic assembly and disassembly processes, where the distinct ends have different rates of kinetics. This results in growth in the direction of the barbed end, with the length of the filament can be maintained by a constant flux of subunits from the pool of monomers in the cell and nucleotide hydrolysis. This process is referred to as *treadmilling* (see fig 3.2 A). However, if one end of the filament is capped, it will continue to grow and apply a pushing force in the outward direction.

3.1.2 Actin networks

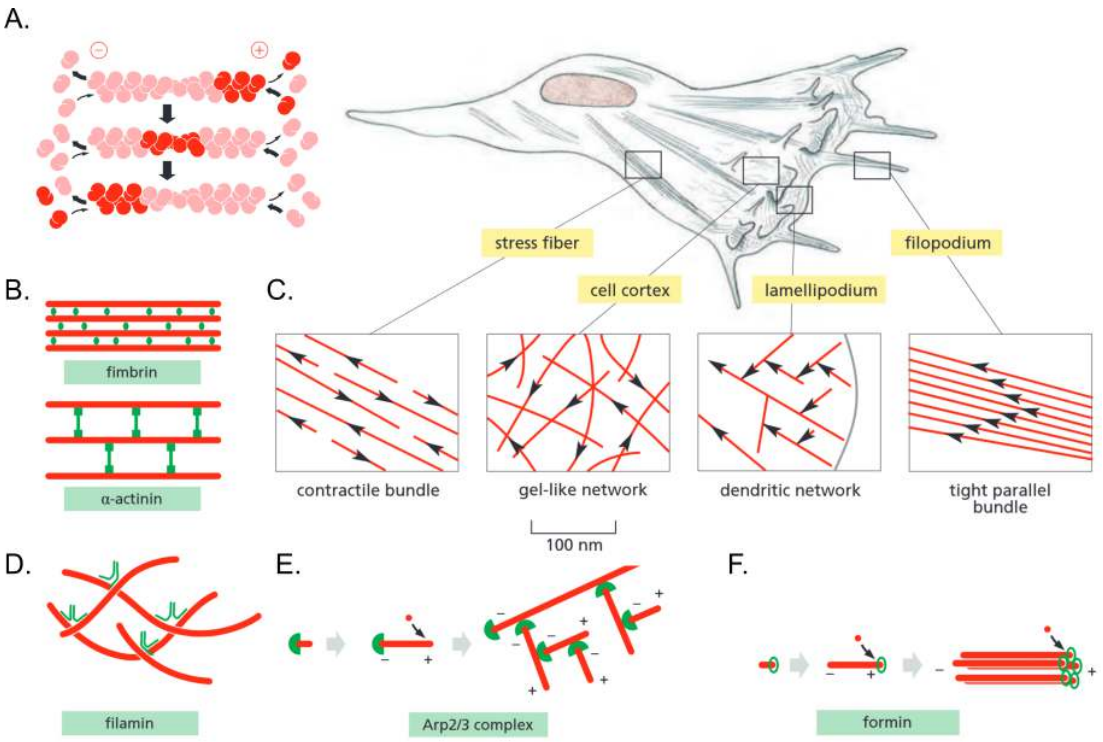

Figure 3.2: **Forms of actin networks**: (A) Actin treadmilling: where highlighted actins move from positive end to negative end as the filament polymerizes and depolymerizes from both ends. (C) In an adherent cells, there are many different kinds of actin structures from contractile network to gel-like cortex. (B,D,E,F) Actin structures can be thought as meshwork of actin filaments (red) with crosslinkers(green). Different crosslinkers produce distinct form of actin network. *Adapted from (Alberts, 2015)*

Actin filaments can also form branched networks, facilitated by the presence of nucleation sites on the filament and proteins containing actin-binding motifs. The actin nucleation can be catalyzed by two primary factors, the ARP 2/3 complex or formins. The ARP 2/3 complex creates a pointed end in the center of a filament, leading to the formation of a new branch from that site. This results in the formation of a tree-like network of branches, capable of generating sufficient pushing forces to move a part of the cell membrane (see fig 3.2 E,F). The formins, in conjunction with profilin, aid in the growth of the filaments, with profilin serving as a staging area for the rapid addition of monomers to the filament. These structures can take the form of dendritic actin networks that enable membrane protrusion at lamellipodia or spike-like projections of the plasma membrane that allow a cell to explore its environment (see fig 3.2 C). The pushing forces generated at the molecular level are of the order of 1 piconewton.

3.1.3 Actin cortex

The actin filaments can also form tight or loose bundles, facilitated by crosslinking proteins. Fimbrins enable multiple actin filaments to arrange in parallel, resulting in closely packed bundles that exclude myosin from connecting to the filaments. On the other hand, α-actinin crosslinks actin filaments with opposite polarity into a loose bundle, allowing myosin to bind and create contractile bundles (see fig 3.2 B). Myosin II oligomerizes into a bipolar short filament that can connect multiple actin filaments and move across them, resulting in a pulling effect (see fig 3.1 B). This movement is driven by ATP hydrolysis making contracting an active process. The loose bundle forms the gel-like network in the cell cortex. Other actin crosslinking proteins can result in different structures. Filamin creates a loose and viscous gel that is essential for migration, while spectrin creates a strong and flexible web-like network of short actin filaments that allows cells to reversibly deform (see fig 3.2 D). The actomyosin bundles in the cortex can generate two orders of magnitude more force than a single filament (Clarke and Martin, 2021).

3.2 Actin structures at a larger scale

During epithelial morphogenesis, individual cells can undergo shape changes by modifying their contractility or actin turnover, resulting in the development of tissue curvature. As mentioned previously, epithelial cells exhibit apicobasal polarity, which results in a non-uniform distribution of the actin cytoskeleton that influences cell shape and tissue architecture.

The geometry of columnar or wedge-like cells in a monolayer determines the specific ways in which they can be organized (Gómez-Gálvez *et al.*, 2021). Columnar cells, when arranged together, produce a flat tissue, while wedge-shaped cells with a narrow top result in convex curvature (see fig 3.4 A). Conversely, concave curvature with a narrow bottom can also be created. By observing the actin cytoskeleton, we can determine the specific mechanisms of tissue shaping (see fig 3.4 B). For example, apical constriction with concentrated actin cortex on the apical surface is involved in multiple convexly curved tissues, such as the invagination of the intestinal crypt, the Drosophila mesoderm, and the vertebrate lens placode (Houssin *et al.*, 2020, Lecuit *et al.*, 2011, Pérez-González *et al.*, 2021).

On the other hand, basal constriction results in opposite curvature, as observed in the optic cup and mid-hind brain fold of zebrafish (Gutzman *et al.*, 2018, Sidhaye and Norden, 2017). However, convex curvature can also be produced through basal expansion, as seen in the Drosophila wing disc (see fig 3.4 A). Certain parts of the wing disc can locally relax the basal side without affecting the apical side, leading to basal expansion (Sui *et al.*, 2018). In addition to the apical and basal surfaces, lateral surfaces can also contract or expand due to myosin II activity, which can cause tissue folding in the wing and leg discs of Drosophila (Monier *et al.*, 2015, Sui *et al.*, 2018). Furthermore, cell-cell rearrangements can be produced by altering junction lengths during germ band extension (Collinet *et al.*, 2015, Yu and Fernandez-Gonzalez,

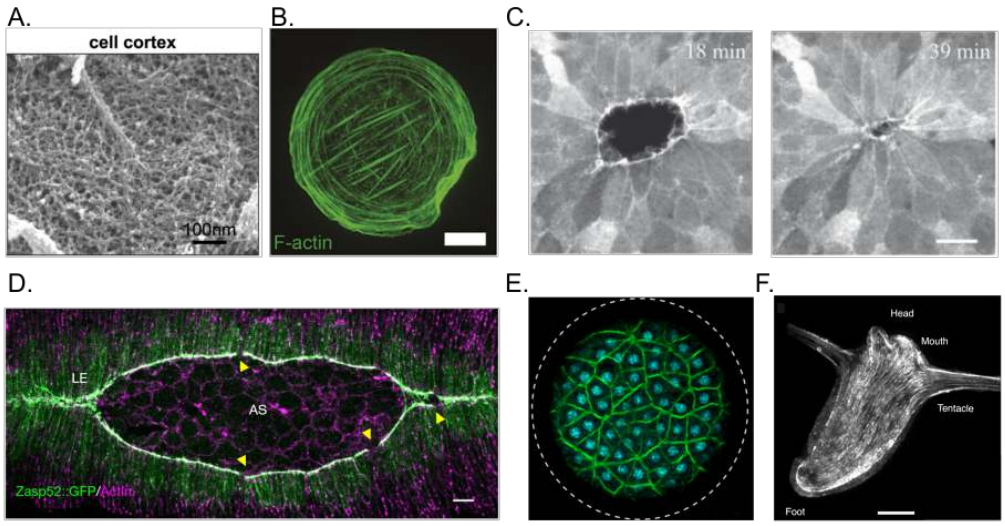

Figure 3.3: **Actin organization at different scales**:(A) Electron micrograph of actin cortex of mitotic Hela cells (Kelkar *et al.*, 2020). (B) Different forms of actin organization in circular fibroblast cell (Jalal *et al.*, 2019) Scale= 10μm. (C) Supracellular actin ring during wound closure (Brugués *et al.*, 2014) Scale= 20μm. (D) Dorsal closure of amnioserosa with actin network (Ducuing and Vincent, 2016) Scale= 10μm. (E) Supra-cellular organization of actin for cellularization of coenocyte. Circle is 60μm (Dudin *et al.*, 2019). (F) Hydra with actin network, whose nematic defects determines morphogenesis (Maroudas-Sacks *et al.*, 2021) Scale= 100μm.

2016) (see fig 3.4 C).

Not only do individual cells undergo coordinated actin reorganization during epithelial morphogenesis, but supracellular actin structures can also emerge at the tissue level (see fig 3.3 A-C). Junctional actomyosin organizes to form bundles connected across multiple cells, allowing for important functions such as wound healing and morphogenesis (Brugués *et al.*, 2014, Clarke and Martin, 2021) (see fig 3.4 D-F). These supracellular networks can exert forces at the scale of the embryo, as observed in cases such as dorsal closure and parasegment boundary formation in Drosophila and epiboly in zebrafish (Calzolari *et al.*, 2014, Ducuing and Vincent, 2016). Additionally, these networks can alter the material properties of specific regions in the embryo, making them more prone to deformation and thus aiding in the formation of folds or invaginations (see fig 3.4 G).

During Drosophila gastrulation, tissue-level actin cortex is altered in the direction of the anterior-posterior axis, providing increased bending strength in that direction. This supports the internalization of the mesoderm by promoting folding in a perpendicular direction (Yevick *et al.*, 2019). Interestingly, highly organized actin bundles are also found in even larger systems such as Hydra, vertebrate smooth muscle, and the heart (Cetera *et al.*, 2014, Helm *et al.*, 2005, Maroudas-Sacks *et al.*, 2021, Palmer *et al.*, 2021) (see fig 3.3 D-F). These bundles assist in generating mechanical force patterns that create coordinated tissue movements at a global

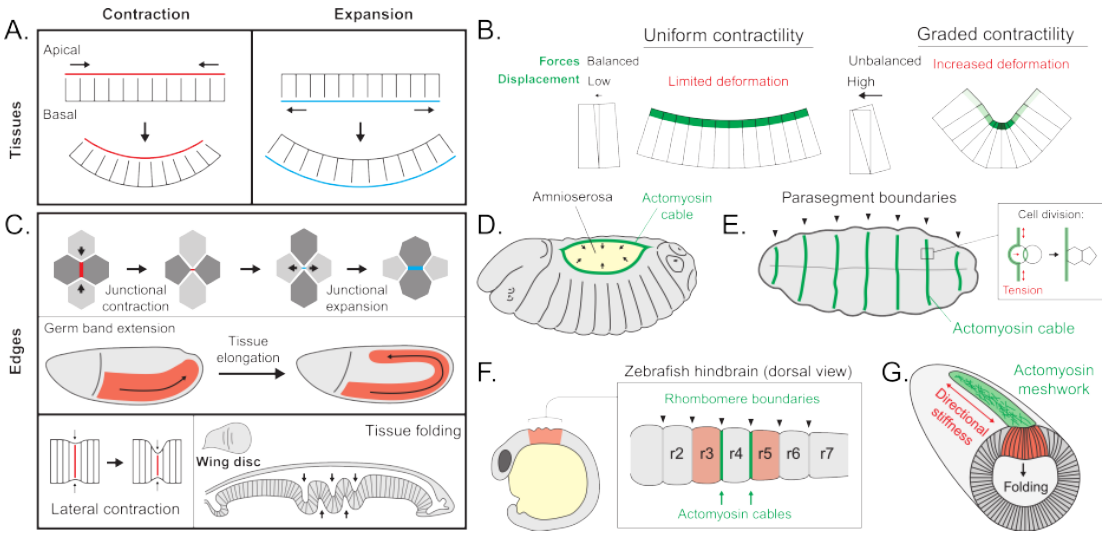

Figure 3.4: **Morphogenesis driven by actin at tissue scale**: (A) Apical contraction or basal relaxation both results in the same curvature. (B) However, amount of deformation will depend on the contractility gradient. (C) Lateral surface of cells can also undergo expansion or contraction leading to cell rearrangements or tissue folding. (D-G) Supracellular actin cables plays vital role in creating boundaries or causing large scale deformations. *Adapted from (Clarke and Martin, 2021)*

scale.

3.3 Timescales of the actin cytoskeleton

Morphogenesis, the process of shaping and forming living structures, occurs at varying time scales and requires the cell cytoskeleton to change its shape accordingly. Rheological and mechanobiological experiments have given us insights into how cells respond to forces and deformations based on their magnitude and rate (see fig 3.5 A; reviewed in (Wyatt *et al.*, 2016)).

For fast deformations (in the range of milliseconds to seconds), cells exhibit elastic behavior, as there is insufficient time for the actin cortex to respond or remodel. The cytoskeleton can store elastic energy and release it. At this scale, there is also flow of cytosol through the cortical mesh, resulting in poroelastic behavior.

When forces or deformations are applied over longer timescales (seconds to minutes), cells exhibit viscoelastic behavior. The actin cortex can flow and is unable to fully store energy. The actin filaments and crosslinkers, such as myosins and actinin, allow the cytoskeleton to remodel in response to mechanical perturbations through turnover in tens of seconds or a few seconds, respectively. Myosin mini filaments, however, can take longer to remodel, up to hundreds of seconds.

At even longer timescales (minutes to hours), cells or tissues may respond through oriented division or rearrangement, allowing them to adapt to persistent forces such as gravity or

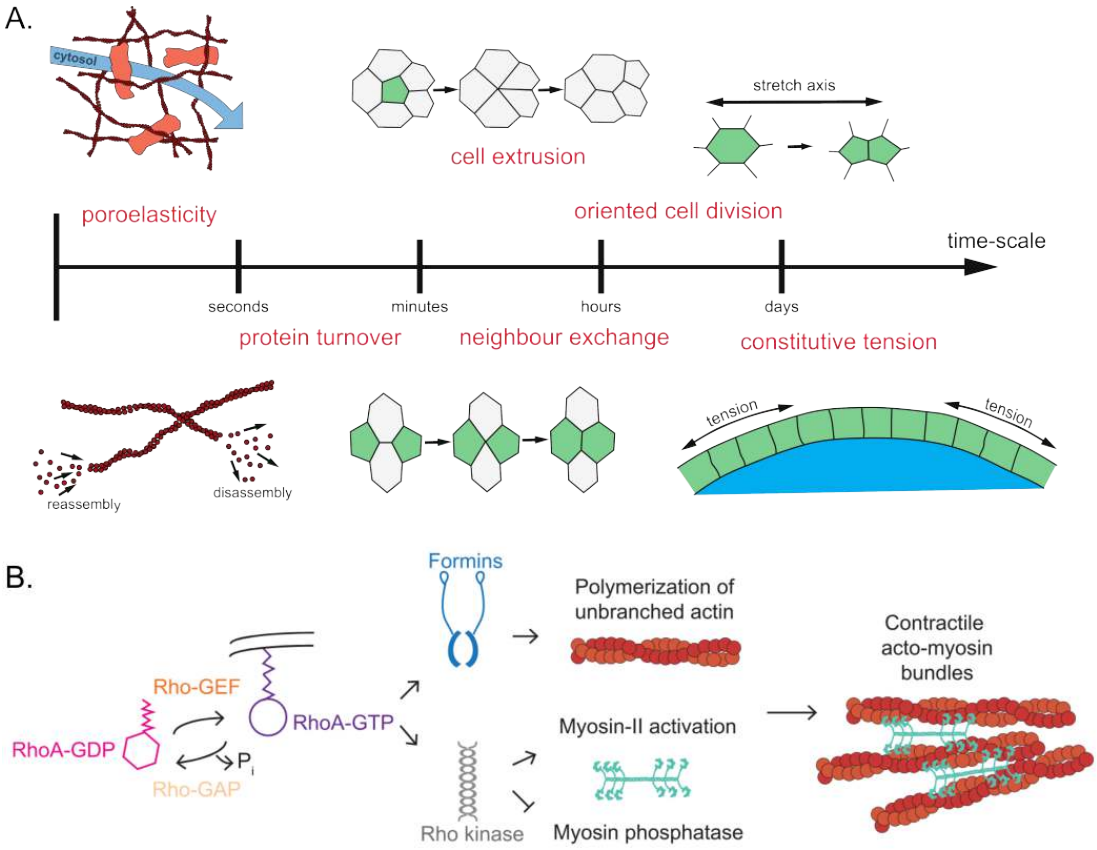

Figure 3.5: **Molecular pathway and timescale of actin network related processes**: (A) Timescales of different actin driven cellular processes, ranging from cytoskeletal fluid deformation to large-scale tissue deformations (Wyatt *et al.*, 2016). (B) Molecular signaling of RhoGTPase. RhoGEFs return GDP for GTP to activate RhoA. In turn RhoA results in actomyosin contractility (Kelkar *et al.*, 2020).

surface tension. Tissues may resemble a viscous fluid and morph into a sphere, such as a blastocyst. Interactions with the extracellular matrix over hours can lead to adjustments in the constitutive tension of tissues based on biophysical and biochemical forces.

3.4 Controlling cortical tension

The magnitude of contractile or tensile forces exerted by cells is greatly influenced by the tissue type and its environment. The signaling pathways regulating the crosslinkers and nucleators of actin bundles are responsive to both external biochemical and biomechanical stimuli (see fig 3.5 B; reviewed by (Kelkar *et al.*, 2020)). The actomyosin bundles, made up of dynamic actin filaments, constantly undergo cycles of contraction, polymerization, and depolymerization, which maintain a homeostatic level of cortical tension in healthy tissues. As a result of the numerous components involved in the actin network, cortical tension can

be readily modulated by pharmacological interventions targeting specific molecular targets (Cartagena-Rivera *et al.*, 2016).

For example, the use of Latrunculin, which binds to actin monomers, can result in the depolymerization of the actin network and reduce contractility. Similarly, inhibiting myosin activity with Blebbistatin leads to a decrease in cortical tension due to its hindrance of myosin II ATPase activity. Conversely, Calyculin-A enhances contractility by accelerating the rate of Myosin II phosphorylation. The stability of the actin network can also be impacted by sequestering ARP 2/3 monomers with CK666, which increases cortical tension. Other factors, such as Rho-GTPases and calcium levels, located further along the signaling pathway, can also affect network stability (Valon *et al.*, 2017).

Optogenetic tools offer a more refined and localized means of controlling contractility. For instance, tools based on the regulation of RhoA can be used to locally regulate cell protrusion, tissue tension, and traction (Valon *et al.*, 2017). A recently developed tool controlling Shroom3 provides even finer control over apical constriction and can be used to recreate tissue folding (Martínez-Ara *et al.*, 2022).

3.5 Modeling active tissue dynamics

The advancement of molecular biology and tissue dynamics has increased our understanding of morphogenesis. However, it is becoming increasingly crucial to interpret biological experiments through theoretical models in order to generate new hypotheses and validate them through further experimentation.

Mathematical models at multiple scales are used to describe both physics and biology. At larger tissue scales, hyperelastic continuum material models could be utilized to describe the behavior of the cardiovascular system (Holzapfel *et al.*, 2019). On smaller scales, agent-based models are used to explain epithelial tissue behavior in terms of cell sorting and reorganization (Voss-Böhme, 2012). This section aims to provide the reader with a brief overview of the relevant modeling approaches in this field.

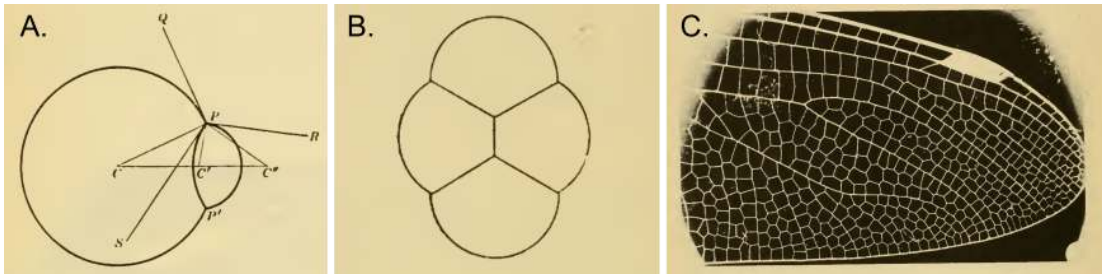

Figure 3.6: **D'Arcy Thompson's forms of tissues:** (A-B) Thompson equates cell aggregates to coalescence of bubbles like in a froth. (C) A dragon fly wing is a clear example of this organization.

3.5.1 Vertex models

D'Arcy Thompson, in his chapter on "The Forms of Tissues," presents an intuitive argument regarding the role of surface tension or capillarity in organizing cells into a tissue (Graner and Riveline, 2017, Thompson, 1979). He observed this phenomenon in a wide range of biological systems, from two connected cells to the organization of cells in a dragonfly wing, which resemble the associations of soap bubbles or foams (see fig 3.6). [1] In the case of monolayered epithelial tissue, its polygonal cellular pattern on its surface enables the easy description and tracking of cell motion and shape change through the use of vertices and edges. Vertex models have proven to be valuable in understanding the complex interactions between cellular shape, the forces generated within epithelial cells, and the mechanical constraints imposed on the tissue from external sources (as reviewed in (Alt *et al.*, 2017)). These models can be two-dimensional or three-dimensional, depending on the system being modeled, but cells are consistently defined as having both an apical and basal surface, as well as lateral interfaces between neighbors. Further complexities have been added to describe specific systems, such as intercalations in three-dimensional epithelia, through the use of a geometric shape known as the Scutoid (reviewed in (Gómez-Gálvez *et al.*, 2021)).

Figure 3.7: **Vertex model for cells in a monolayer** (Gómez-González *et al.*, 2020).

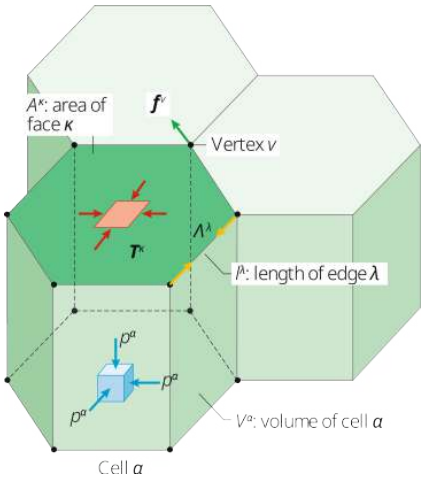

To determine the motion of the vertex, mechanics must be specified. It is often done using the virtual work function (W). There are two components: internal and external.

$$\delta W = \delta W_i + \delta W_e$$

The changes in internal virtual work, δW_i, can result from changes in the cell volumes, in the areas of surfaces, or in the lengths of bonds. By defining the cell pressure, the surface tension, and the line tensions, the differential of the internal virtual work for vertex movements can be written.

$$\delta W_i = \Sigma_{cell\ \alpha}\left(-P^\alpha \delta V^\alpha\right) + \Sigma_{surface\ k}\left(T^k \delta A^k\right) + \Sigma_{edge\ \lambda}\left(\Lambda^\lambda \delta l^\lambda\right) - \Sigma_{vertex\ v}\left(f_i^v \delta x^v\right)$$

Similarly, the external virtual work, δW_e, can be written according to the external forces that come from external mechanical forces applied to the tissue through the matrix, or fluid

[1] "we recognize the appearance of a "froth," precisely resembling that which we can construct by imprisoning a mass of soap-bubbles in a narrow vessel with flat sides of glass; in both cases we see the cell-walls everywhere meeting, by threes, at angles of 120 deg, irrespective of the size of the individual cells: whose relative size, on the other hand, determines the curvature of the partition-walls", writes Thompson

pressure acting on apical or basal cell surfaces.

The state of a monolayer is determined by minimizing the virtual work function, taking into account the molecular complexities that contribute to surface tension and line tensions. In the context of epithelial layers, the actin cortex significantly impacts the tensions along the edges. Vertex model simulations in 2D models demonstrate the important role of interfacial tensions in shaping cell orientation, coordinating collective migration, and facilitating tissue rearrangement through cell division.

In contrast, 3D or 2.5D models capture the physics of various morphogenetic processes, such as the formation of appendages on the drosophila eggshell and the mechanical compartmentalization of intestinal epithelia (Osterfield *et al.*, 2017, Pérez-González *et al.*, 2021). These models offer unique insights into cell packing and the transition between jamming and unjamming (Park *et al.*, 2015, Tang *et al.*, 2022). In some cases, phase transitions from a solid to fluid state result from localized proliferation and oriented divisions, showing that the epithelial tissue behaves as an active material with viscoelastic properties (reviewed in (Lenne and Trivedi, 2022)).

3.5.2 Continuum models

The viscoelastic properties of tissues are captured in vertex models, which are useful for smaller-scale. However, for larger-scale deformations or flows, we can model tissues as a continuous material. There are two tactics for thinking about these models: one focuses on the rheological properties of the tissue, and the other on shape transformations. By thinking of a continuous sheet of cells as an active surface, we can capture the physics of single cells to embryos (Khoromskaia and Salbreux, 2023, Salbreux and Jülicher, 2017).

Continuum models focus on developing reliable constitutive relations and solving initial-boundary-value problems. Constitutive relations describe how materials respond to applied loads, and they depend on the internal constitution of the material. Determining constitutive relations for epithelial monolayers can be challenging because these tissues are much more complex than simple metals or passive polymers (see fig 3.8 A-B). However, their complex material behavior can be understood by characterizing their mechanical response using standard material testing techniques (Humphrey, 2002). Typically, they can be probed mechanically in a biologically relevant manner, such as through biaxial or uniaxial stretching experiments that simulate in vivo tissue behavior (Humphrey *et al.*, 2014). These experiments with epithelial tissues have revealed the viscoelastic nature of these materials (Harris *et al.*, 2012, Khalilgharibi *et al.*, 2019).

Solids, such as rubber, are considered to have elastic properties, allowing them to deform reversibly when subjected to a force. Conversely, fluids are characterized by their viscosity, meaning they flow in response to an applied force. Viscoelastic materials exhibit both solid-like and fluid-like behaviors (see fig 3.8 C). Simple models can represent these behaviors by combining elastic components, represented as springs, and viscous components, represented

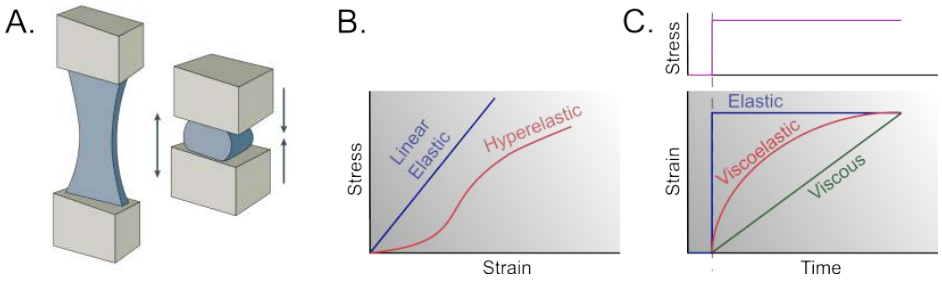

Figure 3.8: **Stress strain behavior of materials**: (A) materials being stretched or compressed. (B) Quasistatic deformations yield stress-strain curves. (C) Creep test where strain response is characterized at constant stress.

as dashpots. The elastic response does not dissipate energy, unlike the viscous response.

$$\sigma = E\epsilon$$

$$\sigma = \eta \frac{d\gamma}{dt}$$

Other material properties like stiffness or Poisson's ratio can be revealed through quasi-static stretching or compression. However, dynamic properties are better understood through frequency sweep, creep, or stress relaxation experiments (Guimarães *et al.*, 2020). Rheological experiments have been extremely valuable in gaining insight into the mechanical response of various biological materials, ranging from reconstituted cytoskeletal proteins to large multicellular aggregates (Cavanaugh *et al.*, 2020, Mofrad, 2009, Xi *et al.*, 2018).

Rheological properties are often linked to physiological state and are crucial for their specific functions (Park *et al.*, 2015, Vedula *et al.*, 2012). For example, heart failure can be caused by a loss of contractility in heart muscle cells, as observed during mechanical remodeling (Humphrey, 2002). Therefore, it is important to assess rheological properties in different microenvironments. Mechanical information such as deformation, deformation rates or velocity fields, traction forces exerted by cells on substrates, and intercellular mechanical stress can provide a more complete picture of tissue rheology when combined with information about cellular architecture obtained through imaging (Roca-Cusachs *et al.*, 2017). These types of experiments shed light on the complex mechanisms of strain stiffening and viscoelastic behavior at different deformation regimes involving various parts of the cytoskeleton.

However, in certain cases like modeling cardiovascular mechanics or the growth of organs, we can rely on hyperelasticity or composite material framework. The basic kinematics assumes a mapping, $x = \chi(X, t)$, deformation from reference to deformed configuration. The deformation gradient and Green's strain tensor are defined.

$$F = \nabla_X(\chi(X, t))); \quad E = \frac{(F^T F - I)}{2}$$

The elastic and growth can be delineated in the deformation gradient through decomposition.

$$F = F_e F_g$$

Here, in the theoretical framework of finite elasticity, one can assume a strain energy function relates to stress. The stress-strain data extracted from the experiment allows for predicting the form of the strain energy function.

$$S = \frac{\delta W}{\delta E}$$

The utilization of hyperelastic models has proven to be effective in capturing the material response in various biological tissues, such as the bladder, heart tissue, skin, and arteries (Holzapfel, 2000). This type of formulation provides a degree of flexibility, as it allows for the inclusion of additional physical constraints, such as the anisotropy of the tissue microstructure or its incompressibility.

Drawing inspiration from composite materials, the utilization of transversely isotropic material models has proven to be instrumental in comprehending the mechanisms behind myocardium infarction and different types of aneurysms (Holzapfel *et al.*, 2019). Minor modifications to these constitutive relations can be used to capture the material response, such as explaining the phenomenon of strain stiffening, or accounting for the inhomogeneity in the material, such as the collagen content and crosslinking in the tissue.

These models are also employed in the understanding of growth and remodeling, through the use of kinematical growth theory (Ambrosi *et al.*, 2019). This theory highlights the existence of residual stresses in growing tissues, which allow for compatible elastic and inelastic growth-induced deformations, leading to a modification of the tissue properties into a spatially inhomogeneous and anisotropic state. This process is of great significance in the field of solid tumor growth mechanobiology, as the residual stresses directly impact tumor aggressiveness, nutrient pathways, necrosis, and angiogenesis.

3.5.3 Active surface models

At the cellular level, the mechanical properties of tissues are largely determined by the biopolymeric cytoskeleton, which consists of filaments and cross-linkers and molecular motors. These components continuously convert energy, ATP to ADP, through contractions or extensions of the network, resulting in a physical gel-like system due to its cross-linked actin filament network. However, the presence of phenomena such as treadmilling, active polymerization-depolymerization of filaments, and the mobility of molecular motors, such as myosin, makes the tissue system an active gel that lacks time-reversal symmetry due to its continuous energy transduction.

Additionally, the filaments are polar, which allows for the acquisition of orientational order. This has led to the modeling of tissues as active gels, similar to modeling active systems, such

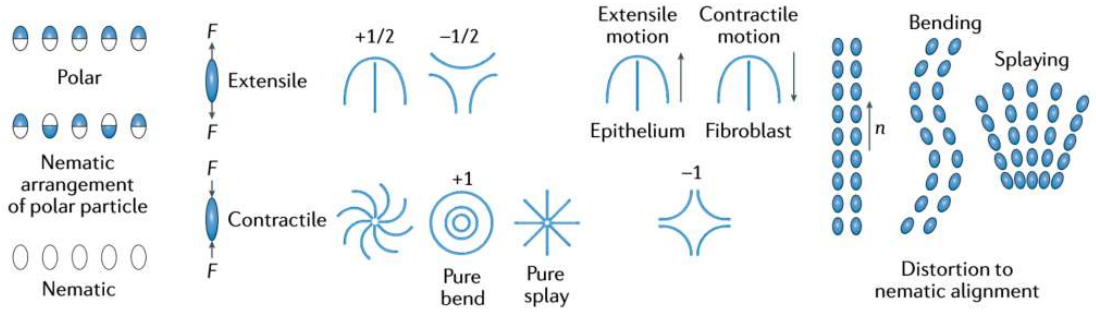

Figure 3.9: **Active nematics**: (Xi *et al.*, 2018)

as flocks of birds and schools of fish, using hydrodynamics of active matter (Jülicher *et al.*, 2018). Active matter systems are a subclass of continuum models used to describe the dynamics of packed active particles, which are based on the liquid crystal theories of soft condensed matter. Like liquid crystals, cells also possess orientation and the ability to move past each other. In this framework, the orientation of filaments in the cytoskeleton or the elongation of cells in the tissue can be characterized by a nematic order parameter matrix (see fig 3.9).

$$Q = \frac{3S}{2}\left(n \otimes n - \frac{I}{3}\right)$$

$$S = [cos2\theta]$$

$$\sigma_{active} = \zeta Q$$

The utilization of this formulation is significant in characterizing the active forces produced by the network. The stress is separated into two components: active and passive. The passive stress arises from the viscoelasticity of the material and the bending, splaying, and twisting of the aligned elements. The active stress, on the other hand, is calculated by combining the strength of activity, represented by the parameter zeta, and the nematic order matrix. The sign of zeta determines the type of force dipole generated; a negative sign results in contraction of the system, while a positive sign leads to expansion along the nematic axis.

The active stress plays a crucial role in the motion of the system and can result in chaotic motion even in low Reynolds number systems, as evidenced in dense bacterial systems of *Bacillus subtilis* where jet flows and turbulent patterns have been observed, as well as in expanding monolayers where independent vortices have been recorded (Blanch-Mercader *et al.*, 2018, Wensink *et al.*, 2012). The nematic equations have proven to be effective in capturing the physics of 2D confined systems and expanding systems (Trepat *et al.*, 2009).

In the context of 3D models, active surfaces are used to describe the actomyosin cortex near cell membranes or epithelium in embryos (Salbreux and Jülicher, 2017). This thin sheet of matter generates internal forces and torques that drive shape changes at the cellular or

tissue level. The resulting three-dimensional structures can be conceptualized as curved, active two-dimensional surfaces. To describe the kinematics of these surfaces, mathematical tools from differential geometry can be applied, using generalized coordinates X, metric tensor g, and curvature tensor C. Forces and torques can be defined in terms of tension (t) and moment (m), where dl is the length of the line element with tangential unit vector v, and the model also considers the mirror and rotation symmetries of the surface elements (see fig 3.10).

Salbreux and Julicher's work has demonstrated that flat active membranes with up-down asymmetry exhibit stability dependent on active tension and active tension-curvature coupling term. This tension-curvature dependency has been observed in the pancreas of mice, where the morphology of epithelial tumors is determined by the interplay of cytoskeletal changes in transformed cells and the existing tubular geometry (Messal *et al.*, 2019). Specifically, small pancreatic ducts produced exophytic growth, whereas large ducts deformed endophytically, consistent with theoretical predictions. Another example shows that curls of high curvature form spontaneously at the free edge of suspended epithelial monolayers, which originate from an enrichment of myosin in the basal domain that generates an active spontaneous curvature (Fouchard *et al.*, 2020). The extent of curling is controlled by the interplay between internal stresses in the monolayer.

Figure 3.10: **Active surface models**: (A) Tissues or cell surfaces can be modeled as surface with stresses and torques along the thickness. (B) Internal and external forces actin on a surface element (Salbreux and Jülicher, 2017)

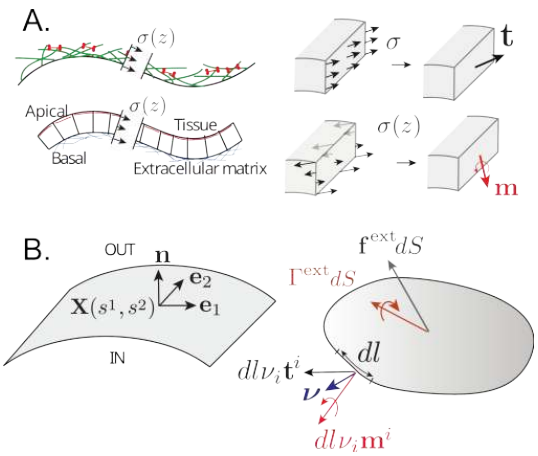

While the molecular level behind epithelial morphogenesis, specifically the actin cytoskeleton, is well understood, there are still gaps in the theoretical and experimental framework that can bridge the gap between molecular dynamics and tissue-scale deformations. Vertex and continuum models have been developed to capture the physics of morphogenesis at the tissue scale, and phenomenological experiments provide insights into the constitutive relations of cytoskeletal components and tissues in specific conditions. However, combining vertex models and active surface mechanics could provide finer control over individual cell surfaces, enabling more precise bottom-up morphogenesis.

Chapter 4

Bottom up morphogenesis

4.1 Learn by building

The mechanics and biology of epithelial tissues are complex, with mechano-chemical signaling and multiscale behavior all intertwined. The lens of active material has been instrumental in illuminating the role of molecular elements in undergoing shape changes during morphogenesis. Mechanistic understanding has been enhanced with new mathematical tools and advanced microscopy, enabling measurement of the forces involved in tissues.

The traditional and successful method for studying mechanics has been to deconstruct the system one component or parameter at a time. By manipulating genes or disrupting cellular processes, we can observe how mechanics change. This perturbative method allows for the alteration of biological systems at various levels, from molecular to tissue, (see fig 4.1) .

However, studying systems like organoids or embryos can only provide limited physical insights into the topological transitions of these structures, as experimental systems have limited physical control and ability to measure forces. An alternative approach is to learn by actively performing morphogenesis or reconstructing biological structures from their basic components.

For years, researchers have broken down biological systems into approachable parts - tissues, cells, proteins - in order to understand the behavior of each component. However, combining existing knowledge of these parts to recreate novel experimental systems could reveal the basic building blocks and effects of scale. This approach would complement top-down approaches in developmental biology. Synthetic biology, a perfect example of reconstruction, seeks to recreate life at various scales, from synthetic proteins to entire cells, in order to gain a deeper understanding of the indispensable components of life.

As active agents exist at every scale, emergent properties can appear at higher scales. Thus, it is essential to focus on higher scales or work with collectives of cells. This reminds me of the example of cars and traffic: Imagine you know the behavior of all individual car components, but this information is not sufficient to understand the behavior of traffic flow. This requires a

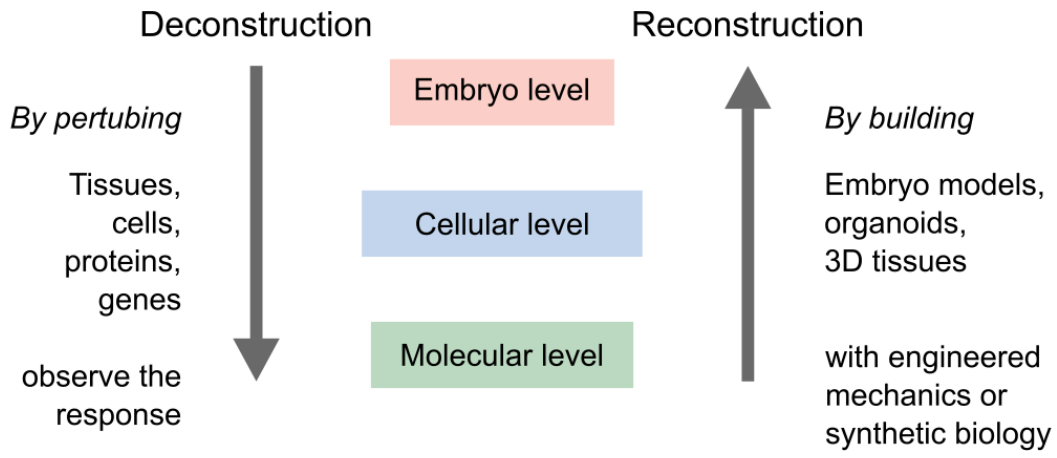

Figure 4.1: **A conceptual representation of two approaches to understanding mechanics: reconstruction (bottom-up) and deconstruction (top-down).** In reality, they are not separate from each other. These methods inform each other, with past top-down research guiding new reconstruction, and new engineered cells or tissues furthering our understanding of the field in innovative directions.

higher level of analysis. [1] Similarly, biological structures exhibit numerous collective behaviors, such as jamming, nematic order, instabilities, or self-organization (Trepat and Sahai, 2018).

Recreating structures from scratch also provides an opportunity to understand the role of physics at different scales. In the spirit of D'Arcy Thompson, we can explore the fundamental properties of matter in biological structures. [2] For instance, we can study the role of surface tension in guiding the shape of cellular aggregates or lumens. In this work, we focus on the mesoscale structures of epithelia ($\sim 10 - 10^4 \mu m$).

We present our efforts to engineer an epithelial structure with a controlled microenvironment that is sensitive to self-organization and mechanical instabilities. The following sections will describe the ways of creating these structures from minimal ingredients.

[1] Matthew Good's commentary provides an insightful perspective on the complexity involved in building cells from interacting molecules. Meanwhile, Xavier Trepat argues that a bottom-up approach does not fully explain the emergent behavior of higher-level structures and emphasizes the need for constructing tissues at the mesoscale. Trepat uses the analogy of traffic jams to illustrate the importance of considering the collective behavior of cells in tissue engineering (Good and Trepat, 2018).

[2]. Thompson writes,'...to seek not for ends but for antecedents is the way of the physicists, who finds causes in what he has learned to recognize as fundamental properties, or inseparable concomitants, or unchanging laws, of matter and of energy." (Thompson, 1979)

4.2 How to build tissue structures?

Before embarking on the construction of an tissue structure, it is important to consider the desired form and function. Despite the diversity in the shapes and functions of tissues, certain elementary shapes can be seen in many cases, resulting from the interplay between physical forces and biochemical signaling. Examples of such shapes include spherical blastocysts, ellipsoidal embryos, or cylindrical vessels.

After considering the desired form and function of the structure, established cell lines are selected and synthetic structures are constructed using various techniques, such as geometry control and localized folding, as discussed in the 2.3 section. The resulting structures can be further studied to understand the interplay between physical forces and biochemical signaling, as well as their potential applications in various biological systems.

4.2.1 Controlling geometry and physical forces

From an engineering perspective, scaffolding is a commonly used approach for constructing synthetic epithelial structures. Scaffolds can be generated through 3D printing or microfabrication techniques, and cells can then be seeded onto the scaffold to attain the desired shape (Torras *et al.*, 2018). This method allows for the creation of a well-controlled microenvironment for the cells in terms of geometry, stiffness, adhesion proteins, and cell culture media (see fig 4.2 A) . Structures generated through this approach can be utilized to investigate tissue behavior in response to forces and curvature.

For instance, cells can be used to form a micro-vessel using a hydrogel with a cylindrical hole (Dessalles *et al.*, 2021). The hydrogel and cells were housed in a microfluidic device that controlled pressure and flow in the vessel, and the authors were able to examine the role of hydrogel poroelastic properties in regulating the dynamics of the vessel. Another exciting study demonstrated the potential of epithelial tissues to form shape-programmable materials by using a collagen scaffold (Mailand *et al.*, 2022).

Scaffolds can also be designed to dynamically change their shape (see fig 4.2 B). For example, a cell monolayer on a flexible membrane can alter its curvature (Blonski *et al.*, 2021), and a combination of stretching and unstretching a cell-laden hydrogel can produce distinctive folds and patterns (Chan *et al.*, 2018). In some cutting-edge studies, researchers have utilized 4D bioprinting, where 3D printed objects undergo transformation over time (Arif *et al.*, 2022). For instance, a flat hydrogel sheet containing endothelial cells and photo-crosslinking can be transformed into a tube (Zhang *et al.*, 2020).

Additionally, the contractility of fibroblasts and hepatoma cells has been utilized to fold 2D structures into 3D shapes (He *et al.*, 2018) (see fig 4.2 C) . Microplates with an origami folding pattern are created, and the cells apply forces to generate a 3D structure. In other scenarios, cells are allowed to self-organize through the imposition of geometric constraints, which enhances the efficiency of organoid-like systems (Gjorevski *et al.*, 2016). In the case of intestinal organoids, controlling the stiffness of the matrix in specific regions leads to growth

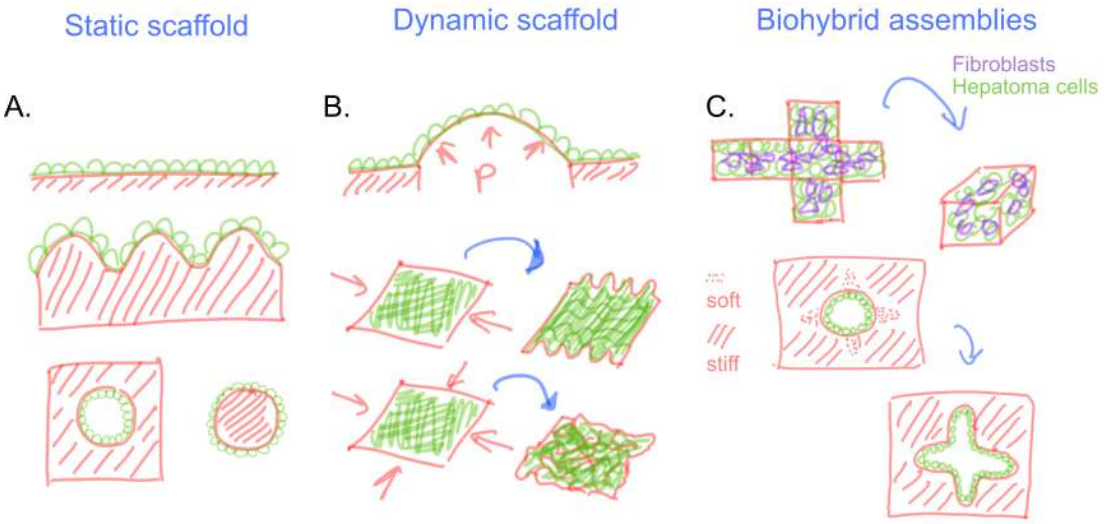

Figure 4.2: **Controlling geometry and physical forces:** The concept of scaffolding can be divided into two categories: static and dynamic scaffolds. (A) Static scaffolds are microfabricated structures that cells can adapt to and respond to geometrical cues, leading to the formation of a specific tissue organization (Brassard *et al.*, 2021). (B) In contrast, dynamic scaffolds consist of cell-laden matrices that are deformable, and their curvature can change dynamically due to external pressure or mechanical forces (Blonski *et al.*, 2021, Chan *et al.*, 2018). (C) Biohybrid assemblies can incorporate active contraction or pushing to create hybrid structures, such as origami folding triggered by fibroblast contraction (He *et al.*, 2018), or cells carving out an intestinal crypt-like geometry from a softer matrix (Gjorevski *et al.*, 2016).

and differentiation at softer areas, producing a highly reproducible structure (Gjorevski *et al.*, 2022).

4.2.2 Manipulating biochemical signaling

Another approach to constructing biological structures involves controlling biochemical signaling to induce shape transformation. This approach utilizes natural processes in embryo morphogenesis, such as apical constriction in ventral furrow formation or cell jamming in the normal elongation of the zebrafish. Optogenetic tools, such as controlling Rho signaling, can be used to induce localized apical constriction with spatiotemporal control (Izquierdo *et al.*, 2018). This technique can also be applied to other proteins, such as Shroom3, to induce synthetic morphogenesis in neural organoids (Martínez-Ara *et al.*, 2022) (see fig 4.3 C).

Epithelial-mesenchymal interaction is another crucial aspect of the tissue folding process. Hughes et al. demonstrated that cell clusters can remodel the matrix to create oriented stresses that lead to budding in tissues (Hughes *et al.*, 2018). By controlling the location and density of these cell clusters, it is possible to manipulate the curvature of the epithelia. Mesenchymal

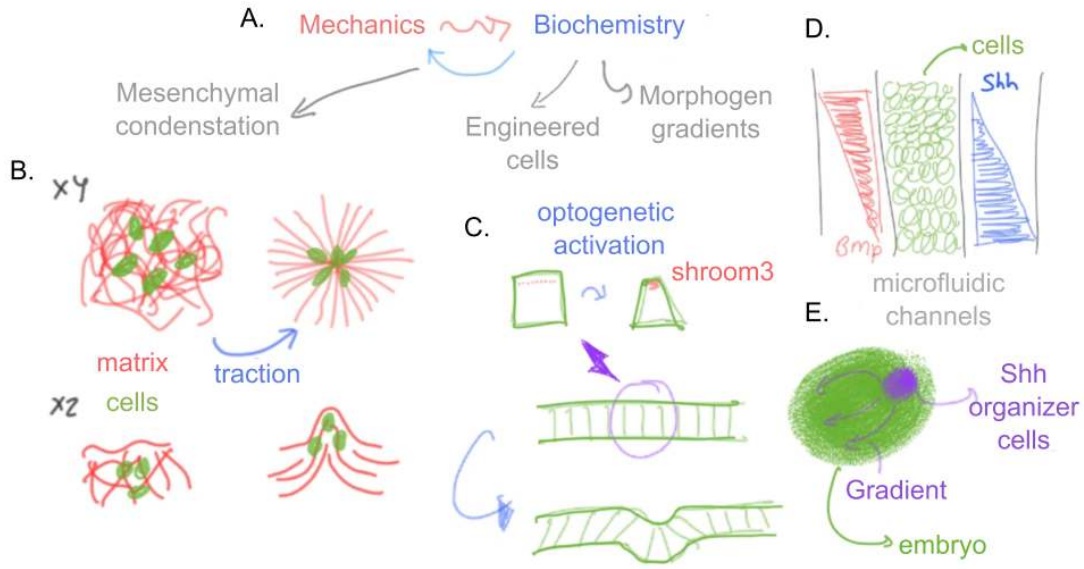

Figure 4.3: **Manipulating biochemical signaling:** Biochemical signaling and mechanics are interdependent in morphogenetic processes (A). The transport of signaling molecules can affect the cytoskeleton and mechanical properties of cells, while mechanical forces can also influence biochemical signaling. Microfluidics (D) is one method used to control biochemical signaling by providing opposing morphogen gradients through multiple channels (Demers *et al.*, 2016). Alternatively, cells can be genetically engineered to undergo apical constriction (C) or produce morphogen gradients (E) locally to form curved geometries (Cederquist *et al.*, 2019, Martínez-Ara *et al.*, 2022). Mesenchyme condensation (B) is another approach used to program curvature in developing tissues (Hughes *et al.*, 2018, Palmquist *et al.*, 2022).

condensation serves as a folding template for the final tissue structure (Palmquist *et al.*, 2022, Shyer *et al.*, 2017) (see fig 4.3 B).

The microenvironment plays a critical role in providing vital signals to tissues and can be manipulated to activate specific cellular functions. Microfluidic techniques can deliver appropriate morphogen gradients to the tissue with precise timing (Hofer and Lutolf, 2021). In vivo, multiple morphogens often act simultaneously. For instance, during neural tube development, there is an opposing gradient of Sonic Hedgehog (SHH) and bone morphogenic protein (BMP). With microfluidic devices, stable gradients can be generated, even in opposite directions (Demers *et al.*, 2016), thus mimicking symmetry-breaking events and directional neural tube patterning (see fig 4.3 D).

Moreover, genetic engineering of specific cells can be utilized to control signaling. Human pluripotent stem cells (hPSCs) can be programmed to express SHH (Cederquist *et al.*, 2019) (see fig 4.3 E). Mixing these cells with others could result in a polarized organoid and a patterned cerebral organoid.

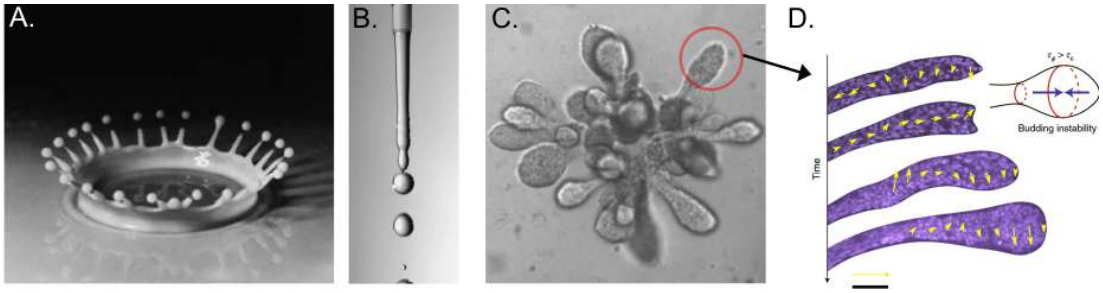

Figure 4.4: **D'Arcy Thompson compares biological budding to splashes** (A) of fluids and Rayleigh-Plateau instability (Thompson, 1979) (B), where liquid splits up into smaller droplets. This mechanism could also be seen in organogenesis of mammary tissue (C, D) (Fernández *et al.*, 2021).

4.2.3 Exploiting mechanical instabilities

Morphogenesis, the process of shaping and formation of biological structures, often involves spontaneous pattern formation or symmetry-breaking events (Ishihara and Tanaka, 2018). These processes are often dictated by mechanical instabilities, which can lead to large deformations in soft matter systems. In material science, these instabilities are typically seen as problematic as they cause rapid breakage. However, in soft matter, large deformations can lead to interesting topological transformations, providing an opportunity for engineers to exploit these instabilities in the development of new actuators or soft robots (reviewed in (Pal *et al.*, 2021)). [3]

The significance of mechanical instabilities was foreseen by D'Arcy Thompson in his comparison of fluid splashes to hydroids (see fig 4.4 A). He wrote that the shapes of a potter's cup, glass blower's bulb, and biological structures are simply glorified splashes formed slowly under conditions of restraint that enhance or reveal their mathematical symmetry (Thompson, 1979). [4] This conjecture has been confirmed through numerous quantitative studies on various systems, including ripples in leaves and wrinkles in the brain (Karzbrun *et al.*, 2018, Liang and Mahadevan, 2009).

There are various instabilities associated with solids and fluids. For example, the Rayleigh-Plateau instability explains why a fluid stream breaks into smaller packets, driven by the fluid's tendency to minimize its surface area due to surface tension. The same instability can arise when fluid is surrounded by an elastic medium, instead of air, provided the surface tensions can overcome the elastic stresses, leading to budding as observed in alveologenesis in

[3] "Mechanical instabilities have provided a unique approach to imbue "material intelligence" into soft machines without requiring the addition of rigid components. For example, binary actuators relying on mechanical instabilities can recreate logic modules and reproduce valving functionality using entirely soft elements.

[4] I cannot recommend enough the chapter "the forms of cell". He states "Many forms are capable of realization under surface-tension, … The subject is a very general one; it is, in its essence, more mathematical than physical; it is part of the mathematics of surfaces, and only comes into relation with surface-tension because this physical phenomenon illustrates and exemplifies, in a concrete way, the simple and symmetrical conditions with which the mathematical theory is capable of dealing."

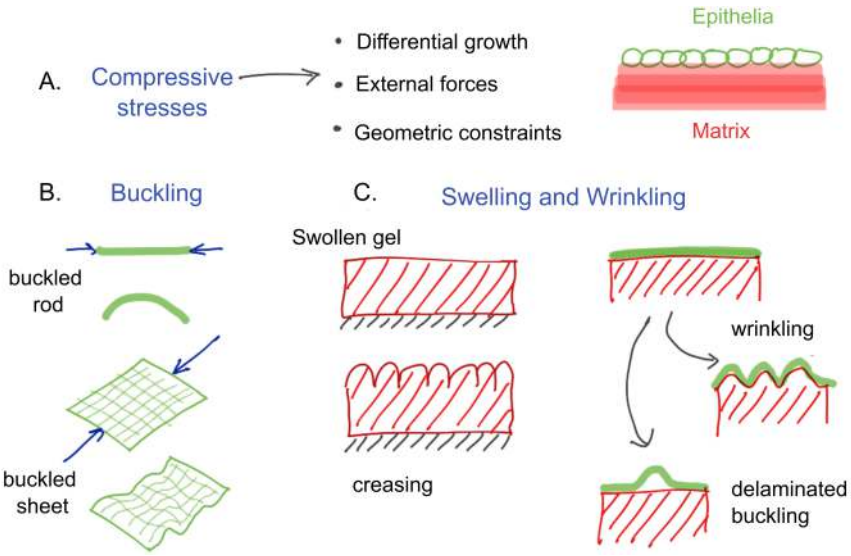

Figure 4.5: **Compressive stresses** occur frequently in many systems (A). We can consider epithelia and matrix as thin sheet supported by a compliant substrate. Thus, the tissue folding could be understood as buckling of sheets (B) or wrinkling or creasing of thin film supported by an hydrogel (C).

human mammary tissue (Fernández *et al.*, 2021) (see fig 4.4 C-D). However, as tissues are active viscoelastic materials surrounded by viscoelastic medium, the timescales of these instabilities change, slowing down to hours instead of milliseconds in water droplets.

There are several types of mechanical instabilities associated with solids and fluids, including Rayleigh-Plateau instability, Kelvin-Helmholtz instability, Rayleigh-Taylor instability, viscous coiling and folding, and large-scale wrinkling and buckling (Gallaire and Brun, 2017, Kourouklis and Nelson, 2018). In this study, we aim to harness these instabilities to recreate epithelial structures.

Applying compressive stresses is one of the easiest ways to induce mechanical instabilities in solids. These stresses can occur in biological systems as a result of differential growth, swelling, or morphogen gradients and can lead to various forms of instabilities, including wrinkling, creasing, and buckling. Buckling occurs when a thin sheet is subjected to in-plane compressive stress, and if the stress is above a critical value, the sheet undergoes out-of-plane deformation instead of in-plane shrinkage (see fig 4.5 B). In contrast, wrinkling and creasing occur in similar compressive stresses, but the thin sheet is typically supported by a compliant substrate.

The creation of biological tissues in vitro has been a subject of great interest in the field of tissue engineering. To reproduce the characteristics of these tissues, researchers have turned to the use of hydrogels. These materials can be mechanically and chemically manipulated to simulate the behavior of biological matrices, which provide support for epithelial structures.

One of the ways in which hydrogels can be used to recreate the behavior of biological tissues is through the application of physical stress. For example, swelling of the hydrogel can cause

it to undergo rapid large volumetric changes, producing crease-like patterns on the surface. If the hydrogel is constrained at the bottom, these creases can become permanent. Alternatively, if the hydrogel is supported by another flexible material, such as another hydrogel or an elastic substrate, the stresses produced during swelling will result in a wrinkling instability (see fig 4.5 A). These instabilities are important for understanding the formation of a variety of structures, including the gyrification of the brain cortex.

In a study by Tallinen et al., the gyrification of the brain cortex was replicated through the programming of materials to produce wrinkling (Tallinen *et al.*, 2016). The researchers created a synthetic brain with an inner core of an inert elastomer and an outer layer of a swellable elastomer. On swelling, the outer layer produced folds that closely matched the process of gyrification (see fig 4.6 A).

Similar mechanisms have been observed in other systems undergoing differential growth, such as the branching of lungs and formation of intestinal villi (Shyer *et al.*, 2013, Varner *et al.*, 2015) (see fig 4.6 B,D). These findings highlight the potential of hydrogels as a tool for understanding the physical mechanisms underlying tissue development. However, it is worth noting that the mechanisms described here are the subject of ongoing research and debate in the field of developmental biology.

The ability to recreate biological tissue growth conditions in vitro has been made possible through the use of hydrogels. Researchers have discovered that by mechanically and chemically controlling the hydrogel, they can generate desired mechanical instabilities (Dervaux and Amar, 2012). This can be accomplished through the swelling or pre-stretching of the gel, or by manually applying compressive stresses.

One way to simulate growth is through the direct stretching or compression of the gel. Chan et al. showed that the patterns produced can be controlled by modulating the shear modulus of the hydrogel with the epithelial layer and stretch (Chan *et al.*, 2018) (see fig 4.5 B). By pre-stretching the hydrogel before seeding cells, they were able to produce folded patterns with different wavelengths depending on the type of pre-stretching applied (uniaxial or biaxial).

Another type of instability in bilayers is delaminated buckling, which is often observed in thin film delamination in furniture. This can be induced through compressive stresses created during growth or collective tension. Recent studies have shown that growing epithelia confined in a sphere undergo delaminated buckling after reaching a critical growth-induced stress (Trushko *et al.*, 2020) (see fig 4.6 C), or through intercellular stresses (Oyama *et al.*, 2021) or by placing a biofilm on top of the epithelial monolayer (Cont *et al.*, 2020).

The formation of the ventral furrow in the drosophila embryo can also be considered as a buckling event. Although there are multiple explanations for this phenomenon, recent studies have shown that the instability leading to the fold is caused by embryo-level forces (Fierling *et al.*, 2022, Guo *et al.*, 2022). Apart from instabilities, it is remarkable that the mechanical information can be encoded in the substrate. For instance, the tension produced by the cells in a pre-stretched membrane, on cutting would lead to curling (Tomba *et al.*, 2022), or through

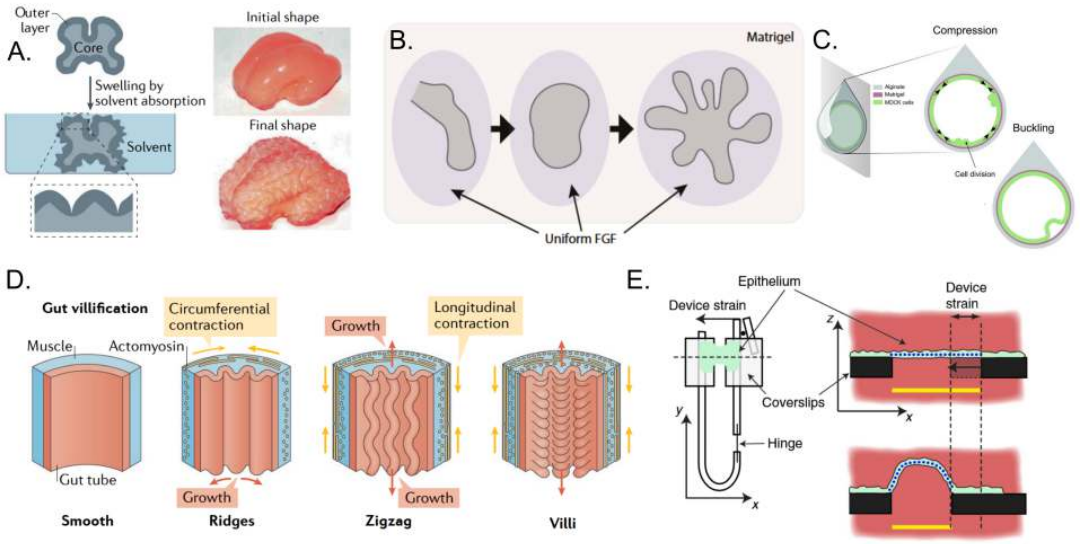

Figure 4.6: **Examples of mechanical instabilities**: (A) Synthetic mini brains illustrate the wrinkling of the outer layer with swelling mimicking gyrification (Tallinen *et al.*, 2016). (B, D) Other way around where inner layer of lung or intestinal epithelia develops folds when embedded into a hydrogel or muscle shell (Shyer *et al.*, 2013, Varner *et al.*, 2015). (C) It is also shown that simple epithelial tissues embedded into a shell would also buckle (Trushko *et al.*, 2020). (D) (Wyatt *et al.*, 2020) used matrix independent tissue with compression to illustrate that the epithelial tissue itself can undergo buckling. *Panel A, D are adpated from (Collinet and Lecuit, 2021) and C from (Matejčić and Trepat, 2020)*

stretching a suspended epithelial layer would also do the same(Fouchard *et al.*, 2020).

It is noteworthy that there is currently only one established method for directly applying compressive stresses to suspended epithelial tissue. The Lab of Guillaume Charras has developed a technique using a cell-laden collagen gel sandwiched between two rods, where the gel is digested with collagenase to create a suspended monolayer (see fig 4.6 E). Through extensive experimentation, they have observed that the compression of more than 35% strain produces transient buckling events (Wyatt *et al.*, 2020). Importantly, the actin cytoskeleton plays a crucial role in buffering deformations in this system.

4.3 Tissue hydraulics

4.3.1 Hydraulic control of morphogenesis

In this thesis, we focus on the role of hydraulic pressure in morphogenesis. It has been well established in the field of developmental biology that fluid pressure plays a significant role in lumen expansion. For instance, in the mouse embryo, cell aggregates form small fluid cavities in intercellular junctions, which grow and coalesce into a large lumen, breaking the symmetry of the embryo, due to the presence of an osmotic pressure gradient ((Dumortier

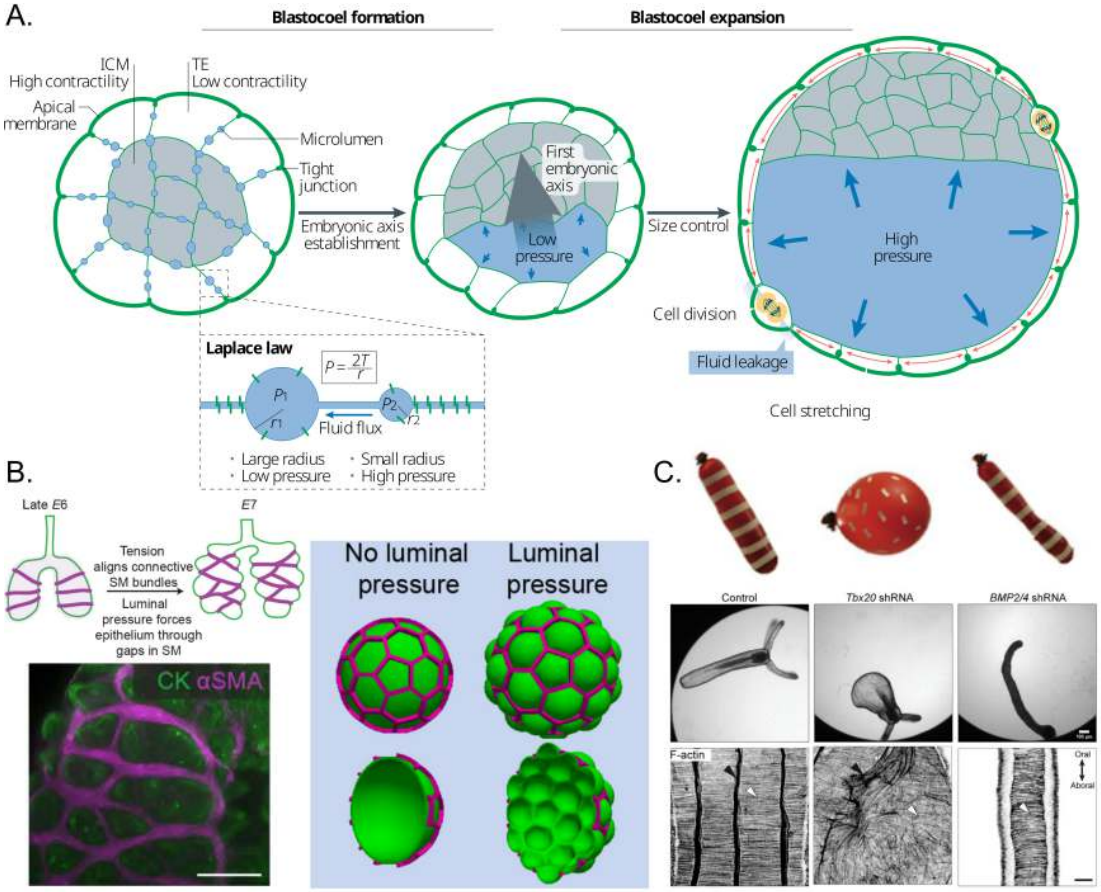

Figure 4.7: **Tissue hydraulics** plays an essential role in establishing (A) embryonic axis through lumen coarsening, and later the pressure regulates the size of the embryo. Laplace's law acts on the spherical cavities between cells to the whole blastocyst (Chan *et al.*, 2019, Collinet and Lecuit, 2021, Dumortier *et al.*, 2019). (B) Interestingly, if the inflated structure is surrounded by a mesh you see a stressball effect, where material inflates through the mesh. Similar phenomena is visible in growth and inflation of the lizard lungs. The smooth muscle constrains the deformation leading to stressball morphogenesis (Palmer *et al.*, 2021). (C) In cnidarians, the different orientation of F-actin leads to different shapes of the organism (Stokkermans *et al.*, 2022).

et al., 2019); reviewed by (Torres-Sánchez *et al.*, 2021), see fig 4.7 A). This process is powered by the pumping of ions and water by the cells, which generates pressure in the fluid-filled cavities, ultimately leading to the formation of spherical embryos. For any inflated spherical shell, the relationship between pressure, curvature, and surface tension can be described by Laplace's law.

$$\sigma = \frac{\Delta P R}{2}$$

The shape that is created under pressure depends on the material properties of the tissue. For example, a homogeneous material would create a uniform curvature, such as a spherical shape, while an anisotropic tissue with oriented cells would result in various shapes, such as cylinders or ellipsoids (Stokkermans *et al.*, 2021) (see fig4.7 C). An interesting example of this phenomenon can be seen in the lobed epithelium of lizard lungs, which resembles the shape of a stress ball. Palmer et al. propose that the smooth muscle network functions as a mesh that constrains the epithelium, much like the outer layer of a stress ball (Palmer *et al.*, 2021) (see fig4.7 B). Upon the application of pressure, the epithelium inflates in the regions between the gaps in the muscles.

For embryos, an increase in pressure results in an increase in tension and stretching of the cells. Once a certain threshold is reached, the cell junctions may leak, causing a reduction in luminal pressure and shrinkage of the embryonic cavity. This system of pressure regulation through leakage acts as a mechanism for size regulation (Chan *et al.*, 2019). At the same time, it polarizes the embryo and promotes cell segregation and fate specification (see fig4.7 A, reviewed by (Chan and Hiiragi, 2020)).

Similar coalescence and lumen coarsening have been observed in other systems (reviewed in (Schliffka and Maître, 2019)). The pressure can also be generated through secretion of the matrix, as seen in the case of the drosophila hindgut with mucins (Syed *et al.*, 2012), or through the secretion of hyaluronic acid in the formation of ear canals in zebrafish otic vesicles (Munjal *et al.*, 2021). Despite numerous in vivo experiments, there are very few systems in which epithelial tissue can be subjected to controlled shape and size in vitro.

4.3.2 Mechanics of domes

Many of the morphogenetic events are called doming because the shape vaguely resemble a spherical cap. For instance, doming of the retina in the eye or zebrafish embryo, or doming during duct formation of mammary or salivary glands. There are typically two mechanisms for these: first, an accumulation of the cells or matrix to create curvature; and second, trans-epithelial transport causing hydraulic pressure-driven shape change. The second kind is remarkable as they mimic various lumenized epithelia in vivo.

This is the most pertinent system to the thesis. I would briefly go into the historical developments in dome mechanics.

Fluid-filled dome formation in epithelial tissue culture has been recorded since 1933 (Cameron, 1953) (see fig 4.8 A). After several decades alongside the development of cell culture techniques, microscopy, and MDCK cell line [5], in 1968, Leighton and colleagues observed that the confluent MDCK cell monolayers formed hemispherical blisters (domes) (Leighton *et al.*,

[5]It is very important to acknowledge the contribution of Madin-Darby canine kidney (MDCK) cells to the field of mechanobiology and enhancing our understanding of tissues in vitro. Stewart H. Madin and Norman B. Darby, Jr. isolated female cocker spaniel dog's kidney tubules cells in 1958. MDCK cells can self-organize in 2D and 3D; form monolayers and stratified layers; and undergo collective migrations. These cells are incredibly robust for experimentation.

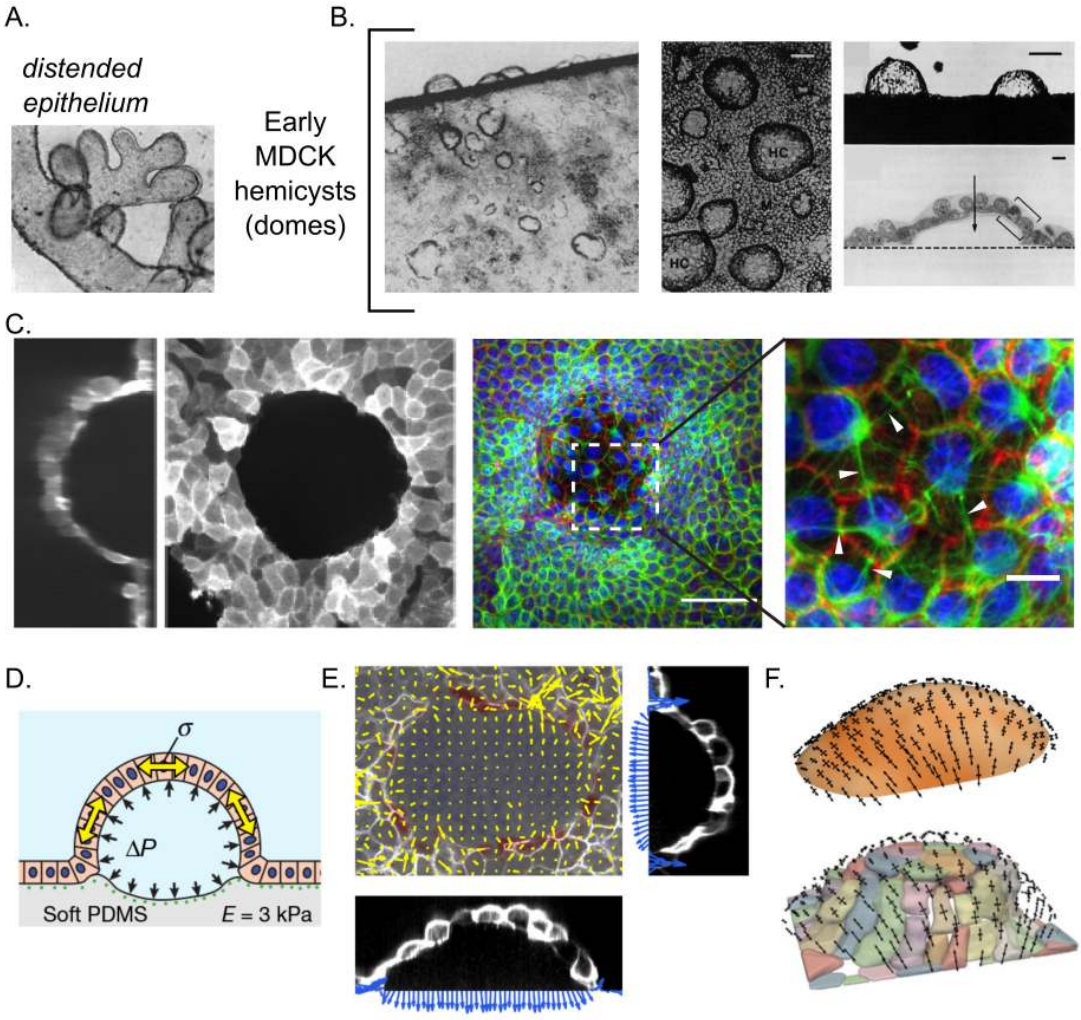

Figure 4.8: **Historical development of epithelial domes**:(A) Distended epithelium was observed in explant cultures in 1930-50s. (B) With MDCK cell line, spontaneously forming domes/hemicysts were characterized (Leighton *et al.*, 1969, Valentich *et al.*, 1979). (C,D) In our lab, shape and size of the domes were controlled with micropatterning adhesion protein (Latorre *et al.*, 2018). The pressure and tension was measured with Laplace's law and traction force microscopy. (E-F) For non-spherical domes, curved monolayer stress microscopy technique was implemented by segmenting the dome shape (Marín-Llauradó *et al.*, 2022).

1969) (see fig 4.8 B). They observed that these are different from renal tubules because the apical surface, with microvilli, was facing outwards. They saw that these fluid-filled structures are dynamically changing size and curvature. They would burst to deflate and leak fluid out in the medium (Valentich *et al.*, 1979). After sometime, they could heal and form the dome again. Later, other cell lines derived from mammalian and amphibian kidneys were often observed to form domes too (Dulbecco and Okada, 1980, Leighton, 1981, Lever, 1979)

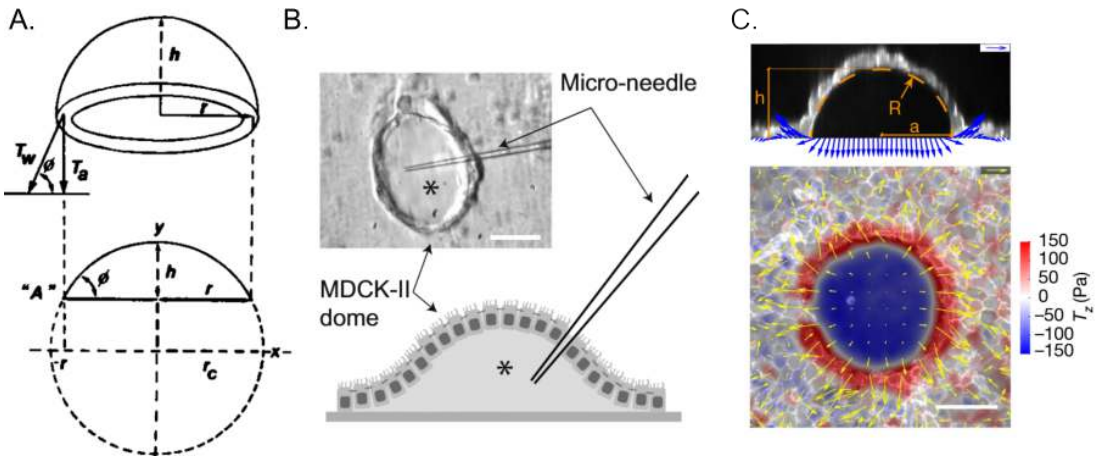

Figure 4.9: **Ways of measuring pressure and tension**: (A) Earlier studies tried to estimate tension through geometry and thickness of the monolayer (Tanner *et al.*, 1983). (B) Later, pressure was measured by puncturing the dome with a micro-needle. However, the measurement of pressure is static, because the dome deflated after the puncturing (Choudhury *et al.*, 2022). (C) Traction force microscopy technique provides a viable non-invasive solution for measuring pressure under to domes (Latorre *et al.*, 2018).

Now the mechanism is clear as the epithelial cells perform critical barrier function alongside controlling the transepithelial flow of ions and water. It was shown that hindering sodium-potassium ion pumping reduces the likelihood of domes (Leighton *et al.*, 1969). Thus, on forming a confluent monolayer the cells perform their function of pumping ions from apical to basal direction (Valentich *et al.*, 1979). If the substrate is solid and impermeable the tissue accumulates enough pressure to delaminate and form a spherical structure.

Most domes observed have been spherical and circular in footprint, indicating uniform tension across the dome. This can be explained by considering the dome as a thin shell under pressure, similar to a bubble, and following Laplace's law. Early studies attempted to infer tension through geometry and pressure measurement (Tanner *et al.*, 1983), finding that the pressure was of the same order as physiological vessels (see fig 4.9 A-B).

One study (Popowicz *et al.*, 1986) identified a "dome curve" when the frequency of domes was plotted against size, observing three classes of domes in terms of size. Smaller domes were observed to swell and increase in size. It was also suggested that there could be different subpopulations of MDCK cells. In the 1990s, many strains were characterized that formed different inflated structures, ranging from normal domes to tubules (Klebe *et al.*, 1995). One cell line, called super dome MDCK, formed larger domes.

Despite research into ion transport, hormone signaling, the role of tight junctions, and external shear stress, the understanding of the mechanics of domes and pressure has remained stagnant due to the lack of tools for measuring tension, pressure, and controlling the shape and size of these structures.

The work of Ernest Latorre in our laboratory has led to the development of a system for

controlling the size of domes and studying the relationship between tension and pressure (Latorre *et al.*, 2018) (see fig 4.8 C-D). By utilizing protein patterning techniques, Latorre was able to create non-adhesive circular regions on soft PDMS gel, which, when seeded with MDCK cells, led to the formation of domes. The gel was embedded with beads to allow for the calculation of traction forces and pressures exerted by the monolayer (see fig 4.9 C). This system allowed for a deeper understanding of the rheology of tissue and the role of the cytoskeleton. He observed that stretching the actin cortex leads to dilution, and that tension reaches a stable value regardless of strain. He also observed the surprising phenomenon of superelasticity, where cells are heterogeneously stretched in the dome when tension is uniform. To further understand the role of actin and keratin bundles in providing superelasticity, Latorre et al. developed a vertex model through which they could understand the instability triggered by actin dilution, and rescued by intermediate filaments.

Ariadna Marin-Llaurado extended Latorre's work by examining domes of varying sizes and shapes (see fig 4.8 E). This study found that different-sized spherical domes have similar tensions, and that pressure is compensated according to curvature. Marin-Llaurado couldn't rely on a simple formula for tension calculation, because the tension in non-spherical domes is non-uniform (Marín-Llauradó *et al.*, 2022). They used confocal microscopy to map dome curvature and calculated stresses computationally using a novel method called cMSM (curved Monolayer Stress Microscopy) (see fig 4.8 F). This method infers stresses just through geometry and pressure as in Young-Laplace relation.It doesn't need to make any assumptions related to material properties. The results showed that cells tended to align along the principal stress direction.

The mechanics of osmotic and hydraulic gradients are also crucial to understand. Chaudhary et al. demonstrated that kidney cells act like a mechanobiological pump (Choudhury *et al.*, 2022). Using a two-layer microfluidic chip, the team was able to measure and apply pressure differences across an epithelial monolayer and observe that the tissue acted like a mechanical pump that stalls at high pressure. Remarkably, they discovered that diseased kidney cells pump in a different direction than healthy ones. They were able to control both osmotic and hydraulic pressure. Another study by Ishida-Ishihara et al. investigated the connection between osmotic pressure and extracellular matrix swelling (Ishida-Ishihara *et al.*, 2020). The researchers found that osmotic gradients trigger Aquaporin transport channels, leading to dome formation through Matrigel swelling. However, these domes are gel-filled structures that differ from fluid-filled domes.

MDCK domes provide a model system for studying transport, cell fate, and tissue dynamics with a curvature. However, control over luminal pressure in these structures remains a challenge.

Chapter 5

Structure of the thesis

5.1 What is to be done?

Morphogenesis is a process of deformation or growth of the tissue under the combination of endogenous and exogenous mechanical forces that include contractility of the epithelium itself and the surrounding matrix as well as hydraulic pressure from the lumen. These stresses are applied to different material components of the tissues, such as cells and the extracellular matrix, that display distinct viscoelastic properties and remodeling time scales. Understanding how the complex interplay between tissue stresses and viscoelastic properties gives rise to specific morphogenetic events in vivo poses outstanding technical and conceptual challenges. These include difficulties to disentangle the relative role of the distinct components involved in a system, the lack of tools for quantitative measurements of stresses and mechanical properties, and the inability to impose controlled stresses over a broad range of amplitudes and rates.

As a complementary strategy, bottom-up approaches aim at understanding the role of each component of the system and its morphogenetic potential, with the ultimate goal of building complexity through rational engineering of the building blocks that form functional tissue. These approaches have been successful at engineering elementary morphogenetic processes such as epithelial bending or buckling. However, despite the emerging success of bottom-up approaches, we still lack tools to simultaneously measure and control the shape and stress of 3D epithelia. In addition, we lack computational models that integrate cellular and tissue shape with the subcellular determinants of epithelial mechanics such as the contractility, turnover, and viscoelasticity of the actomyosin cortex.

The focus of this thesis is to investigate the mechanics of epithelial tissues. Understanding the principles that govern tissue form and function is critical for two main reasons. Firstly, it allows us to comprehend the fundamental physical rules of biology. Secondly, it provides inspiration for new engineering tools and design principles. We use cutting-edge technologies such as 3D printing, microfluidics, and 3D cell cultures to individually control morphogenetic driving factors. This approach enables us to study tissues from a material science perspective,

which is particularly useful for probing the intricate mechanisms involved in the generation of forces and shape changes at the cellular and tissue levels. Furthermore, this approach has the potential to lead to the discovery of emergent phenomena and enable the building of novel tissue forms and assemblies.

5.2 Objectives

General aim of the thesis

Explore the mechanics of epithelial layers subjected to controlled pressure.

Specific aims of the thesis

General aims are divided into specific goals:

1. Develop a new technology to build a three-dimensional epithelia by using controlled hydrostatic pressure.
2. Characterize material response of the pressurized epithelial tissue.
3. Explore the mechanics of epithelial folds.

5.3 Thesis outline

Results are presented in Part 2 with four chapters addressing all the aims and conclusions.

- Chapter 6 will detail the construction of an experimental system for physically controlling epithelial monolayers. This chapter will showcase the main result of the PhD, a novel microfluidic system that generates 3D epithelia with controlled pressure and shape. I will explain the motivation for the device and provide a summary of failed or attempted methods used in constructing the device.
- Chapter 7 will focus on using the microfluidic device to understand epithelial mechanics. In this chapter, I will report the results of rheological experiments and relate them to the computational framework. We show that the shape and rheology of the epithelia are driven by the viscoelasticity of the actomyosin cortex. Additionally, we will make predictions related to tissue buckling.
- Chapter 8 will describe the buckling instability in pressurized epithelia. We found that rapid deflation produces a buckling instability that leads to the formation of epithelial folds. Buckling occurs across different length scales to overcome compressive stresses, and folding patterns become more complex with increasing size. I will discuss the potential of guiding the folds by controlling the shape and size of the epithelia.

- Finally, in Chapter 9, I will summarize our findings and report our conclusions.

In summary, we present a microfluidic-based technique to impose a controlled deformation on an epithelial monolayer while continuously monitoring its state of stress. This technique allows us to investigate the active viscoelasticity of epithelial layers over physiological time scales. We also present a 3D model of the epithelium, which explains the observed phenomena using the active viscoelastic properties of the actomyosin cortex. Additionally, we demonstrate that these viscoelastic properties, along with adhesion micropatterning, can be utilized to engineer epithelial wrinkles with predictable geometry.

Part II

Results

Chapter 6

A microfluidic system for generating 3D epithelia with controlled pressure and shape

6.1 Introduction

To create three-dimensional epithelial structures in vitro from planar epithelial monolayers, we chose to begin with already existing system of epithelial domes developed by Ernest Latorre and improved Ariadna Marin. In this system, Madin-Darby canine kidney (MDCK) cell monolayer is seeded on substrate which is patterned with circular non adhesive regions. The cells invade these non adhesive regions and form a cohesive monolayer everywhere in 24 to 48 hours. Due to the tendency of these cells to actively pump ions in apical to basal direction, the cells delaminate from the impermeable substrate, like glass or soft PDMS gel, to form a spherical cap structure in the circular patterns, called epithelial domes. Latorre and Marin studies show that they could form variety of the structures of controlled shape and size, ranging from circular to rectangular shaped structures.

At the same time, the system enabled the use of 3D traction force microscopy, which allows for measurement of pressure. It utilizes the deformation of the soft PDMS gel embedded with beads to characterize the forces and pressures applied by the cells on substrate. It is ingenious way of measuring pressure as compared to the past method of puncturing the epithelial domes with a microneedle. This allowed for characterization of rheology of epithelia and revealed interesting material properties such as superelasticity of cells while stretching.

However, the process of forming epithelial domes is dependent on ion pumping mechanism of the domes. We can call them spontaneous domes. Thus, the timescales for the dome stretching are not controlled. The process could be accelerated marginally by few hours through use of drugs like Forskolin, which can activate transepithelial channels of NA+/K+/Cl-. We wanted to build the epithelial structure at will which requires pressure control. At the

same time, we wanted to have measurement of lumen pressure and tissue tension.

6.2 Monolayer inflator

Drawing upon the inspiration from organ on chip microfluidic devices, we though they would be perfect system for controlling pressure, cell culture, and enable us to image at high resolution. For example, lungs-on-chip device which is a two layers separated with a porous membrane with the channel in top layer for epithelia and another one for endothelia. This is all assembled on a thin glass which allows for high quality imaging.

Therefore, we conceived the idea of monolayer inflator device, where we will use two layer microfluidic channel which will have one side for epithelial monolayer and another on for application of the pressure. The epithelial monolayer side will be micropatterned with protein with non/less-adhesive regions for dome formation. We reasoned that cells will attach everywhere even in less adhesive region. When applying pressure the cells will delaminate from the weakest point of adhesion and form a dome.

We decided use the classical PDMS material for building the microfluidic chip because of ease of use. We attempted making devices from plastic stickers and photopolymerizable glue, but they were unsuccessful and had issues due to leakage or lack of bio-compatibility.

Figure about the basic schematic. comparing natural domes to cool domes

6.3 Fabrication of the device

The structure of the device is in four layers: glass, bottom channel, porous membrane, and top channel. All layers bonded to each other by using ozone plasma activation.

All the device has to be mounted on a thin glass enabling high quality imaging. There are options for using thicker glass slides but for measurement of the curvature of domes, or monitoring cell stretching would require thinner glass of number 1.5.

For the same reason, the bottom channel has to be thin enough to make it as close as possible. This is due to the working distance of most of the confocal microscope objectives. As it is typically between $200\mu m$ to $1000\mu m$. We chose to fabricate this layer for $100\mu m$ such that it is thick enough to handle manually but not too thin too cause microfluidic problems of pressure and flow. We used spin coating method to fabricate thin PDMS layer and then used a desktop cutting machine to cut the channel out of it.

Primary purpose of the porous membrane is allow for pressure application and not let cells pass through from cell channel to pressure channel. We started with $10\mu m$ membrane considering the literature. We tried to use PDMS $100\mu m$ thin layer with $10\mu m$ pores, but the microfabrication using photolithography was unsuccessful. We were producing $10\mu m$ pillars with $100\mu m$ height the aspect ratio was too high for use to get upright domes. Thus, we decided use plastic (PET) membranes with $10\mu m$ pores. The thin ($10\mu m$ thick) plastic sheets, very easy to handle, but the bonding with PDMS was not very sturdy there were bonding failures or leakages because membrane wrinkling.

Later, we decided to attach the PDMS thin layer to a small piece of membrane. The middle PDMS thin layer will have a 1.2*mm* hole exposing the membrane to pressure. We chose this dimension because it is approximately the size of the field of view of 10X objective.

The top channel was chosen to be a big block of 5*mm* thickness with a channel of 1*mm* thickness engraved in it. The thickness of this was chosen in an ad hoc way. The only consideration was that the block has to be thick enough to be able to plug in tubing for application of pressure. Because the dimensions were so big we could use a 3D printer to create a mold with a channel. The way we construct the device, there are two channels crossing each other perpendicularly. Therefore we needed to add 4 inlets in the big block. Two for inlets for bottom channel and other two to seed cells.

We bond all these layers in two steps with ozone plasma cleaner. First we bond glass to bottom channel and simultaneously middle layer to top channel. After these are bonded, we bond them to each other with membrane sandwiched in the middle.

process of making the devices

6.4 Protein patterning and inverted cell culture

After few trials, we immediately realize that the whole device has to be contained in petri because of the cell culture medium. When we put the glass slide in a larger petri dish. The liquid would go underneath the glass, any leakages during pressure application would cause spillage in microscope. Thus, we designed all the setup to be fitting in a glass bottomed dish.

In case of spontaneous domes, the domes were seeded on a soft PDMS gel in a glass bottomed dish. Thus, the top surface is exposed to any chemical treatment including micro-contact printing, where a PDMS block with a topography is put in contact with surface to pattern adhesion proteins. Later, to have more control and flexibility of patterning proteins, PRIMO technique was used. This uses an inverted microscope to etch protein patterns in the substrate.

For our setup, it was impossible to use micro-contact printing because the whole device is sealed and bonded. Thus, we decided to use PRIMO technique. This technique was optimized for glass and soft PDMS substrates. Thus, we had to optimize the technique for our setup with plastic substrate, which involved increasing laser power and protein concentration. In the end, we had successful protein patterning.

We had to optimize the cell seeding too, in other setup cells can just be seeded in a dish. However, in the channel, the cell seeding required high concentration of cells compared to typical spontaneous dome experiment. We would seed 30×10^6 cells/ml for one hour and then wash away the cells which didn't attach within one hour.

In early experiments, we would have to cells attached to the surface and protein patterns, but on application of pressure there were very few events dome formation. Another thing was that the quality of the imaging was terrible, we were imaging through the porous membrane. The domes in the top channel would have cells further away from the microscope objective. Upon closer look we noticed cells were filtering through the membrane from top to bottom

primo method, + all the upside down business

and protein coating was better on the bottom channel side than the top.

To prevent cells crossing the membrane, we decided to use membrane of smaller pore size like 400nm. However, imaging green channel 488nm was impossible through 400nm pores. Here, we decide to change the side of seeding cells from top to bottom. This improved two things. First, imaging would be better as the cells and dome would be closer to objective. Second, cells would be seeded on the good side of the protein pattern.

We call it "upside down" cell culture, where upon seeding cells in bottom channel we would flip the device immediately to make sure cells are attached on the membrane not the glass. We have to wash the channel thoroughly, otherwise cells might attach on the glass which also obstruct the imagine of the domes.

Even with these improvements, the ultimate challenge was to make sure cell monolayer cover the non adhesive regions. To resolve this issue, we had to increase the protein concentration in these regions so that cells could attach there. The cells would be attached to these regions will be attached weakly and would detach there first to form a dome.

6.5 Pressure control

After optimization of protein patterning, cell culture conditions, and confocal microscopy, we dealt with pressure control. The previous studies showed that the pressure under the dome is around 100Pa. The idea for us was to use hydrostatic as the pressure required to form dome is so low, 100Pa is 1cm of water column.

In early trials, I was using pipette tips to apply pressure. One side pipette tip would be blocked and other was used to apply pressure by adjusting the height of liquid. However, the pipette tips are not the best because they are prone to bubbles and also if there's a leak the media just flows out. Later, we used Polytetrafluoroethylene tubing connected to a 15ml tube. We could match the height of the device with the height of air-liquid interface in the tube. This means that there is a zero pressure on the monolayer. Upon increasing the height of the tube by 2cm we would apply 200Pa pressure on the monolayer causing it to delaminate and form domes.

With tubing, we have to be attentive to the cavitation or bubbles getting trapped in the cell channel. To ameliorate the bubble issues, we would put the media in vacuum chamber. It would get rid of nascent bubbles which get bigger with time. Also during inserting the tubing, we could easily introduce bubbles again. To solve this, we use the two inlets for each channel by flushing the fresh media from the reservoir to fill up the tube without the bubbles and remove any pre-existing bubbles.

We used an automatic translation stage which can be programmed to lift the reservoir. We measure the pressure by keeping track of the height of the stage and the zero pressure position. With this stage, we could apply pressure in the range of $0 \rightarrow 1500Pa$. Although, by setting it lower we could even apply negative pressure. For typical experiments done for this thesis, we used the range of $-200 \rightarrow 1300Pa$.

schemetic of pressure control

6.6 Imaging the epithelial domes

Finally, we were able to form domes according to the pattern and control pressure at will. Domes would not inflate right away as they have to detach from the porous membrane. They would delaminate at pressures $50 - 100Pa$ then we could image the dome in confocal microscopy. We would use 40x objective to image a dome with membrane marked in $488nm$ channel and protein pattern in $644nm$. Labeled adhesion protein made it easier for us to track and anticipate the formation of the domes. The confocal microscopy stack of $100\mu m$ tall dome with step size of $0.5\mu m$ would take $5min$. This is much slower than we can actually deform the dome by changing pressure. At first, to characterize the epithelial mechanics, we were mainly interested in spherical domes at constant pressure. We could monitor pressure, cell shape, and tissue curvature easily, enabling us to utilize the Laplace's law to calculate tension.

confocal, line scale, and lightsheet dome

$$\sigma = \frac{\Delta P R}{2}$$

In previous studies, the domes were shown to be dynamic but the dynamics was slow and domes could be recorded at much slower rate of $5min$. In our case, the domes could be inflated and deflated in matters of seconds. We could monitor them by looking at the base of the dome, where monolayer would come in and out of the view. This would not be enough to quantitatively track the state of the dome.

For the studying rheology, it would be of our interest to be able monitor dynamic response of the domes at faster pressure rates or shorter timescales. In this case, we would only be interested in the dynamics of the dome strain and curvature. Due to its symmetry, we could image only the mid section of the dome and get all the information needed to characterize the material response of the dome.

Using the line scanning mode of a Zeiss Airy Scan Microscope, we could selectively image a single line of pixel across the midsection of the dome and take a confocal z-stack along the height of the dome. This will give us a cross-section of the dome in a fraction of the time of normal stack. Along with piezo stage movement enabled, we were able to image $100\mu m$ tall dome within $4s$. We could even track the dome height evolution through kymograph of the central part of the dome. However, it is important to note that this form of imaging is useful to keep track of the dome strain and curvature, but the quality is of cells imaged is quite low. In some cases, where the fluorescent expression of cells on the top of the domes is not adequate, we have much noisy data.

6.7 Light-sheet MOLI

Later in my PhD, for observing cellular or sub-cellular changes, we could utilize the light sheet microscope. The microscope in our lab, has two immersion-upright objectives at 45 degrees to

the horizontal plane. With our expertise at fabricating devices, we were able to design new setup which would have cells and porous membrane exposed to the top for imaging.

We decided to invert the normal MOLI device and simplify the setup for fabrication. For this, we needed a pressure channel and middle layer with hole and porous membrane. The device had to be thick enough to plug in the tubing. The whole device and channels are large so we could fabricate the mold for this using normal 3D printer. We created a ridge-like protrusion so that pressure channel and hole of seeding cells is manufactured in one go. The bonding of the device was done by gluing the device to a microscope slide with unpolymerized PDMS. We were able to primo pattern the device by flipping it upside down. Seeding cells in this setup is easier as the cell seeding part is exposed.

As expected, we were able to apply pressure with the same system as before and form domes. We could see the features which were impossible to see in other imaging strategies.

light sheet device

6.8 Summary and Discussion

We have developed a microfluidic chip to form 3D curved epithelia. It is a multilevel device, which has two layers separated by a porous membrane. We can seed cells on the membrane 'upside down' way in the bottom channel, so that when dome forms it is closer to the microscope objective. The pressure in this system is applied using hydrostatic pressure by changing the height of the reservoir. This experimental setup enabled us to control pressure under the dome dynamically, and obtain high quality confocal images. We also developed imaging strategies to capture dynamics of these 3D structures faster using line scanning mode of confocal microscope or light sheet microscope.

It is worth acknowledging that even though the method of forming 3D epithelia described here feels obvious and easy, it is not. We had to go through many iterations of this device and many other methods we tried and failed.

We formed the domes and were able to monitor cells and tissue behavior. The pressure, tension, and curvature could be measured by applying Laplace law for spherical cap domes. As shown in previous studies, the most interesting part of the system is that the complex material such as epithelial tissue to maintain mechanical equilibrium has to adopt a spherical cap shape for circular footprint. This uniform curvature and pressure implies uniform tension, for this we don't even need material properties of the tissue. However, in case of the non-spherical geometry, there would be anisotropic stresses which would require computational model to solve an inverse problem to go from geometry to forces.

The geometry of the domes is controlled through the protein pattern. But it could delaminate further too. This has been shown in spontaneous domes where the researchers found that the most domes had circular footprint. Also, in case of the domes which were instructed to form around a sharp corner would blunt itself with delamination. We would have to keep this in mind while creating particular geometry.

There is an interplay between tissue tension and adhesion forces. As cell-cell junctions

discussion panels

are much stronger than cell-substrate adhesion, if we consider that the tension exceeds the adhesion forces at the base of the dome it would lead to detachment and delamination of the domes.

Also, another aspect to think about is that we have created unintentionally a peeling system, where we are able to see tissue being peeled off from the substrate. and if the dome remains spherical, we could even calculate forces required to break cell-substrate adhesion and identify the role of the molecular components of focal adhesion. However, we are more interested in learning more about the mechanics of epithelial tissue under controlled pressure.

Part III

Appendices

Appendix A

Methods and Materials

A.1 Fabrication of microfluidic devices

Polydimethylsiloxane (PDMS) gels (Sylgard PDMS kit, Dow Corning) were used to make the microfluidic devices. PDMS was synthesized by mixing the curing agent and elastomer in $1:9$ weight ratio. This mixture was centrifuged for $2min$ at $900rpm$ to remove air bubbles. The unpolymerized PDMS was poured into a mold or spun to obtain the desired shape. There are four parts to the device (fig S1X showing device scheme). First is the top block, a thick PDMS block with four inlets and one channel for the application of hydraulic pressure. The second is a $200\mu m$ thin PDMS layer with a $1.2mm$ diameter hole in the center with a $400nm$ porous membrane (Polycarbonate filtration membrane $0.4\mu m$, Whatman membranes) attached to it. The third is another $200\mu m$ thin PDMS layer with a channel for seeding the cells. Lastly, all these PDMS parts are attached to, the fourth part, a glass-bottomed $35mm$ dish ($35mm$, no. 0 coverslip thickness, Cellvis). The top block was made using replica molding in a 3D printed mold. This mold was 3D printed with vat polymerization and a digital light processing 3D printer (Solus DLP 3D Printer with SolusProto resin). The mold's surface was then silanized using Trichlorosilane (Trichloro(1H,1H,2H,2H-perfluorooctyl) silane, Merck) for preventing adhesion with unpolymerized PDMS. PDMS was poured into the mold and degassed for one hour. PDMS is cured with a hot plate at 100 deg C for $30min$. Once cured, PDMS is removed, cut into devices, and punched with $1.5mm$. $200\mu m$ thin PDMS layers were made by spin coating $4.5ml$ unpolymerized PDMS on a $15cm$ dish at $500rpm$ for $1min$. These dishes were incubated in an oven at 80 deg C to polymerize for $12hr$. These thin sheets were cut into the parts of devices using a Silhouette cutting machine (Silhouette Cameo 4, Silhouette America). The sheets were attached to a Silhouette cutting mat and then Silhouette software was fed with the pattern of the device layers. A sharp cutting tool in the machine cut the PDMS along the pattern. These cut PDMS were peeled off with help of 70% ethanol. These devices are assembled with the aid of ozone plasma cleaner (PCD-002-CE, Harrick Plasma). Glass bottomed dishes and thin PDMS layers with cell channels were treated for 1 min under plasma. Then bonded together

by placing the layers in contact for 2 hr at 80 C. Similarly, the top block and thin membrane with porous membrane were also bonded. These layers were later bonded together again using plasma cleaner.

A.2 Patterning protein on the device

The devices were filled with 96% ethanol for removing air bubbles. Then, devices are treated with 5% v/v (3-aminopropyl) triethoxysilane (Merck) diluted in 96% ethanol for 3min and rinse three times with 96% ethanol. Later the devices were filled with MilliQ water to remove ethanol traces. PRIMO (Alveole Lab) was used to pattern adhesion-promoting protein. For this setup, devices were incubated with PLL (Poly-L-lysine solution, Merck) for 1hr, subsequently with SVA PEG (50mg/ml in 8.24pH HEPES) for 30min, and rinsed with HEPES. Before using PRIMO, devices were filled with a photoinitiator. Desired protein pattern was loaded into the PRIMO software (Leonardo, Alveole Lab). PRIMO uses a microscope to shine the laser in the specific region according to the loaded pattern to cut PEG chains. Samples were rinsed with phosphate-buffered saline (PBS, Merck). Then the samples were filled with fibronectin and fibrinogen (100$\mu g/ml$ Fibronectin in 2% Far-red fibrinogen solution in 1X PBS) solution for 5 min. Then samples were rinsed again with 1X PBS. Fibrinogen labels the fibronectin with Far-red signal to image the coated protein pattern.

A.3 Cell culture in the device

To image cell shape and tissue structure Madin-Darby Canine Kidney (MDCK) cells expressing CIBN-GFP-CAAX were used for the experiments. CIBN-GFP-CAAX labels plasma membrane. These cells were cultured in Dulbecco's Modified Eagle Medium (DMEM, Gibco Thermofisher) with 10% v/v fetal bovine serum (FBS, Gibco, Thermofisher), L-glutamine (Thermofisher), 100$\mu g/ml$ streptomycin and penicillin. Cells were incubated at 37 deg C with a 5% CO_2 condition. Before seeding cells in the device, it is filled with a cell culture medium. Cells are trypsinized and diluted at a concentration of $25x10^6$ cells/ml. The cell channel of the device is filled with 30μl of cell solution and incubated for cell adhesion. After one hour of incubation, devices are rinsed with media to remove unattached cells. Devices were kept 24hr in the incubation for the growth of a monolayer before the experiment. Application and measurement of the pressure The pressure is applied via hydrostatic forces similar to the previous studies (Choudhury *et al.*, 2022, Palmer *et al.*, 2021). The two channels in the chip were separated by the porous membrane. Cells are on the bottom side of the membrane. The pressure in the channel (top side of the membrane) is used to inflate the structures on the top. This channel has one inlet and one outlet for removing bubbles. The inlet is connected to a 35 ml reservoir of cell culture medium (in a 50 ml falcon tube) by tubing (PTFE Tubing 1/16" OD for Microfluidics, Darwin microfluidics) and the outlet is connected to a shutoff valve (Microfluidic Sample Injection / Shut-off Valve, Darwin microfluidics). Once bubbles are removed, closing the valve

would apply the pressure on the basal side of the cells according to the difference between the height of the fluid level. All tubings are connected to the chip with a steel insert (Stainless steel 90 deg Bent PDMS Couplers, Darwin microfluidics). We are able to find zero by matching the height of the device to the liquid and air interface in the reservoir. This is confirmed with the experiments, where on applying pressure domes form but on reduction in pressure to zero domes deflate.

A.4 Confocal Microscopy

For timelapse imaging of domes at a larger time interval (> 1 min), an inverted Nikon microscope with a spinning disk confocal unit (CSU-W1, Yokogawa) was used with Nikon 40x, 20x, and 10x air lenses. For shorter time intervals (< 10 s), a Zeiss LSM880 inverted confocal microscope was used with laser scanning mode. Fast imaging was enabled by imaging a single line in the middle of the dome. Fabrication method for the Light-Sheet device The devices used with the light-sheet microscope consisted of a single PDMS block bonded to a glass microscope slide (76x26 mm, RS Components BPB016). The blocks were made using a 3D printed mold (Ultimaker 3 with Ultimaker PLA Printer Filament 1616). PDMS was mixed, centrifuged, degassed, and cured as described above for the normal devices. Once cured, the PDMS was removed, cut into individual devices and punched with a 1.5mm biopsy punch. The PDMS blocks were then attached glass slides using a thin layer of unpolymerized PDMS, that was coated onto the glass slides using a spatula. The devices were then kept on a hotplate at 100C for 30mins to allow the PDMS bonding to fully cure. The 400nm porous membranes were then attached to the devices. The edges of the membrane were carefully dipped into unpolymerized PDMS, before being placed flat on the top of the device. Particular care was taken to ensure the centre of the membrane over the punched pressure-application hole remained free of PDMS. The devices were then kept at 65C for 1 hour to allow the PDMS bonding to fully cure.

A.5 Device protein patterning and cell culture in Light-Sheet device

The light-sheet devices were protein patterned and cell cultured using the same methods and steps as outlined above for the normal devices, with the one minor addition of the use of a simple PDMS and glass cap for a few critical steps. The porous membrane for pressure application, and thus the site of protein patterning and cell seeding, for the light-sheet devices is exposed and on the top side of the devices. This mostly allowed for easy application of reagents as a droplet could be applied and aspirated directly, however for the more sensitive steps in the procedure, a simple PDMS and glass device was used to create a temporary covered channel over the porous membrane to regulate the procedure and ensure the treatment of the devices was highly standardized. Specifically, the cap was used for the application of

photoinhibitor during PRIMO, and for the application of cell solution during cell attachment. The caps were fabricated using $2cm \times 2cm$ squares of a $400\mu m$ thick PDMS layer, with a keyhole shape cut in from the side. Each PDMS piece was then stuck to a 18mm diameter coverslip (18mm, no.1 Cover glasses circular, Marienfeld 0111580) using the innate attraction between the surfaces. The experimental apparatus and measurements for the light-sheet devices were the same as the normal devices as outlined above.

A.6 Light-sheet microscopy

The imaging of the light-sheet devices was done with a dual-illumination inverted Selective Plane Illumination Microscope (diSPIM) (QuVi SPIM, Luxendo, Brucker) with Nikon 40x immersion lenses (Nikon CFI Apo 40x W 0.8 NA NIR water immersion objective). For the buckling experiments, only single objective illumination and detection was used. Quantification of the dome areal strain and tension

As mentioned earlier, the domes were imaged in 3D with confocal microscopy. We used ImageJ to manually section the dome in the middle in the YZ plane, XZ plane is a plane parallel to the monolayer, with Reslice function along the Z axis. This section was used to calculate the height h, radius of curvature R, and base radius a. Strain ϵ and tension σ were calculated as,

$$\epsilon = h^2/a^2$$
$$\sigma = 0.5PR$$

The raw data was extracted in ImageJ and then MATLAB was used to compute and plot the strain and tension.

A.7 Analysis of the kymographs

For cyclic pressure or buckling experiments, the domes were imaged at low resolution and high noise levels to capture fast dynamics. The previous method of manually quantifying each time point is not feasible. Thus, we used the ImageJ function of the Reslice function along the time axis. We resliced it along the Y-time axis in the middle of the dome, such that we get a kymograph of height as a function of time. Also, we performed the reslicing along the XT axis at the plane of the monolayer, such that we get the kymograph of the base radius with respect to time. These kymographs were in form of images save manually with ImageJ. A custom-built MATLAB code was used to digitize the kymographs, where maximum intensity along each time was considered as the current dome height position. The first 30 s of the experiment pressure is zero, so the unstretched monolayer position is determined from those time points. Dome height is calculated with the difference between the current position and the initial position. Base radius is calculated similarly by subtracting two sides. The radius of curvature

is calculated using the relation between the base and height of the dome.

$$R = \frac{h^2 + a^2}{2h}$$

A.8 Qualitative analysis of the buckling event

Whether domes are buckling or not was determined manually checking every frame during the deflation. If dome maintains the smooth circular geometry in XZ plane during the deflation, we mark the dome as “not buckling”. However, if the dome has a visual discontinuity in the curvature or a kink it is then considered to be “buckling”.

Imaging the fast events in XY plane was done in an ad hoc manner. To capture the folds, the dome as imaged closer to the apical surface of the monolayer. The type of fold was determined by carefully observing the way which monolayer makes contact with the imaging plane. If there is one point of contact in the centre and spreads outwards, it is considered as accumulation along the periphery. In case where there are multiple points of contact and they all join in the middle, it is considered as a network of folds.

Bibliography

Are All Fish the Same Shape If You Stretch Them? The Victorian Tale of On Growth and Form. https://writings.stephenwolfram.com/2017/10/are-all-fish-the-same-shape-if-you-stretch-them-the-victorian-tale-of-on-growth-and-form/.

The 100-Year-Old Challenge to Darwin That Is Still Making Waves in Research. *Nature* **544**, 138 (2017a).

A Ton for Thompson's Tome. *Nature Physics* **13**, 315 (2017b).

B. Alberts. *Molecular Biology of the Cell.* sixth edition ed. (Garland Science, Taylor and Francis Group, New York, NY, 2015).

S. Alt, P. Ganguly, and G. Salbreux. Vertex Models: From Cell Mechanics to Tissue Morphogenesis. *Philosophical Transactions of the Royal Society B: Biological Sciences* **372**, 20150520 (2017).

D. Ambrosi, M. Ben Amar, C. J. Cyron, A. DeSimone, A. Goriely, J. D. Humphrey, and E. Kuhl. Growth and Remodelling of Living Tissues: Perspectives, Challenges and Opportunities. *Journal of The Royal Society Interface* **16**, 20190233 (2019).

Z. U. Arif, M. Y. Khalid, W. Ahmed, and H. Arshad. A Review on Four-Dimensional (4D) Bioprinting in Pursuit of Advanced Tissue Engineering Applications. *Bioprinting* **27**, e00203 (2022).

L. Balasubramaniam, A. Doostmohammadi, T. B. Saw, G. H. N. S. Narayana, R. Mueller, T. Dang, M. Thomas, S. Gupta, S. Sonam, A. S. Yap, Y. Toyama, R.-M. Mège, J. M. Yeomans, and B. Ladoux. Investigating the Nature of Active Forces in Tissues Reveals How Contractile Cells Can Form Extensile Monolayers. *Nature Materials* **20**, 1156 (2021).

G. Bao and S. Suresh. Cell and Molecular Mechanics of Biological Materials. *Nature Materials* **2**, 715 (2003).

N. Barker. Adult Intestinal Stem Cells: Critical Drivers of Epithelial Homeostasis and Regeneration. *Nature Reviews Molecular Cell Biology* **15**, 19 (2014).

C. Blanch-Mercader, V. Yashunsky, S. Garcia, G. Duclos, L. Giomi, and P. Silberzan. Turbulent Dynamics of Epithelial Cell Cultures. *Physical Review Letters* **120**, 208101 (2018).

S. Blonski, J. Aureille, S. Badawi, D. Zaremba, L. Pernet, A. Grichine, S. Fraboulet, P. M. Korczyk, P. Recho, C. Guilluy, and M. E. Dolega. Direction of Epithelial Folding Defines Impact of Mechanical Forces on Epithelial State. *Developmental Cell* **56**, 3222 (2021).

V. Braga. Spatial Integration of E-cadherin Adhesion, Signalling and the Epithelial Cytoskeleton. *Current Opinion in Cell Biology* Cell Dynamics. **42**, 138 (2016).

J. A. Brassard, M. Nikolaev, T. Hübscher, M. Hofer, and M. P. Lutolf. Recapitulating Macro-Scale Tissue Self-Organization through Organoid Bioprinting. *Nature Materials* **20**, 22 (2021).

K. A. Breau, M. T. Ok, I. Gomez-Martinez, J. Burclaff, N. P. Kohn, and S. T. Magness. Efficient Transgenesis and Homology-Directed Gene Targeting in Monolayers of Primary Human Small Intestinal and Colonic Epithelial Stem Cells. *Stem Cell Reports* **17**, 1493 (2022).

T. M. Brown and E. Fee. Rudolf Carl Virchow. *American Journal of Public Health* **96**, 2104 (2006).

A. Brugués, E. Anon, V. Conte, J. H. Veldhuis, M. Gupta, J. Colombelli, J. J. Muñoz, G. W. Brodland, B. Ladoux, and X. Trepat. Forces Driving Epithelial Wound Healing. *Nature Physics* **10**, 683 (2014).

D. M. Bryant and K. E. Mostov. From Cells to Organs: Building Polarized Tissue. *Nature Reviews Molecular Cell Biology* **9**, 887 (2008).

S. Calzolari, J. Terriente, and C. Pujades. Cell Segregation in the Vertebrate Hindbrain Relies on Actomyosin Cables Located at the Interhombomeric Boundaries. *The EMBO Journal* **33**, 686 (2014).

G. Cameron. Secretory Activity of the Chorioid Plexus in Tissue Culture. *The Anatomical Record* **117**, 115 (1953).

O. Campàs, T. Mammoto, S. Hasso, R. A. Sperling, D. O'Connell, A. G. Bischof, R. Maas, D. A. Weitz, L. Mahadevan, and D. E. Ingber. Quantifying Cell-Generated Mechanical Forces within Living Embryonic Tissues. *Nature Methods* **11**, 183 (2014).

F. M. Carlier, C. de Fays, and C. Pilette. Epithelial Barrier Dysfunction in Chronic Respiratory Diseases. *Frontiers in Physiology* **12** (2021).

A. X. Cartagena-Rivera, J. S. Logue, C. M. Waterman, and R. S. Chadwick. Actomyosin Cortical Mechanical Properties in Nonadherent Cells Determined by Atomic Force Microscopy. *Biophysical Journal* **110**, 2528 (2016).

L. Casares, R. Vincent, D. Zalvidea, N. Campillo, D. Navajas, M. Arroyo, and X. Trepat. Hydraulic Fracture during Epithelial Stretching. *Nature Materials* **14**, 343 (2015).

K. E. Cavanaugh, M. F. Staddon, S. Banerjee, and M. L. Gardel. Adaptive Viscoelasticity of Epithelial Cell Junctions: From Models to Methods. *Current Opinion in Genetics & Development* **63**, 86 (2020).

G. Y. Cederquist, J. J. Asciolla, J. Tchieu, R. M. Walsh, D. Cornacchia, M. D. Resh, and L. Studer. Specification of Positional Identity in Forebrain Organoids. *Nature Biotechnology* **37**, 436 (2019).

M. Cetera, G. R. Ramirez-San Juan, P. W. Oakes, L. Lewellyn, M. J. Fairchild, G. Tanentzapf, M. L. Gardel, and S. Horne-Badovinac. Epithelial Rotation Promotes the Global Alignment of Contractile Actin Bundles during Drosophila Egg Chamber Elongation. *Nature Communications* **5**, 5511 (2014).

C. J. Chan and T. Hiiragi. Integration of Luminal Pressure and Signalling in Tissue Self-Organization. *Development* **147**, dev181297 (2020).

C. J. Chan, M. Costanzo, T. Ruiz-Herrero, G. Mönke, R. J. Petrie, M. Bergert, A. Diz-Muñoz, L. Mahadevan, and T. Hiiragi. Hydraulic Control of Mammalian Embryo Size and Cell Fate. *Nature* **571**, 112 (2019).

H. F. Chan, R. Zhao, G. A. Parada, H. Meng, K. W. Leong, L. G. Griffith, and X. Zhao. Folding Artificial Mucosa with Cell-Laden Hydrogels Guided by Mechanics Models. *Proceedings of the National Academy of Sciences* **115**, 7503 (2018).

J. Chen, A.-C. Sayadian, N. Lowe, H. E. Lovegrove, and D. S. Johnston. An Alternative Mode of Epithelial Polarity in the Drosophila Midgut. *PLOS Biology* **16**, e3000041 (2018).

M. I. Choudhury, Y. Li, P. Mistriotis, A. C. N. Vasconcelos, E. E. Dixon, J. Yang, M. Benson, D. Maity, R. Walker, L. Martin, F. Koroma, F. Qian, K. Konstantopoulos, O. M. Woodward, and S. X. Sun. Kidney Epithelial Cells Are Active Mechano-Biological Fluid Pumps. *Nature Communications* **13**, 2317 (2022).

D. N. Clarke and A. C. Martin. Actin-Based Force Generation and Cell Adhesion in Tissue Morphogenesis. *Current Biology* **31**, R667 (2021).

C. Collinet and T. Lecuit. Programmed and Self-Organized Flow of Information during Morphogenesis. *Nature Reviews Molecular Cell Biology* **22**, 245 (2021).

C. Collinet, M. Rauzi, P.-F. Lenne, and T. Lecuit. Local and Tissue-Scale Forces Drive Oriented Junction Growth during Tissue Extension. *Nature Cell Biology* **17**, 1247 (2015).

A. Cont, T. Rossy, Z. Al-Mayyah, and A. Persat. Biofilms Deform Soft Surfaces and Disrupt Epithelia. *eLife* **9**, e56533 (2020).

M. Deforet, V. Hakim, H. G. Yevick, G. Duclos, and P. Silberzan. Emergence of Collective Modes and Tri-Dimensional Structures from Epithelial Confinement. *Nature Communications* **5**, 3747 (2014).

C. J. Demers, P. Soundararajan, P. Chennampally, G. A. Cox, J. Briscoe, S. D. Collins, and R. L. Smith. Development-on-Chip: In Vitro Neural Tube Patterning with a Microfluidic Device. *Development* **143**, 1884 (2016).

J. Dervaux and M. B. Amar. Mechanical Instabilities of Gels. *Annual Review of Condensed Matter Physics* **3**, 311 (2012).

C. A. Dessalles, C. Ramón-Lozano, A. Babataheri, and A. I. Barakat. Luminal Flow Actuation Generates Coupled Shear and Strain in a Microvessel-on-Chip. *Biofabrication* **14**, 015003 (2021).

M. E. Dolega, M. Delarue, F. Ingremeau, J. Prost, A. Delon, and G. Cappello. Cell-like Pressure Sensors Reveal Increase of Mechanical Stress towards the Core of Multicellular Spheroids under Compression. *Nature Communications* **8**, 14056 (2017).

A. Ducuing and S. Vincent. The Actin Cable Is Dispensable in Directing Dorsal Closure Dynamics but Neutralizes Mechanical Stress to Prevent Scarring in the Drosophila Embryo. *Nature Cell Biology* **18**, 1149 (2016).

O. Dudin, A. Ondracka, X. Grau-Bové, A. A. Haraldsen, A. Toyoda, H. Suga, J. Bråte, and I. Ruiz-Trillo. A Unicellular Relative of Animals Generates a Layer of Polarized Cells by Actomyosin-Dependent Cellularization. *eLife* **8**, e49801 (2019).

R. Dulbecco and S. Okada. Differentiation and Morphogenesis of Mammary Cells in Vitro. *Proceedings of the Royal Society of London. Series B. Biological Sciences* **208**, 399 (1980).

J. G. Dumortier, M. L. Verge-Serandour, A. F. Tortorelli, A. Mielke, L. de Plater, H. Turlier, and J.-L. Maître. Hydraulic Fracturing and Active Coarsening Position the Lumen of the Mouse Blastocyst. *Science* (2019). 10.1126/science.aaw7709.

J. Duque, A. Bonfanti, J. Fouchard, E. Ferber, A. Harris, A. J. Kabla, and G. T. Charras. Fracture in Living Cell Monolayers. (2023).

G. T. Eisenhoffer and J. Rosenblatt. Bringing Balance by Force: Live Cell Extrusion Controls Epithelial Cell Numbers. *Trends in Cell Biology* **23**, 185 (2013).

A. Elosegui-Artola, I. Andreu, A. E. M. Beedle, A. Lezamiz, M. Uroz, A. J. Kosmalska, R. Oria, J. Z. Kechagia, P. Rico-Lastres, A.-L. Le Roux, C. M. Shanahan, X. Trepat, D. Navajas, S. Garcia-Manyes, and P. Roca-Cusachs. Force Triggers YAP Nuclear Entry by Regulating Transport across Nuclear Pores. *Cell* **171**, 1397 (2017).

A. Elosegui-Artola, A. Gupta, A. J. Najibi, B. R. Seo, R. Garry, C. M. Tringides, I. de Lázaro, M. Darnell, W. Gu, Q. Zhou, D. A. Weitz, L. Mahadevan, and D. J. Mooney. Matrix Viscoelasticity Controls Spatiotemporal Tissue Organization. *Nature Materials* , 1 (2022).

A. Elosegui-Artola, R. Oria, Y. Chen, A. Kosmalska, C. Pérez-González, N. Castro, C. Zhu, X. Trepat, and P. Roca-Cusachs. Mechanical Regulation of a Molecular Clutch Defines Force Transmission and Transduction in Response to Matrix Rigidity. *Nature Cell Biology* **18**, 540 (2016).

A. J. Engler, S. Sen, H. L. Sweeney, and D. E. Discher. Matrix Elasticity Directs Stem Cell Lineage Specification. *Cell* **126**, 677 (2006).

A. Fasano, B. Baudry, D. W. Pumplin, S. S. Wasserman, B. D. Tall, J. M. Ketley, and J. B. Kaper. Vibrio Cholerae Produces a Second Enterotoxin, Which Affects Intestinal Tight Junctions. *Proceedings of the National Academy of Sciences* **88**, 5242 (1991).

P. A. Fernández, B. Buchmann, A. Goychuk, L. K. Engelbrecht, M. K. Raich, C. H. Scheel, E. Frey, and A. R. Bausch. Surface-Tension-Induced Budding Drives Alveologenesis in Human Mammary Gland Organoids. *Nature Physics* **17**, 1130 (2021).

J. Fierling, A. John, B. Delorme, A. Torzynski, G. B. Blanchard, C. M. Lye, A. Popkova, G. Malandain, B. Sanson, J. Étienne, P. Marmottant, C. Quilliet, and M. Rauzi. Embryo-Scale Epithelial Buckling Forms a Propagating Furrow That Initiates Gastrulation. *Nature Communications* **13**, 3348 (2022).

J. Firmin, N. Ecker, D. R. Danon, V. B. Lange, H. Turlier, C. Patrat, and J.-L. Maître. Mechanics of Human Embryo Compaction. (2022).

D. A. Fletcher and R. D. Mullins. Cell Mechanics and the Cytoskeleton. *Nature* **463**, 485 (2010).

I. C. Fortunato and R. Sunyer. The Forces behind Directed Cell Migration. *Biophysica* **2**, 548 (2022).

J. Fouchard, T. P. J. Wyatt, A. Proag, A. Lisica, N. Khalilgharibi, P. Recho, M. Suzanne, A. Kabla, and G. Charras. Curling of Epithelial Monolayers Reveals Coupling between Active Bending and Tissue Tension. *Proceedings of the National Academy of Sciences* **117**, 9377 (2020).

F. Gallaire and P.-T. Brun. Fluid Dynamic Instabilities: Theory and Application to Pattern Forming in Complex Media. *Philosophical Transactions of the Royal Society A: Mathematical, Physical and Engineering Sciences* **375**, 20160155 (2017).

N. Gjorevski, M. Nikolaev, T. E. Brown, O. Mitrofanova, N. Brandenberg, F. W. DelRio, F. M. Yavitt, P. Liberali, K. S. Anseth, and M. P. Lutolf. Tissue Geometry Drives Deterministic Organoid Patterning. *Science* (2022). 10.1126/science.aaw9021.

N. Gjorevski, N. Sachs, A. Manfrin, S. Giger, M. E. Bragina, P. Ordóñez-Morán, H. Clevers, and M. P. Lutolf. Designer Matrices for Intestinal Stem Cell and Organoid Culture. *Nature* **539**, 560 (2016).

B. G. Godard and C.-P. Heisenberg. Cell Division and Tissue Mechanics. *Current Opinion in Cell Biology* Cell Dynamics. **60**, 114 (2019).

P. Gómez-Gálvez, P. Vicente-Munuera, S. Anbari, J. Buceta, and L. M. Escudero. The Complex Three-Dimensional Organization of Epithelial Tissues. *Development* **148**, dev195669 (2021).

M. Gómez-González, E. Latorre, M. Arroyo, and X. Trepat. Measuring Mechanical Stress in Living Tissues. *Nature Reviews Physics* **2**, 300 (2020).

M. Good and X. Trepat. Cell Parts to Complex Processes, from the Bottom Up. *Nature* **563**, 188 (2018).

N. Gorfinkiel and A. Martinez Arias. The Cell in the Age of the Genomic Revolution: Cell Regulatory Networks. *Cells & Development* Quantitative Cell and Developmental Biology. **168**, 203720 (2021).

F. Graner and D. Riveline. 'The Forms of Tissues, or Cell-aggregates': D'Arcy Thompson's Influence and Its Limits. *Development* **144**, 4226 (2017).

P. Guillamat, C. Blanch-Mercader, G. Pernollet, K. Kruse, and A. Roux. Integer Topological Defects Organize Stresses Driving Tissue Morphogenesis. *Nature Materials* **21**, 588 (2022).

C. Guillot and T. Lecuit. Mechanics of Epithelial Tissue Homeostasis and Morphogenesis. *Science* **340**, 1185 (2013).

C. F. Guimarães, L. Gasperini, A. P. Marques, and R. L. Reis. The Stiffness of Living Tissues and Its Implications for Tissue Engineering. *Nature Reviews Materials* **5**, 351 (2020).

H. Guo, M. Swan, and B. He. Optogenetic Inhibition of Actomyosin Reveals Mechanical Bistability of the Mesoderm Epithelium during Drosophila Mesoderm Invagination. *eLife* **11**, e69082 (2022).

J. H. Gutzman, E. Graeden, I. Brachmann, S. Yamazoe, J. K. Chen, and H. Sive. Basal Constriction during Midbrain–Hindbrain Boundary Morphogenesis Is Mediated by Wnt5b and Focal Adhesion Kinase. *Biology Open* **7**, bio034520 (2018).

J. Guyon, P.-O. Strale, I. Romero-Garmendia, A. Bikfalvi, V. Studer, and T. Daubon. Co-Culture of Glioblastoma Stem-like Cells on Patterned Neurons to Study Migration and Cellular Interactions. *Journal of Visualized Experiments* , 62213 (2021).

S. L. Haigo and D. Bilder. Global Tissue Revolutions in a Morphogenetic Movement Controlling Elongation. *Science* **331**, 1071 (2011).

C. Halley. Public Dissection Was a Gruesome Spectacle. https://daily.jstor.org/public-dissection-gruesome-spectacle/ (2019).

A. K. Harris, P. Wild, and D. Stopak. Silicone Rubber Substrata: A New Wrinkle in the Study of Cell Locomotion. *Science* **208**, 177 (1980).

A. R. Harris, L. Peter, J. Bellis, B. Baum, A. J. Kabla, and G. T. Charras. Characterizing the Mechanics of Cultured Cell Monolayers. *Proceedings of the National Academy of Sciences* **109**, 16449 (2012).

M. Hatzfeld, R. Keil, and T. M. Magin. Desmosomes and Intermediate Filaments: Their Consequences for Tissue Mechanics. *Cold Spring Harbor Perspectives in Biology* **9**, a029157 (2017).

Q. He, T. Okajima, H. Onoe, A. Subagyo, K. Sueoka, and K. Kuribayashi-Shigetomi. Origami-Based Self-Folding of Co-Cultured NIH/3T3 and HepG2 Cells into 3D Microstructures. *Scientific Reports* **8**, 4556 (2018).

N. C. Heer and A. C. Martin. Tension, Contraction and Tissue Morphogenesis. *Development* **144**, 4249 (2017).

P. Helm, M. F. Beg, M. I. Miller, and R. L. Winslow. Measuring and Mapping Cardiac Fiber and Laminar Architecture Using Diffusion Tensor MR Imaging. *Annals of the New York Academy of Sciences* **1047**, 296 (2005).

M. Hofer and M. P. Lutolf. Engineering Organoids. *Nature Reviews Materials* **6**, 402 (2021).

G. A. Holzapfel. *Nonlinear Solid Mechanics: A Continuum Approach for Engineering* (Wiley, 2000).

G. A. Holzapfel, R. W. Ogden, and S. Sherifova. On Fibre Dispersion Modelling of Soft Biological Tissues: A Review. *Proceedings of the Royal Society A: Mathematical, Physical and Engineering Sciences* **475**, 20180736 (2019).

N. S. Houssin, J. B. Martin, V. Coppola, S. O. Yoon, and T. F. Plageman. Formation and Contraction of Multicellular Actomyosin Cables Facilitate Lens Placode Invagination. *Developmental Biology* **462**, 36 (2020).

A. J. Hughes, H. Miyazaki, M. C. Coyle, J. Zhang, M. T. Laurie, D. Chu, Z. Vavrušová, R. A. Schneider, O. D. Klein, and Z. J. Gartner. Engineered Tissue Folding by Mechanical Compaction of the Mesenchyme. *Developmental Cell* **44**, 165 (2018).

D. Huh, B. D. Matthews, A. Mammoto, M. Montoya-Zavala, H. Y. Hsin, and D. E. Ingber. Reconstituting Organ-Level Lung Functions on a Chip. *Science* **328**, 1662 (2010).

J. D. Humphrey. *Cardiovascular Solid Mechanics* (Springer New York, New York, NY, 2002).

J. D. Humphrey, E. R. Dufresne, and M. A. Schwartz. Mechanotransduction and Extracellular Matrix Homeostasis. *Nature Reviews Molecular Cell Biology* **15**, 802 (2014).

D. E. Ingber. From Mechanobiology to Developmentally Inspired Engineering. *Philosophical Transactions of the Royal Society B: Biological Sciences* **373**, 20170323 (2018).

S. Ishida-Ishihara, M. Akiyama, K. Furusawa, I. Naguro, H. Ryuno, T. Sushida, S. Ishihara, and H. Haga. Osmotic Gradient Induces Stable Dome Morphogenesis on Extracellular Matrix. *Journal of Cell Science* , jcs.243865 (2020).

T. Ishiguro, H. Ohata, A. Sato, K. Yamawaki, T. Enomoto, and K. Okamoto. Tumor-Derived Spheroids: Relevance to Cancer Stem Cells and Clinical Applications. *Cancer Science* **108**, 283 (2017).

K. Ishihara and E. M. Tanaka. Spontaneous Symmetry Breaking and Pattern Formation of Organoids. *Current Opinion in Systems Biology* • Big Data Acquisition and Analysis • Development and Differentiation. **11**, 123 (2018).

E. Izquierdo, T. Quinkler, and S. De Renzis. Guided Morphogenesis through Optogenetic Activation of Rho Signalling during Early Drosophila Embryogenesis. *Nature Communications* **9**, 2366 (2018).

S. Jalal, S. Shi, V. Acharya, R. Y.-J. Huang, V. Viasnoff, A. D. Bershadsky, and Y. H. Tee. Actin Cytoskeleton Self-Organization in Single Epithelial Cells and Fibroblasts under Isotropic Confinement. *Journal of Cell Science* **132**, jcs220780 (2019).

F. Jülicher, S. W. Grill, and G. Salbreux. Hydrodynamic Theory of Active Matter. *Reports on Progress in Physics* **81**, 076601 (2018).

E. Karzbrun, A. H. Khankhel, H. C. Megale, S. M. K. Glasauer, Y. Wyle, G. Britton, A. Warmflash, K. S. Kosik, E. D. Siggia, B. I. Shraiman, and S. J. Streichan. Human Neural Tube Morphogenesis in Vitro by Geometric Constraints. *Nature* **599**, 268 (2021).

E. Karzbrun, A. Kshirsagar, S. R. Cohen, J. H. Hanna, and O. Reiner. Human Brain Organoids on a Chip Reveal the Physics of Folding. *Nature Physics* **14**, 515 (2018).

J. Z. Kechagia, J. Ivaska, and P. Roca-Cusachs. Integrins as Biomechanical Sensors of the Microenvironment. *Nature Reviews Molecular Cell Biology* **20**, 457 (2019).

M. Kelkar, P. Bohec, and G. Charras. Mechanics of the Cellular Actin Cortex: From Signalling to Shape Change. *Current Opinion in Cell Biology* **66**, 69 (2020).

N. Khalilgharibi, J. Fouchard, N. Asadipour, R. Barrientos, M. Duda, A. Bonfanti, A. Yonis, A. Harris, P. Mosaffa, Y. Fujita, A. Kabla, Y. Mao, B. Baum, J. J. Muñoz, M. Miodownik, and G. Charras. Stress Relaxation in Epithelial Monolayers Is Controlled by the Actomyosin Cortex. *Nature Physics* **15**, 839 (2019).

D. Khoromskaia and G. Salbreux. Active Morphogenesis of Patterned Epithelial Shells. *eLife* **12**, e75878 (2023).

E. J. Y. Kim, E. Korotkevich, and T. Hiiragi. Coordination of Cell Polarity, Mechanics and Fate in Tissue Self-organization. *Trends in Cell Biology* **28**, 541 (2018).

R. J. Klebe, A. Grant, G. Grant, and P. Ghosh. Cyclic-AMP Deficient MDCK Cells Form Tubules. *Journal of Cellular Biochemistry* **59**, 453 (1995).

A. P. Kourouklis and C. M. Nelson. Modeling Branching Morphogenesis Using Materials with Programmable Mechanical Instabilities. *Current Opinion in Biomedical Engineering* Tissue Engineering and Regenerative Medicine / Biomaterials. **6**, 66 (2018).

A. Kumar, J. K. Placone, and A. J. Engler. Understanding the Extracellular Forces That Determine Cell Fate and Maintenance. *Development* **144**, 4261 (2017).

A. Labernadie and X. Trepat. Sticking, Steering, Squeezing and Shearing: Cell Movements Driven by Heterotypic Mechanical Forces. *Current Opinion in Cell Biology* **54**, 57 (2018).

B. Ladoux and R.-M. Mège. Mechanobiology of Collective Cell Behaviours. *Nature Reviews Molecular Cell Biology* **18**, 743 (2017).

E. Latorre, S. Kale, L. Casares, M. Gómez-González, M. Uroz, L. Valon, R. V. Nair, E. Garreta, N. Montserrat, A. del Campo, B. Ladoux, M. Arroyo, and X. Trepat. Active Superelasticity in Three-Dimensional Epithelia of Controlled Shape. *Nature* **563**, 203 (2018).

T. Lecuit, P.-F. Lenne, and E. Munro. Force Generation, Transmission, and Integration during Cell and Tissue Morphogenesis. *Annual Review of Cell and Developmental Biology* **27**, 157 (2011).

S. E. Leggett, A. M. Hruska, M. Guo, and I. Y. Wong. The Epithelial-Mesenchymal Transition and the Cytoskeleton in Bioengineered Systems. *Cell Communication and Signaling* **19**, 32 (2021).

J. Leighton. BRIEF HISTORY OF ACTIVE TRANSPORT IN CULTURE. *Annals of the New York Academy of Sciences* **372**, 352 (1981).

J. Leighton, Z. Brada, L. W. Estes, and G. Justh. Secretory Activity and Oncogenicity of a Cell Line (MDCK) Derived from Canine Kidney. *Science* **163**, 472 (1969).

P.-F. Lenne and V. Trivedi. Sculpting Tissues by Phase Transitions. *Nature Communications* **13**, 664 (2022).

J. E. Lever. Regulation of Dome Formation in Differentiated Epithelial Cell Cultures. *Journal of Supramolecular Structure* **12**, 259 (1979).

H. Liang and L. Mahadevan. The Shape of a Long Leaf. *Proceedings of the National Academy of Sciences* **106**, 22049 (2009).

A. J. Lomakin, C. J. Cattin, D. Cuvelier, Z. Alraies, M. Molina, G. P. F. Nader, N. Srivastava, P. J. Sáez, J. M. Garcia-Arcos, I. Y. Zhitnyak, A. Bhargava, M. K. Driscoll, E. S. Welf, R. Fiolka, R. J. Petrie, N. S. De Silva, J. M. González-Granado, N. Manel, A. M. Lennon-Duménil, D. J. Müller, and M. Piel. The Nucleus Acts as a Ruler Tailoring Cell Responses to Spatial Constraints. *Science* **370**, eaba2894 (2020).

M. Luciano, S.-L. Xue, W. H. De Vos, L. Redondo-Morata, M. Surin, F. Lafont, E. Hannezo, and S. Gabriele. Cell Monolayers Sense Curvature by Exploiting Active Mechanics and Nuclear Mechanoadaptation. *Nature Physics* **17**, 1382 (2021).

K. MacCord. Epithelium. (2012).

E. Mailand, E. Özelçi, J. Kim, M. Rüegg, O. Chaliotis, J. Märki, N. Bouklas, and M. S. Sakar. Tissue Engineering with Mechanically Induced Solid-Fluid Transitions. *Advanced Materials* **34**, 2106149 (2022).

A. Malandrino, M. Mak, R. D. Kamm, and E. Moeendarbary. Complex Mechanics of the Heterogeneous Extracellular Matrix in Cancer. *Extreme Mechanics Letters* **21**, 25 (2018).

A. M. Marchiando, W. V. Graham, and J. R. Turner. Epithelial Barriers in Homeostasis and Disease. *Annual Review of Pathology: Mechanisms of Disease* **5**, 119 (2010).

A. Marín-Llauradó, S. Kale, A. Ouzeri, R. Sunyer, A. Torres-Sánchez, E. Latorre, M. Gómez-González, P. Roca-Cusachs, M. Arroyo, and X. Trepat. Mapping Mechanical Stress in Curved Epithelia of Designed Size and Shape. (2022).

Y. Maroudas-Sacks, L. Garion, L. Shani-Zerbib, A. Livshits, E. Braun, and K. Keren. Topological Defects in the Nematic Order of Actin Fibres as Organization Centres of Hydra Morphogenesis. *Nature Physics* **17**, 251 (2021).

A. C. Martin, M. Kaschube, and E. F. Wieschaus. Pulsed Contractions of an Actin–Myosin Network Drive Apical Constriction. *Nature* **457**, 495 (2009).

G. Martínez-Ara, N. Taberner, M. Takayama, E. Sandaltzopoulou, C. E. Villava, M. Bosch-Padrós, N. Takata, X. Trepat, M. Eiraku, and M. Ebisuya. Optogenetic Control of Apical Constriction Induces Synthetic Morphogenesis in Mammalian Tissues. *Nature Communications* **13**, 5400 (2022).

M. Matejčić and X. Trepat. Buckling Up from the Bottom. *Developmental Cell* **54**, 569 (2020).

A. F. Mertz, Y. Che, S. Banerjee, J. M. Goldstein, K. A. Rosowski, S. F. Revilla, C. M. Niessen, M. C. Marchetti, E. R. Dufresne, and V. Horsley. Cadherin-Based Intercellular Adhesions

Organize Epithelial Cell–Matrix Traction Forces. *Proceedings of the National Academy of Sciences* **110**, 842 (2013).

H. A. Messal, S. Alt, R. M. M. Ferreira, C. Gribben, V. M.-Y. Wang, C. G. Cotoi, G. Salbreux, and A. Behrens. Tissue Curvature and Apicobasal Mechanical Tension Imbalance Instruct Cancer Morphogenesis. *Nature* **566**, 126 (2019).

M. R. Mofrad. Rheology of the Cytoskeleton. *Annual Review of Fluid Mechanics* **41**, 433 (2009).

A. Mongera, M. Pochitaloff, H. J. Gustafson, G. A. Stooke-Vaughan, P. Rowghanian, S. Kim, and O. Campàs. Mechanics of the Cellular Microenvironment as Probed by Cells in Vivo during Zebrafish Presomitic Mesoderm Differentiation. *Nature Materials* **22**, 135 (2023).

B. Monier, M. Gettings, G. Gay, T. Mangeat, S. Schott, A. Guarner, and M. Suzanne. Apico-Basal Forces Exerted by Apoptotic Cells Drive Epithelium Folding. *Nature* **518**, 245 (2015).

R. Morizane and J. V. Bonventre. Generation of Nephron Progenitor Cells and Kidney Organoids from Human Pluripotent Stem Cells. *Nature Protocols* **12**, 195 (2017).

J. M. Mullin, N. Agostino, E. Rendon-Huerta, and J. J. Thornton. Keynote Review: Epithelial and Endothelial Barriers in Human Disease. *Drug Discovery Today* **10**, 395 (2005).

J. M. Muncie, N. M. E. Ayad, J. N. Lakins, X. Xue, J. Fu, and V. M. Weaver. Mechanical Tension Promotes Formation of Gastrulation-like Nodes and Patterns Mesoderm Specification in Human Embryonic Stem Cells. *Developmental Cell* **55**, 679 (2020).

A. Munjal, E. Hannezo, T. Y. C. Tsai, T. J. Mitchison, and S. G. Megason. Extracellular Hyaluronate Pressure Shaped by Cellular Tethers Drives Tissue Morphogenesis. *Cell* **184**, 6313 (2021).

C. M. Nelson, J. P. Gleghorn, M.-F. Pang, J. M. Jaslove, K. Goodwin, V. D. Varner, E. Miller, D. C. Radisky, and H. A. Stone. Microfluidic Chest Cavities Reveal That Transmural Pressure Controls the Rate of Lung Development. *Development* **144**, 4328 (2017).

C. M. Nelson, J. L. Inman, and M. J. Bissell. Three-Dimensional Lithographically Defined Organotypic Tissue Arrays for Quantitative Analysis of Morphogenesis and Neoplastic Progression. *Nature Protocols* **3**, 674 (2008).

C. M. Nelson, R. P. Jean, J. L. Tan, W. F. Liu, N. J. Sniadecki, A. A. Spector, and C. S. Chen. Emergent Patterns of Growth Controlled by Multicellular Form and Mechanics. *Proceedings of the National Academy of Sciences* **102**, 11594 (2005).

G. Odell, G. Oster, P. Alberch, and B. Burnside. The Mechanical Basis of Morphogenesis. *Developmental Biology* **85**, 446 (1981).

S. Okuda, N. Takata, Y. Hasegawa, M. Kawada, Y. Inoue, T. Adachi, Y. Sasai, and M. Eiraku. Strain-Triggered Mechanical Feedback in Self-Organizing Optic-Cup Morphogenesis. *Science Advances* **4**, eaau1354 (2018).

D. Oriola, M. Marin-Riera, K. Anlaş, N. Gritti, M. Sanaki-Matsumiya, G. Aalderink, M. Ebisuya, J. Sharpe, and V. Trivedi. Arrested Coalescence of Multicellular Aggregates. *Soft Matter* **18**, 3771 (2022).

M. Osterfield, C. A. Berg, and S. Y. Shvartsman. Epithelial Patterning, Morphogenesis, and Evolution: Drosophila Eggshell as a Model. *Developmental Cell* **41**, 337 (2017).

T. G. Oyama, K. Oyama, H. Miyoshi, and M. Taguchi. 3D Cell Sheets Formed via Cell-Driven Buckling-Delamination of Patterned Thin Films. *Materials & Design* **208**, 109975 (2021).

Ö. Özgüç, L. de Plater, V. Kapoor, A. F. Tortorelli, A. G. Clark, and J.-L. Maître. Cortical Softening Elicits Zygotic Contractility during Mouse Preimplantation Development. *PLOS Biology* **20**, e3001593 (2022).

A. Pal, V. Restrepo, D. Goswami, and R. V. Martinez. Exploiting Mechanical Instabilities in Soft Robotics: Control, Sensing, and Actuation. *Advanced Materials* **33**, 2006939 (2021).

M. E. Pallarès, I. Pi-Jaumà, I. C. Fortunato, V. Grazu, M. Gómez-González, P. Roca-Cusachs, J. M. de la Fuente, R. Alert, R. Sunyer, J. Casademunt, and X. Trepat. Stiffness-Dependent Active Wetting Enables Optimal Collective Cell Durotaxis. *Nature Physics* , 1 (2022).

M. A. Palmer, B. A. Nerger, K. Goodwin, A. Sudhakar, S. B. Lemke, P. T. Ravindran, J. E. Toettcher, A. Košmrlj, and C. M. Nelson. Stress Ball Morphogenesis: How the Lizard Builds Its Lung. *Science Advances* **7**, eabk0161 (2021).

K. H. Palmquist, S. F. Tiemann, F. L. Ezzeddine, S. Yang, C. R. Pfeifer, A. Erzberger, A. R. Rodrigues, and A. E. Shyer. Reciprocal Cell-ECM Dynamics Generate Supracellular Fluidity Underlying Spontaneous Follicle Patterning. *Cell* **185**, 1960 (2022).

J.-A. Park, J. H. Kim, D. Bi, J. A. Mitchel, N. T. Qazvini, K. Tantisira, C. Y. Park, M. McGill, S.-H. Kim, B. Gweon, J. Notbohm, R. Steward Jr, S. Burger, S. H. Randell, A. T. Kho, D. T. Tambe, C. Hardin, S. A. Shore, E. Israel, D. A. Weitz, D. J. Tschumperlin, E. P. Henske, S. T. Weiss, M. L. Manning, J. P. Butler, J. M. Drazen, and J. J. Fredberg. Unjamming and Cell Shape in the Asthmatic Airway Epithelium. *Nature Materials* **14**, 1040 (2015).

C. Pérez-González, R. Alert, C. Blanch-Mercader, M. Gómez-González, T. Kolodziej, E. Bazellieres, J. Casademunt, and X. Trepat. Active Wetting of Epithelial Tissues. *Nature Physics* **15**, 79 (2019).

C. Pérez-González, G. Ceada, F. Greco, M. Matejčić, M. Gómez-González, N. Castro, A. Menendez, S. Kale, D. Krndija, A. G. Clark, V. R. Gannavarapu, A. Álvarez-Varela, P. Roca-Cusachs,

E. Batlle, D. M. Vignjevic, M. Arroyo, and X. Trepat. Mechanical Compartmentalization of the Intestinal Organoid Enables Crypt Folding and Collective Cell Migration. *Nature Cell Biology* **23**, 745 (2021).

P. Popowicz, J. Kurzyca, and S. Popowicz. "Dome-curve" — Three Size Classes of Domes of MDCK Epithelial Monolayer. *Experimental pathology* **29**, 147 (1986).

L. S. Prahl, C. M. Porter, J. Liu, J. M. Viola, and A. J. Hughes. Independent Control over Cell Patterning and Adhesion on Hydrogel Substrates for Tissue Interface Mechanobiology. (2022).

P. Roca-Cusachs, V. Conte, and X. Trepat. Quantifying Forces in Cell Biology. *Nature Cell Biology* **19**, 742 (2017).

G. Salbreux and F. Jülicher. Mechanics of Active Surfaces. *Physical Review E* **96**, 032404 (2017).

P. Samal, C. van Blitterswijk, R. Truckenmüller, and S. Giselbrecht. Grow with the Flow: When Morphogenesis Meets Microfluidics. *Advanced Materials* **31**, 1805764 (2019).

S. Sances, R. Ho, G. Vatine, D. West, A. Laperle, A. Meyer, M. Godoy, P. S. Kay, B. Mandefro, S. Hatata, C. Hinojosa, N. Wen, D. Sareen, G. A. Hamilton, and C. N. Svendsen. Human iPSC-Derived Endothelial Cells and Microengineered Organ-Chip Enhance Neuronal Development. *Stem Cell Reports* **10**, 1222 (2018).

B. Schamberger, A. Roschger, R. Ziege, K. Anselme, M. B. Amar, M. Bykowski, A. P. G. Castro, A. Cipitria, R. Coles, R. Dimova, M. Eder, S. Ehrig, L. M. Escudero, M. E. Evans, P. R. Fernandes, P. Fratzl, L. Geris, N. Gierlinger, E. Hannezo, A. Iglič, J. J. K. Kirkensgaard, P. Kollmannsberger, Ł. Kowalewska, N. A. Kurniawan, I. Papantoniou, L. Pieuchot, T. H. V. Pires, L. Renner, A. Sageman-Furnas, G. E. Schröder-Turk, A. Sengupta, V. R. Sharma, A. Tagua, C. Tomba, X. Trepat, S. L. Waters, E. Yeo, C. M. Bidan, and J. W. C. Dunlop. Curvature in Biological Systems: Its Quantification, Emergence and Implications across the Scales. *Advanced Materials* , e2206110 (2022).

M. F. Schliffka and J.-L. Maître. Stay Hydrated: Basolateral Fluids Shaping Tissues. *Current Opinion in Genetics & Development* Developmental Mechanisms, Patterning and Evolution. **57**, 70 (2019).

F. Schöck and N. Perrimon. Molecular Mechanisms of Epithelial Morphogenesis. *Annual Review of Cell and Developmental Biology* **18**, 463 (2002).

X. Serra-Picamal, V. Conte, R. Vincent, E. Anon, D. T. Tambe, E. Bazellieres, J. P. Butler, J. J. Fredberg, and X. Trepat. Mechanical Waves during Tissue Expansion. *Nature Physics* **8**, 628 (2012).

F. Serwane, A. Mongera, P. Rowghanian, D. A. Kealhofer, A. A. Lucio, Z. M. Hockenbery, and O. Campàs. In Vivo Quantification of Spatially Varying Mechanical Properties in Developing Tissues. *Nature Methods* **14**, 181 (2017).

G. Shah, K. Thierbach, B. Schmid, J. Waschke, A. Reade, M. Hlawitschka, I. Roeder, N. Scherf, and J. Huisken. Multi-Scale Imaging and Analysis Identify Pan-Embryo Cell Dynamics of Germlayer Formation in Zebrafish. *Nature Communications* **10**, 5753 (2019).

A. Shellard and R. Mayor. Collective Durotaxis along a Self-Generated Stiffness Gradient in Vivo. *Nature* **600**, 690 (2021).

A. E. Shyer, A. R. Rodrigues, G. G. Schroeder, E. Kassianidou, S. Kumar, and R. M. Harland. Emergent Cellular Self-Organization and Mechanosensation Initiate Follicle Pattern in the Avian Skin. *Science* **357**, 811 (2017).

A. E. Shyer, T. Tallinen, N. L. Nerurkar, Z. Wei, E. S. Gil, D. L. Kaplan, C. J. Tabin, and L. Mahadevan. Villification: How the Gut Gets Its Villi. *Science* **342**, 212 (2013).

J. Sidhaye and C. Norden. Concerted Action of Neuroepithelial Basal Shrinkage and Active Epithelial Migration Ensures Efficient Optic Cup Morphogenesis. *eLife* **6**, e22689 (2017).

A. E. Stanton, X. Tong, and F. Yang. Extracellular Matrix Type Modulates Mechanotransduction of Stem Cells. *Acta Biomaterialia* **96**, 310 (2019).

A. Stokkermans, A. Chakrabarti, K. Subramanian, L. Wang, S. Yin, P. Moghe, P. Steenbergen, G. Mönke, T. Hiiragi, R. Prevedel, L. Mahadevan, and A. Ikmi. Muscular Hydraulics Drive Larva-Polyp Morphogenesis. *Current Biology* **32**, 4707 (2022).

A. Stokkermans, A. Chakrabarti, L. Wang, P. Moghe, K. Subramanian, P. Steenbergen, G. Mönke, T. Hiiragi, R. Prevedel, L. Mahadevan, and A. Ikmi. Ethology of Morphogenesis Reveals the Design Principles of Cnidarian Size and Shape Development. (2021).

L. Sui, S. Alt, M. Weigert, N. Dye, S. Eaton, F. Jug, E. W. Myers, F. Jülicher, G. Salbreux, and C. Dahmann. Differential Lateral and Basal Tension Drive Folding of Drosophila Wing Discs through Two Distinct Mechanisms. *Nature Communications* **9**, 4620 (2018).

R. Sunyer, V. Conte, J. Escribano, A. Elosegui-Artola, A. Labernadie, L. Valon, D. Navajas, J. M. García-Aznar, J. J. Muñoz, P. Roca-Cusachs, and X. Trepat. Collective Cell Durotaxis Emerges from Long-Range Intercellular Force Transmission. *Science* **353**, 1157 (2016).

Z. A. Syed, A.-L. Bougé, S. Byri, T. M. Chavoshi, E. Tång, H. Bouhin, I. F. van Dijk-Härd, and A. Uv. A Luminal Glycoprotein Drives Dose-Dependent Diameter Expansion of the Drosophila Melanogaster Hindgut Tube. *PLOS Genetics* **8**, e1002850 (2012).

T. Tallinen, J. Y. Chung, F. Rousseau, N. Girard, J. Lefèvre, and L. Mahadevan. On the Growth and Form of Cortical Convolutions. *Nature Physics* **12**, 588 (2016).

D. T. Tambe, C. Corey Hardin, T. E. Angelini, K. Rajendran, C. Y. Park, X. Serra-Picamal, E. H. Zhou, M. H. Zaman, J. P. Butler, D. A. Weitz, J. J. Fredberg, and X. Trepat. Collective Cell Guidance by Cooperative Intercellular Forces. *Nature Materials* **10**, 469 (2011).

W. Tang, A. Das, A. F. Pegoraro, Y. L. Han, J. Huang, D. A. Roberts, H. Yang, J. J. Fredberg, D. N. Kotton, D. Bi, and M. Guo. Collective Curvature Sensing and Fluidity in Three-Dimensional Multicellular Systems. *Nature Physics* **18**, 1371 (2022).

C. Tanner, D. Frambach, and D. Misfeldt. Transepithelial Transport in Cell Culture. A Theoretical and Experimental Analysis of the Biophysical Properties of Domes. *Biophysical Journal* **43**, 183 (1983).

J. P. Thiery, H. Acloque, R. Y. J. Huang, and M. A. Nieto. Epithelial-Mesenchymal Transitions in Development and Disease. *Cell* **139**, 871 (2009).

D. W. Thompson. *On Growth and Form.* repr ed. (Univ. Pr, Cambridge, 1979).

S. Tlili, E. Gauquelin, B. Li, O. Cardoso, B. Ladoux, H. Delanoë-Ayari, and F. Graner. Collective Cell Migration without Proliferation: Density Determines Cell Velocity and Wave Velocity. *Royal Society Open Science* **5**, 172421 (2018).

C. Tomba, V. Luchnikov, L. Barberi, C. Blanch-Mercader, and A. Roux. Epithelial Cells Adapt to Curvature Induction via Transient Active Osmotic Swelling. *Developmental Cell* **57**, 1257 (2022).

N. Torras, M. García-Díaz, V. Fernández-Majada, and E. Martínez. Mimicking Epithelial Tissues in Three-Dimensional Cell Culture Models. *Frontiers in Bioengineering and Biotechnology* **6** (2018).

A. Torres-Sánchez, M. Kerr Winter, and G. Salbreux. Tissue Hydraulics: Physics of Lumen Formation and Interaction. *Cells & Development* Quantitative Cell and Developmental Biology. **168**, 203724 (2021).

X. Trepat and E. Sahai. Mesoscale Physical Principles of Collective Cell Organization. *Nature Physics* **14**, 671 (2018).

X. Trepat, M. R. Wasserman, T. E. Angelini, E. Millet, D. A. Weitz, J. P. Butler, and J. J. Fredberg. Physical Forces during Collective Cell Migration. *Nature Physics* **5**, 426 (2009).

A. Trushko, I. Di Meglio, A. Merzouki, C. Blanch-Mercader, S. Abuhattum, J. Guck, K. Alessandri, P. Nassoy, K. Kruse, B. Chopard, and A. Roux. Buckling of an Epithelium Growing under Spherical Confinement. *Developmental Cell* **54**, 655 (2020).

J. D. Valentich, R. Tchao, and J. Leighton. Hemicyst Formation Stimulated by Cyclic AMP in Dog Kidney Cell Line MDCK. *Journal of Cellular Physiology* **100**, 291 (1979).

L. Valon, A. Marín-Llauradó, T. Wyatt, G. Charras, and X. Trepat. Optogenetic Control of Cellular Forces and Mechanotransduction. *Nature Communications* **8**, 14396 (2017).

V. D. Varner, J. P. Gleghorn, E. Miller, D. C. Radisky, and C. M. Nelson. Mechanically Patterning the Embryonic Airway Epithelium. *Proceedings of the National Academy of Sciences* **112**, 9230 (2015).

S. R. K. Vedula, M. C. Leong, T. L. Lai, P. Hersen, A. J. Kabla, C. T. Lim, and B. Ladoux. Emerging Modes of Collective Cell Migration Induced by Geometrical Constraints. *Proceedings of the National Academy of Sciences* **109**, 12974 (2012).

J. V. Veenvliet, P.-F. Lenne, D. A. Turner, I. Nachman, and V. Trivedi. Sculpting with Stem Cells: How Models of Embryo Development Take Shape. *Development* **148**, dev192914 (2021).

V. Venturini, F. Pezzano, F. Català Castro, H.-M. Häkkinen, S. Jiménez-Delgado, M. Colomer-Rosell, M. Marro, Q. Tolosa-Ramon, S. Paz-López, M. A. Valverde, J. Weghuber, P. Loza-Alvarez, M. Krieg, S. Wieser, and V. Ruprecht. The Nucleus Measures Shape Changes for Cellular Proprioception to Control Dynamic Cell Behavior. *Science* **370**, eaba2644 (2020).

S. Vianello and M. P. Lutolf. Understanding the Mechanobiology of Early Mammalian Development through Bioengineered Models. *Developmental Cell* **48**, 751 (2019).

T. Vignaud, L. Blanchoin, and M. Théry. Directed Cytoskeleton Self-Organization. *Trends in Cell Biology* Special Issue – Synthetic Cell Biology. **22**, 671 (2012).

R. Virchow, F. Chance, J. Goodsir, K. C. London, and P. I. of Berlin. *Cellular Pathology as Based upon Physiological and Pathological Histology; Twenty Lectures Delivered in the Pathological Institute of Berlin during the Months of February, March, and April, 1858* (John Churchill, London, 1860) pp. 1–546.

A. Voss-Böhme. Multi-Scale Modeling in Morphogenesis: A Critical Analysis of the Cellular Potts Model. *PLOS ONE* **7**, e42852 (2012).

K. Wagh, M. Ishikawa, D. A. Garcia, D. A. Stavreva, A. Upadhyaya, and G. L. Hager. Mechanical Regulation of Transcription: Recent Advances. *Trends in Cell Biology* **31**, 457 (2021).

D. A. C. Walma and K. M. Yamada. The Extracellular Matrix in Development. *Development* **147**, dev175596 (2020).

A. Warmflash, B. Sorre, F. Etoc, E. D. Siggia, and A. H. Brivanlou. A Method to Recapitulate Early Embryonic Spatial Patterning in Human Embryonic Stem Cells. *Nature Methods* **11**, 847 (2014).

C. M. Waters, E. Roan, and D. Navajas. Mechanobiology in Lung Epithelial Cells: Measurements, Perturbations, and Responses. *Comprehensive Physiology* **2**, 1 (2012).

Q. Wen and P. A. Janmey. Polymer Physics of the Cytoskeleton. *Current Opinion in Solid State and Materials Science* **15**, 177 (2011).

H. H. Wensink, J. Dunkel, S. Heidenreich, K. Drescher, R. E. Goldstein, H. Löwen, and J. M. Yeomans. Meso-Scale Turbulence in Living Fluids. *Proceedings of the National Academy of Sciences* **109**, 14308 (2012).

S. Wolfram. The Scientist Who Cracked Biological Mysteries With Math | Backchannel. *Wired* (2017).

N. A. Wright and R. Poulsom. Omnis Cellula e Cellula Revisited: Cell Biology as the Foundation of Pathology. *The Journal of Pathology* **226**, 145 (2012).

T. Wyatt, B. Baum, and G. Charras. A Question of Time: Tissue Adaptation to Mechanical Forces. *Current Opinion in Cell Biology* Cell Architecture. **38**, 68 (2016).

T. P. J. Wyatt, J. Fouchard, A. Lisica, N. Khalilgharibi, B. Baum, P. Recho, A. J. Kabla, and G. T. Charras. Actomyosin Controls Planarity and Folding of Epithelia in Response to Compression. *Nature Materials* **19**, 109 (2020).

T. P. J. Wyatt, A. R. Harris, M. Lam, Q. Cheng, J. Bellis, A. Dimitracopoulos, A. J. Kabla, G. T. Charras, and B. Baum. Emergence of Homeostatic Epithelial Packing and Stress Dissipation through Divisions Oriented along the Long Cell Axis. *Proceedings of the National Academy of Sciences* **112**, 5726 (2015).

W. Xi, T. B. Saw, D. Delacour, C. T. Lim, and B. Ladoux. Material Approaches to Active Tissue Mechanics. *Nature Reviews Materials* **4**, 23 (2018).

T. Yeung, P. C. Georges, L. A. Flanagan, B. Marg, M. Ortiz, M. Funaki, N. Zahir, W. Ming, V. Weaver, and P. A. Janmey. Effects of Substrate Stiffness on Cell Morphology, Cytoskeletal Structure, and Adhesion. *Cell Motility* **60**, 24 (2005).

H. G. Yevick, P. W. Miller, J. Dunkel, and A. C. Martin. Structural Redundancy in Supracellular Actomyosin Networks Enables Robust Tissue Folding. *Developmental Cell* **50**, 586 (2019).

J. C. Yu and R. Fernandez-Gonzalez. Local Mechanical Forces Promote Polarized Junctional Assembly and Axis Elongation in Drosophila. *eLife* **5**, e10757 (2016).

F. Zampieri, M. Coen, and G. Gabbiani. The Prehistory of the Cytoskeleton Concept. *Cytoskeleton* **71**, 464 (2014).

L. Zhang, Y. Xiang, H. Zhang, L. Cheng, X. Mao, N. An, L. Zhang, J. Zhou, L. Deng, Y. Zhang, X. Sun, H. A. Santos, and W. Cui. A Biomimetic 3D-Self-Forming Approach for Microvascular Scaffolds. *Advanced Science* **7**, 1903553 (2020).